USGS
science for a changing world

Prepared in cooperation with the Department of Agriculture Natural Resources Conservation Service and Grant County Soil Conservation District

Evaluation of Salinity and Nutrient Conditions in the Heart River Basin, North Dakota, 1970–2020

Scientific Investigations Report 2022–5013

U.S. Department of the Interior
U.S. Geological Survey

Cover: Photograph showing the Heart River north of Carson, North Dakota (left). Photograph by Chad Skettreberg, Western Heart River Irrigation District.

Photograph showing Antelope Creek looking upstream at the North Dakota Department of Environmental Quality site 385583 (right). Photograph by Joel Galloway, U.S. Geological Survey.

Evaluation of Salinity and Nutrient Conditions in the Heart River Basin, North Dakota, 1970–2020

By Wyatt S. Tatge, Rochelle A. Nustad, and Joel M. Galloway

Prepared in cooperation with the Department of Agriculture Natural Resources Conservation Service and Grant County Soil Conservation District

Scientific Investigations Report 2022–5013

U.S. Geological Survey, Reston, Virginia: 2022

Suggested citation:
Tatge, W.S., Nustad, R.A., and Galloway, J.M., 2022, Evaluation of salinity and nutrient conditions in the Heart River Basin, North Dakota, 1970–2020: U.S. Geological Survey Scientific Investigations Report 2022–5013, 76 p., https://doi.org/10.3133/sir20225013.

Associated data for this publication:
Tatge, W.S., Nustad, R.A., and Galloway, J.M., 2022, Data and scripts used in water-quality trend and load analysis in the Heart River Basin, North Dakota, 1970–2020: U.S. Geological Survey data release, https://doi.org/10.5066/P987APZ8.

U.S. Geological Survey, 2020, USGS water data for the Nation: U.S. Geological Survey National Water Information System database, https://doi.org/10.5066/F7P55KJN.

ISSN 2328-0328 (online)

Acknowledgments

The authors gratefully acknowledge funding provided by the U.S. Department of Agriculture Natural Resources Conservation Service and the Grant County Soil Conservation District. The authors gratefully acknowledge the support of the Western Heart River Irrigation District, particularly Chad Skretteberg as the project's visionary. The authors gratefully acknowledge the support from personnel at the North Dakota Department of Environmental Quality. The authors sincerely thank all field personnel and science-support staff in the Heart River Basin who collect and quality assure water-quality and streamflow data, making this type of analysis possible.

The authors wish to acknowledge numerous U.S. Geological Survey personnel for providing insightful edits and comments for this report.

Contents

Figures

Tables

Conversion Factors

U.S. customary units to International System of Units

Multiply	By	To obtain
	Length	
foot (ft)	0.3048	meter (m)
mile (mi)	1.609	kilometer (km)
	Area	
acre	4,047	square meter (m^2)
acre	0.4047	hectare (ha)
acre	0.4047	square hectometer (hm^2)
acre	0.004047	square kilometer (km^2)
square mile (mi^2)	259.0	hectare (ha)
square mile (mi^2)	2.590	square kilometer (km^2)
	Volume	
acre-foot (acre-ft)	1,233	cubic meter (m^3)
acre-foot (acre-ft)	0.001233	cubic hectometer (hm^3)
	Flow rate	
cubic foot per second (ft^3/s)	0.02832	cubic meter per second (m^3/s)
	Mass	
pound, avoirdupois (lb)	0.4536	kilogram (kg)
ton, short (2,000 lb)	0.9072	metric ton (t)
ton per year per square mile ($ton/yr/mi^2$)	0.3503	metric ton per year per square kilometer ($kg/yr/km^2$)

Temperature in degrees Celsius (°C) may be converted to degrees Fahrenheit (°F) as follows:

$$°F = (1.8 \times °C) + 32.$$

Temperature in degrees Fahrenheit (°F) may be converted to degrees Celsius (°C) as follows:

$$°C = (°F - 32) / 1.8.$$

Amount of substance concentrations in millimole per liter (mmol/L) may be converted to milligrams per liter as follows: mg/L = mmol/L x molar mass of compound (g/mol).

Molality in millimole per kilogram (mmol/kg) may be converted to milligram per kilogram as follows: mg/L = mmol/kg of compound x molar mass of compound.

Datum

Vertical coordinate information is referenced to the North American Vertical Datum of 1988 (NAVD 88).

Horizontal coordinate information is referenced to the North American Datum of 1983 (NAD 83).

Elevation, as used in this report, refers to distance above the vertical datum.

Supplemental Information

Specific conductance is given in microsiemens per centimeter at 25 degrees Celsius (µS/cm at 25 °C).

Concentrations of chemical constituents in water are given in either milligrams per liter (mg/L) or micrograms per liter (µg/L).

Abbreviations

AMLE	adjusted maximum likelihood estimator
Ca-montmorillonite	calcium montmorillonite
EGRET	Exploration and Graphics for RivEr Trends
FAGMC	flow-averaged geometric mean concentration
K-feldspar	potassium feldspar
Na-montmorillonite	sodium montmorillonite
NRCS	Natural Resources Conservation Service
NWIS	National Water Information System
R^2	coefficient of determination
SAR	sodium adsorption ratio
SEP	standard error of prediction
SI	saturation index
TDS	total dissolved solids
USGS	U.S. Geological Survey
WQP	Water Quality Portal

Evaluation of Salinity and Nutrient Conditions in the Heart River Basin, North Dakota, 1970–2020

By Wyatt S. Tatge, Rochelle A. Nustad, and Joel M. Galloway

Abstract

The Heart River Basin is predominantly an agricultural basin in western North Dakota and is approximately 3,350 square miles. The U.S. Geological Survey, in cooperation with the U.S. Department of Agriculture Natural Resources Conservation Service and the Grant County Soil Conservation District, completed a study to assess spatial and temporal patterns of water quality in the Heart River Basin. The purpose of this report is to describe the methods and results of a study to evaluate salinity and nutrients in the Heart River Basin in western North Dakota. Water-quality and streamflow data used in the study were compiled from 1970 to 2020 using the National Water Quality Monitoring Council Water Quality Portal and National Water Information System.

Changes in streamflow characteristics were investigated at three sites from 1970 to 2020, and changes in water quality were investigated at four sites from 1974 to 2019. Streamflow analysis indicated decreasing streamflow from 1970 until the late 1990s followed by increasing streamflow through 2020, with the largest increase in the 7-day minimum streamflow or base flow. For the historical water-quality trend period (1974–2019), total dissolved solids, sulfate, sodium, chloride, and sodium adsorption ratio concentrations have increased since the mid-1970s through 2019. Potassium concentrations during the historical period remained mostly constant with some small fluctuations. Calcium and magnesium concentrations increased since the mid-1970s at all sites, except for a decrease at one site between 1974 and 1999. During the recent trend period (1999–2019), increasing concentrations in total dissolved solids, sulfate, sodium, chloride, calcium, magnesium, and sodium adsorption ratios were observed across the Heart River Basin. The magnitude of the increases was smaller at tributary sites compared to main-stem sites. During the recent period, potassium was mostly constant, although small (−0.9 milligram per liter or less) decreases on tributaries and minor (1.3 milligrams per liter) increases on the main-stem sites were detected. Unlike dissolved ion concentrations, significant increases in nutrient concentrations were not detected from 1999 to 2019, but nitrate plus nitrite concentrations most likely decreased upstream from Lake Tschida.

Inverse modeling for period 1 (1974–99) in model zone 1 (Heart River reach from site 5 to site 6) had eight reasonable models that indicated the clay mineral-water interactions and dissolution of evaporites control the geochemistry. Results of the inverse modeling for period 2 (1999–2019) in model zone 1 also had eight reasonable models that indicated that the dissolution of evaporites was the major geochemical control. Results of the geochemical modeling for period 1 (1974–99) in model zone 2 (Heart River and Sweetbriar Creek reach from sites 20 and 21 to site 22) produced seven reasonable models, and the geochemical control of the system was the dissolution of sulfate evaporite minerals. Geochemical modeling results for period 2 (1999–2019) in model zone 2 produced 11 reasonable models and was also controlled by the dissolution of sulfate evaporite minerals. Differences between the two model zones indicated that geology controls some of the water-quality changes in the Heart River Basin.

Loads were estimated for total dissolved solids, sulfate, sodium, and chloride and total phosphorus. Annual loads estimated for the Heart River from 2013 through 2020 at the Heart River site upstream from Lake Tschida (site 5) and near Mandan (site 22) were generally greatest in 2014 and least in 2016 for total dissolved solids, sulfate, sodium, and chloride. Most of the annual loads of total dissolved solids, sulfate, sodium, and chloride are delivered in March through July in the Heart River at these sites and are likely from snowmelt and spring and summer rains. The mean annual yields of total dissolved solids and sodium from 2013 to 2020 generally were largest in Big Muddy Creek (site 18), whereas yields of sulfate and chloride were largest at Sweetbriar Creek (site 21) compared to the other selected sites in the Heart River Basin. Larger yields of total dissolved solids, sulfate, sodium, and chloride at sites located on Big Muddy Creek and Sweet Briar Creek in the lower Heart River Basin were likely a result of differences in geology and soils upstream from the selected sites.

A mass balance of total dissolved solids, sulfate, sodium, and chloride was estimated for the lower Heart River Basin, specifically the reach below Lake Tschida to Mandan (site 7 to site 22). Intervening flow was the largest contributor to the dissolved ion loads in the lower Heart River Basin and is an important part of understanding the transport of dissolved ions in the basin. The intervening load can include groundwater discharge, irrigation return flow, local runoff, and input

from smaller ephemeral tributaries. Tributaries in the lower Heart River Basin contributed portions of the total dissolved solids, sulfate, sodium, and chloride loads at the Heart River near Mandan (site 22) that generally were proportional to the streamflow contributions.

Annual loads for total phosphorus between 2013 and 2020 at the Heart River site upstream from Lake Tschida (site 5) and near Mandan (site 22) generally were largest in 2019 and smallest in 2016. Most of the total phosphorus loads for main-stem sites 5 and 22 were transported in March, April, and June, likely from snowmelt and early summer rains. The mean annual yields of total phosphorus for 2013–20 were largest on the main-stem site upstream from Lake Tschida (site 5) and Sweetbriar Creek (site 21), whereas the smallest yields were in Big Muddy Creek (site 18). Much of the phosphorus that enters Lake Tschida from the upper basin does not get transported downstream to the lower basin, and much of the phosphorus in the lower basin was attributed to intervening flow.

Introduction

The Heart River Basin is predominantly an agricultural basin in western North Dakota and is approximately 3,350 square miles (Maderak, 1966; North Dakota Department of Environmental Quality, 2021a; fig. 1). Agricultural practices including irrigation, grazing, and crop management can affect water quality in the Heart River in terms of salinity and nutrient enrichment. In recent years, dissolved ion concentrations in rivers and streams across North Dakota have been increasing (Galloway and others, 2012; Nustad and Vecchia, 2020). The Western Heart River Irrigation District uses water from the Heart River to irrigate approximately 7,660 acres of the 13,000 acres of irrigable land in the lower portion of the basin downstream from Lake Tschida (Chad Skretteberg, Western Heart River Irrigation District, written commun., 2021; Simonds, 1996; fig. 1). Concerns about salinity in soils of irrigated land have prompted the need to develop a management plan to minimize the buildup of salts in sensitive soils in the area. The development of a plan requires an understanding of the processes controlling salinity on irrigated lands. An understanding of aspects of irrigation was needed, such as how irrigation type (pivot or flood), irrigation-application timing and rates, and irrigation water quality, affect the salinity of different soil types.

An additional concern in the basin is the effect of conservation and agricultural management practices on nutrient concentrations in the Heart River and its tributaries. Excess nutrients coming off the landscape to surface waters can lead to increased frequency and severity of algal blooms in lakes. North Dakota lakes, including Lake Tschida, are experiencing increased occurrence and severity of harmful algal blooms, or blooms containing toxin-producing blue-green algae (North Dakota Department of Environmental Quality, 2021b). An understanding of spatial and temporal variability of nutrient concentrations is important in understanding how activities on the landscape, including agricultural management and conservation practices, have affected nutrient concentrations.

The U.S. Geological Survey (USGS), in cooperation with the U.S. Department of Agriculture's Natural Resources Conservation Service (NRCS) and the Grant County Soil Conservation District, completed a study to assess spatial and temporal patterns of water quality in the Heart River Basin. Streamflow analysis, statistical summarization of water quality, trend analysis, geochemical modeling, and mass balance computation were completed to provide a better understanding of salinity and nutrient dynamics in the basin.

Purpose and Scope

The purpose of this report is to describe the methods and results of a study to evaluate salinity and nutrients in the Heart River Basin in western North Dakota. Water-quality and streamflow data used in the study were compiled from 1970 to 2020 using the National Water Quality Monitoring Council Water Quality Portal (WQP; National Water Quality Monitoring Council, 2020) and National Water Information System (NWIS) database (U.S. Geological Survey, 2020). Streamflow characteristics were analyzed from 1970 to 2020 to examine hydroclimatic patterns that may explain changes in water quality in the Heart River Basin over time. Statistics were computed for selected constituents and sites (fig. 1) to describe spatial patterns in concentration across the basin. Water-quality trend analysis was completed for chosen sites with sufficient data to evaluate how selected water-quality constituents have changed over time. Water-quality trends were analyzed for a recent trend period (1999–2019) at two tributary sites (Green River near New Hradec, North Dakota [site 1] and Antelope Creek near Carson, N. Dak. [site 10]; fig. 1) and two main-stem sites (Heart River near Richardton, N. Dak. [site 5] and Heart River near Mandan, N. Dak. [site 22]) and for a historical trend period (1974–2019) for one tributary site (site 1) and two main-stem sites (sites 5 and 22). Geochemical modeling was used to evaluate chemical reactions relating to salinity in two reaches of the Heart River for two different periods (1974–99 and 1999–2019). Constituent loads and yields were estimated for selected sites in the Heart River Basin from 2013 to 2020 for total dissolved solids (TDS), sulfate, sodium, chloride, and total phosphorus. Monthly, annual, and total loads were computed for each site and constituent, and mean annual yields were computed to normalize loads to the drainage area upstream from the selected sites. Total loads for the period of 2013–20 were used to estimate a simplified mass balance in the lower Heart River Basin to identify areas in the basin that have the largest contributions of constituent mass in the Heart River.

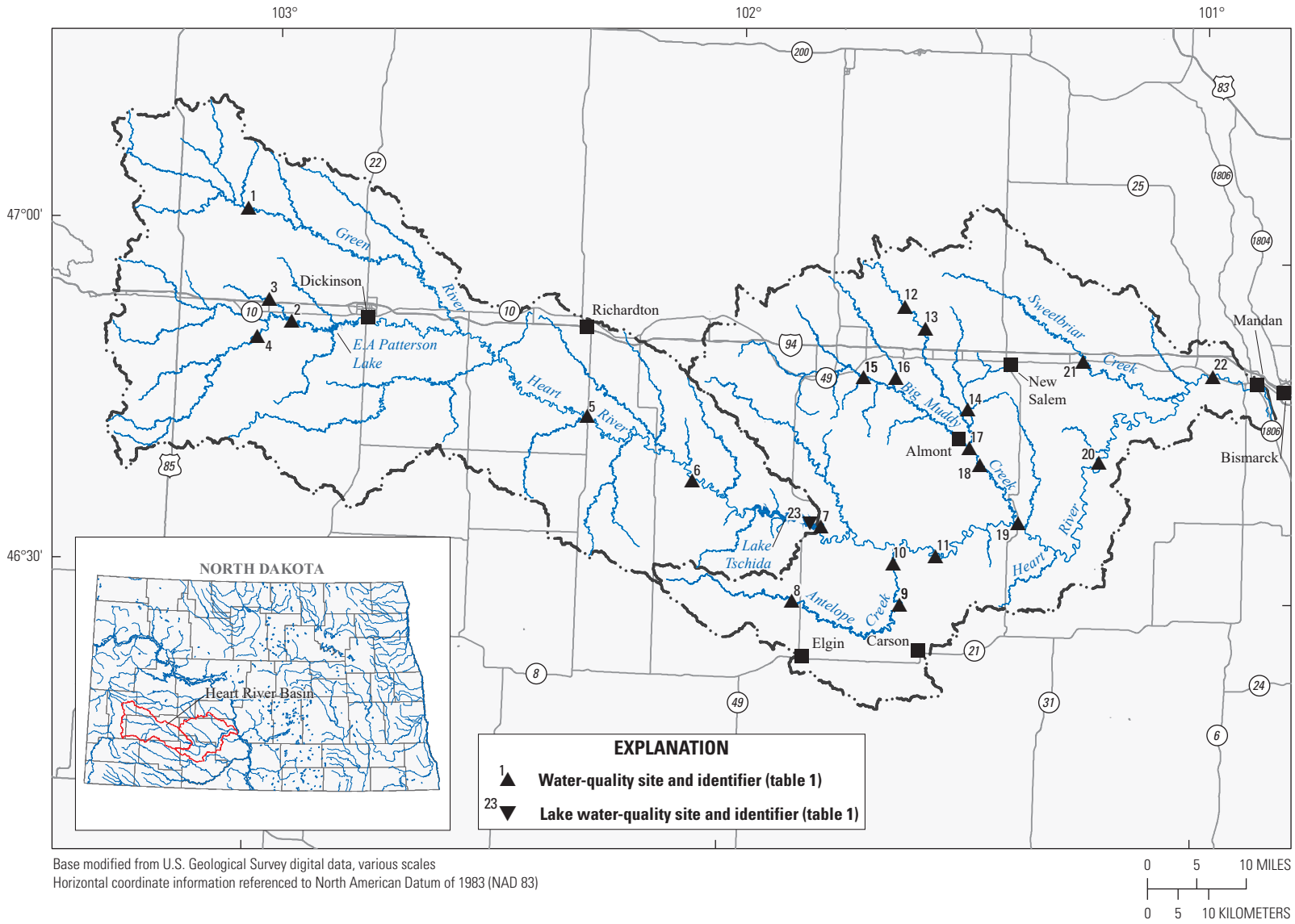

Figure 1. Location of study area and water-quality sites in Heart River Basin, North Dakota.

Description of Study Area

The Heart River Basin, located in western North Dakota, is approximately 120 miles long and about 30 miles wide with a contributing drainage area of about 3,350 square miles (Maderak, 1966; North Dakota Department of Environmental Quality, 2021a; fig. 1). The elevation ranges from about 1,650 feet above North American Vertical Datum 1988 (NAVD 88) at its mouth near Mandan, N. Dak., to about 2,900 feet above NAVD 88 in Billings County, N. Dak (not shown). The Heart River is a dendritic system (Ritter and others, 2011) located between the Knife River to the north and the Cannonball River to the south (not shown). The Heart River is impounded by two dams, the Dickinson Dam (E.A. Patterson Lake) in the upper basin near Dickinson, N. Dak., and the Heart Butte Dam (Lake Tschida) in the central portion of the basin (fig. 1). In this report, the "upper" Heart River Basin refers to the area above Heart Butte Dam (Lake Tschida), and the "lower" basin is the area below Heart Butte Dam (Lake Tschida). Dickinson Dam was completed in 1950 (Linenberger, 1996), and Heart Butte Dam was completed in 1949 (Simonds, 1996). Both reservoirs are operated by the Bureau of Reclamation as water supplies for irrigation, recreation, and flood control as part of the Pick-Sloan Missouri Basin Program. Additionally, E.A. Patterson Lake serves as a water supply for the City of Dickinson, N. Dak.

Western North Dakota geology generally consists of shales, sandstones, and alluvial materials. Specific formations underlying the Heart River Basin are the Ludlow, Cannonball, Bullion Creek, Sentinel Butte, Golden Valley, Chadron, and Brule Formations (figs. 2*A* and 3; Murphy and others, 2009).

The dominant formations in the basin were the Ludlow, Cannonball, and Bullion Creek Formations. The Paleocene Ludlow Formation is considered the basal unit of the Fort Union Group (fig. 3; Carlson, 1983). The Ludlow Formation is characterized by brown or gray with yellowish-brown or gray claystone, siltstone, and sandstone beds alternating with lignite or lignitic shale beds (Carlson, 1982, 1983; Murphy and others, 2009). The Paleocene Cannonball Formation is a marine deposit that overlayed the Ludlow Formation in western North Dakota (fig. 3; Murphy and others, 2009). This formation is characterized by alternating beds of sandstone, siltstone, and mudstones, with mudstones as the dominate lithology (Carlson, 1982, 1983; Murphy and others, 2009). The Paleocene Bullion Creek Formation (formerly Tongue River Formation pre-1977) is a nonmarine deposit that overlies the Cannonball Formation in western North Dakota (fig. 3; Murphy and others, 2009). The Bullion Creek Formation consists of interbedded layers of clay, silt, sand, and lignite (Clayton and others, 1977). The descriptions of these units were used to determine mineral types for geochemical modeling.

Land use in the basin is dominated by agriculture, with 45 percent of the land used for grasslands, 39 percent used for cultivated crops, and 9 percent used for hay or pastureland (Homer and others, 2015; fig. 2*B*). Grasslands are defined as areas with 80 percent or more of the total vegetation being graminoid or herbaceous (Homer and others, 2015). Additionally, grassland is not subjected to intensive management practices but may be used for grazing (Homer and others, 2015). Cultivated crops are areas used to produce annual crops and are managed intensively (Homer and others, 2015). Hay/pastureland are areas of grasses, legumes, or grass-legume mixes planted for grazing or production of seed (Homer and others, 2015). In the upper basin, there is a higher percentage of cultivated crops compared to the lower basin (43 and 35 percent, respectively), whereas in the lower basin there is a higher percentage of grassland compared to the upper basin (51 and 39 percent, respectively) (Homer and others, 2015). To support the agriculture in the subhumid climate of the basin, irrigation began in the late 1940s (Bureau of Reclamation, 2021). Conversion from flood to pivot irrigation practices has been occurring within the basin since the late 1990s (Chad Skretteberg, Western Heart River Irrigation District, written commun., 2021; James Weigel, Bureau of Reclamation, written commun., 2021). Only about 1 percent of the land use is urban (Homer and others, 2015), with two major cities in the basin, Dickinson and Mandan, N. Dak., having populations of 17,787 and 18,331, respectively (U.S. Census Bureau, 2010).

Soil characteristics in the basin have slight variations but are dominated by hydrologic soil groups C and D that cover about 71 percent of the basin (Soil Survey Staff, 2020; fig. 2*C*). Hydrologic soil groups are based on the saturated hydraulic conductivity of the least transmissive layer, depth to impermeable layer, and depth to a water table (U.S. Department of Agriculture, 1972). The hydrologic soil group generally is defined by how well the soil transmits water when fully saturated in each unit (U.S. Department of Agriculture, 1972). The soils are grouped by A, B, C, and D soils where the A and B soils transmit water through the soil column well and the C and D soils do not transmit water well and generally are not well drained naturally (U.S. Department of Agriculture, 1972). Within the basin, the hydrologic group A and B soils generally are present along the streams and rivers in the basin, which was expected because these consist of alluvium and terrace deposits (fig. 2*C*). The group C and D soils were generally formed on top of the local bedrock, which consists of mostly shales (fig. 2*A*, *B*).

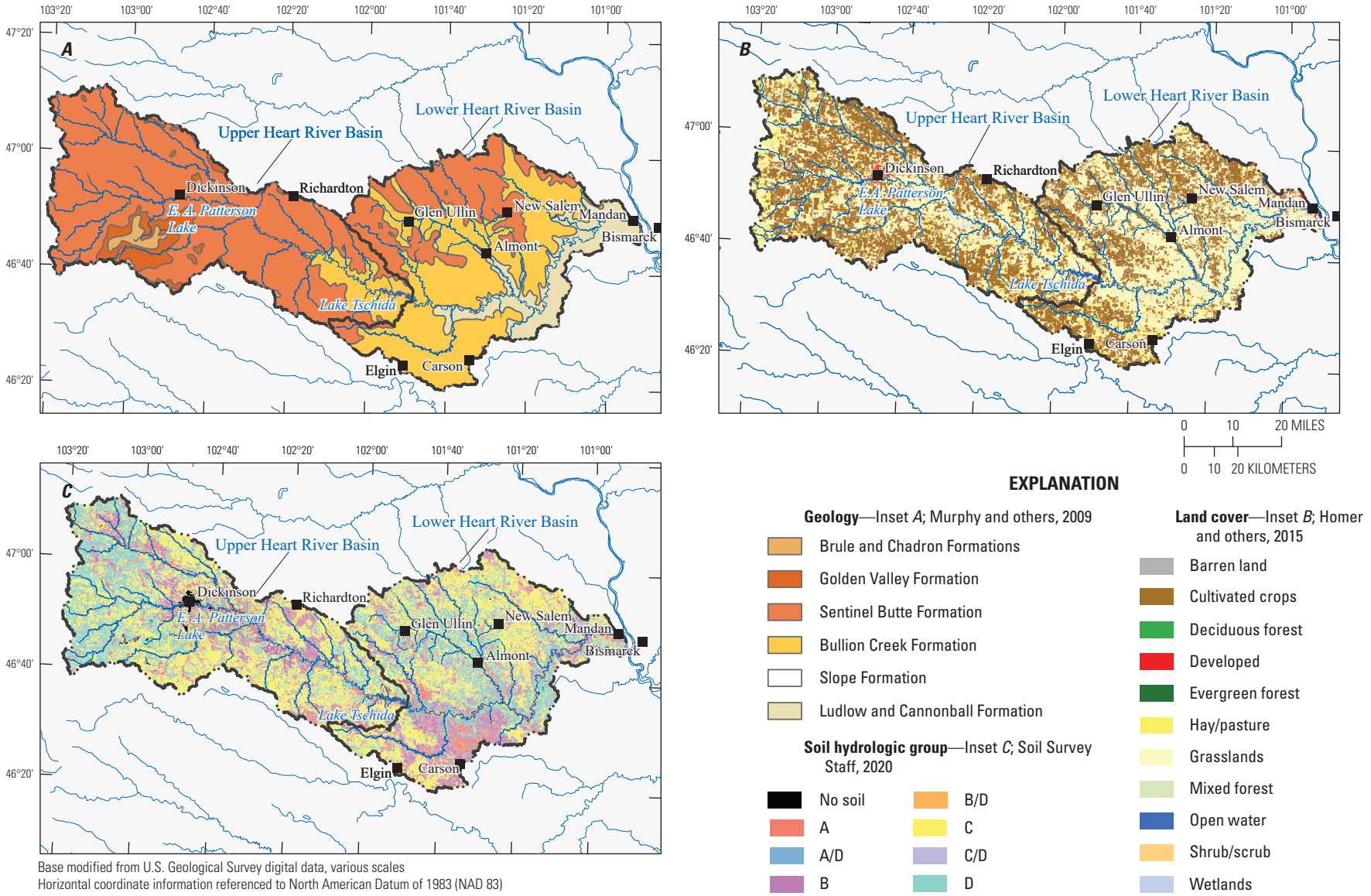

Base modified from U.S. Geological Survey digital data, various scales
Horizontal coordinate information referenced to North American Datum of 1983 (NAD 83)

Figure 2. Geology, land use, and hydrologic soil groups for the Heart River Basin. *A*, Surficial geology; *B*, land use; and *C*, hydrologic soil groups.

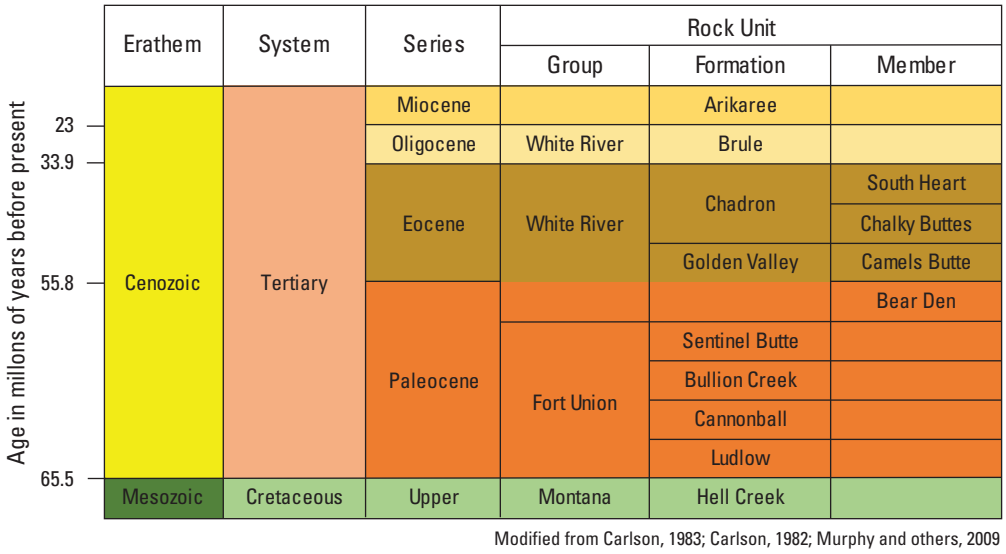

Figure 3. Stratigraphic column of geologic units in the Heart River Basin.

Methods of Analysis

Water-quality and streamflow data were used in the analysis of streamflow characteristics, water-quality trends, geochemical modeling, load estimation, and mass balance. Water-quality data used in the study were compiled for the period of 1970–2020 from the National Water Quality Monitoring Council WQP (National Water Quality Monitoring Council, 2020). Constituents related to salinity and nutrients in the Heart River Basin were selected. Streamflow data for selected sites were obtained from the USGS NWIS database (U.S. Geological Survey, 2020). Streamflow responds to climatic variability, often referred to as hydroclimatic variability. Because variability in streamflow can have a large effect on water-quality concentrations in streams, an analysis of hydroclimate was done. Summary statistics were computed for sites to describe spatial patterns across the basin. Trends for selected sites with sufficient data were analyzed using R–QWTREND (Vecchia and Nustad, 2020) to evaluate how selected water-quality constituents have changed over time. Inverse geochemical modeling using PHREEQC (Parkhurst, 1995) was completed to evaluate geochemical reactions related to increases in salinity in selected reaches of the Heart River. Constituent loads and yields were estimated for selected sites and used in a simple mass balance to identify areas in the lower Heart River Basin that have the largest contributions of constituent mass to the Heart River. Scripts and data used to perform analyses for this study are available in a USGS data release (Tatge and others, 2022).

Streamflow Analysis

Streamflow changes were analyzed in the Heart River Basin using the flow history component of Exploration and Graphics for RivEr Trends (EGRET) program (Hirsch and De Cicco, 2015). The flow history component provides tabular and graphic output for several streamflow statistics that can be used to assess how streamflow may be changing over time. Sites were selected for use in the EGRET analysis that had long term (50 years minimum) flow records with little to no missing data for the period of 1970–2020 and were also used for water-quality trend analysis. Sites 1, 5, and 22 (table 1 and fig. 1) were selected for the EGRET analysis. The flow history in EGRET provides a statistical description of long-term variability in streamflow using the daily streamflow record for a given streamgage.

Four streamflow statistics were selected for streamflow analysis and plotted to analyze changes in streamflow from 1970 to 2020. Using the flow history component of EGRET, plots of the smoothed trend in annual maximum daily, annual mean daily, and annual 7-day minimum were used to identify long-term changes in streamflow. The smoothing methods used by EGRET are described in detail in Hirsch and De Cicco (2015). The results of the EGRET analyses aided in the interpretation of the historical and recent water-quality trends.

A complete record of daily streamflow is required for the analysis of water-quality trends and the estimation of constituent loads. Sites on Antelope, Big Muddy, and Sweetbriar Creeks (site 10, Big Muddy Creek near Almont, N. Dak. [site 18], and Sweetbriar Creek near Judson, N. Dak. [site 21], respectively; fig. 1 and table 1) were operated as seasonal streamgages, where streamflow data were generally only recorded from April through September of each year, requiring an estimation of daily streamflow for the remaining months to use in the various analyses. Streamflow was

Table 1. Selected sites with water-quality data in the Heart River Basin, 1970–2020.

[USGS, U.S. Geological Survey; NDDEQ, North Dakota Department of Environmental Quality; --, no data; N. Dak., North Dakota; SA, streamflow analysis; SS, statistical summary; RT, recent trends; HT, historical trends; L, loads]

Site number (fig. 1)	USGS site number	NDDEQ site number	Site name	Latitude, decimal degrees	Longitude, decimal degrees	Analysis type
1	06344600	--	Green River near New Hradec, N. Dak.	47.02779	−103.0532	SA, SS, RT, HT
2	06343000	--	Heart River near South Heart, N. Dak.	46.86557	−102.9485	SS
3	06342970	--	North Creek near South Heart, N. Dak.	46.89557	−102.9991	SS
4	06342900	--	South Branch Heart R near South Heart, N. Dak.	46.84001	−103.0205	SS
5	06345500	380160	Heart River near Richardton, N. Dak.	46.74556	−102.3083	SA, SS, RT, HT, L
6	06345780	--	Heart River above Lake Tschida near Glen Ullin, N. Dak.	46.65695	−102.0793	SS
7	6346500	--	Heart River Below Heart Butte Dam near Glen Ullin, N. Dak.	46.59723	−101.8018	SS, L
8	--	385584	Antelope Creek	46.48623	−101.858	SS
9	--	380064	Antelope Creek—west of Carson	46.48598	−101.6291	SS
10	06347000	385582	Antelope Creek near Carson, N. Dak.	46.54528	−101.6454	SS, RT, L
11	06347030	553166	Heart River near Carson, N. Dak.	46.55919	−101.556	SS
12	--	385562	Hailstone Creek	46.92348	−101.6381	SS
13	--	385563	Hailstone Creek	46.89171	−101.5927	SS
14	--	385564	Sims Creek	46.77556	−101.4968	SS
15	--	385587	Big Muddy Creek	46.81875	−101.7216	SS
16	--	385588	Wilson Creek	46.81883	−101.6522	SS
17	--	385565	Hailstone Creek	46.71853	−101.4901	SS
18	06347500	385078	Big Muddy Creek Near Almont, N. Dak.	46.69445	−101.4674	SS, L
19	06348000	--	Heart River near Lark, N. Dak.	46.61028	−101.3821	SS
20	06348300	553252	Heart River at Stark Bridge near Judson, N. Dak.	46.70333	−101.2136	SS, L
21	06348500	--	Sweetbriar Creek near Judson, N. Dak.	46.85111	−101.2532	SS, L
22	06349000	380151	Heart River near Mandan, N. Dak.	46.83388	−100.9746	SA, SS, RT, HT, L
23[1]	06346000	--	Lake Tschida Near Glen Ullin, N. Dak.	46.59528	−100.8094	L[1]

[1]Water-quality data from site 23 used with streamflow data from site 7 to estimate loads at site 7.

estimated between the months of October and March using nearby streamgages with recorded data for those months and similar contributing drainage areas. The USGS streamgage on the Cannonball River at Regent, N. Dak (USGS site number 06350000) was used to estimate streamflow at site 10; Spring Creek at Zap, N. Dak. (USGS site number 0634000) was used to estimate streamflow at site 18; and Square Butte Creek below Center, N. Dak. (USGS site number 06342260) was used to estimate streamflow at site 21 (fig. 1). Streamflow from 1950 to 2020 from paired sites was compared using a regression analysis of daily streamflow. The Leaps package in R (Lumley, 2020) was used to evaluate the possible subsets of models, and the coefficient of determination (R^2) was used to evaluate the possible models.

Constituent and Site Selection

All available water-quality data in the Heart River Basin were initially compiled for the period of 1970–2020 from the WQP (National Water Quality Monitoring Council, 2020) to evaluate their use in the various analyses described in this report. The WQP contains water-quality data collected by multiple agencies for the area of interest including data from the U.S. Environmental Protection Agency, the USGS NWIS, and North Dakota Department of Environmental Quality databases. USGS streamflow data associated with water-quality sites were compiled from the USGS NWIS (U.S. Geological Survey, 2020).

Constituents were selected based on their relevance to salinity and nutrient dynamics in the Heart River Basin. For evaluating salinity, TDS, dissolved ions (sulfate, sodium, chloride, potassium, calcium, magnesium, bicarbonate), silica, sodium adsorption ratio (SAR), and physical properties (specific conductance and pH) were selected. For nutrient dynamics, ammonia, nitrate plus nitrite, filtered (dissolved) phosphorus and unfiltered (total) phosphorus were selected (table 2).

Sites were initially selected based on available data for the selected water-quality constituents. Sites that had fewer than 10 samples collected between 1970 and 2020 were removed. Some sites were colocated because data were collected by different agencies or groups at the same location and had different site identification numbers depending on the agency. Where appropriate, the data from colocated sites were combined. Six sites in the basin had colocated sites where data were combined (site 5; site 10; Heart River near Carson, N. Dak. [site 11]; site 18; Heart River at Stark Bridge near Judson, N. Dak. [site 20]; and site 22; table 1).

Many of the selected constituents had censored values or values that represent concentrations too low to be accurately quantified (Oblinger Childress and others, 1999). The censoring level can change through time and among laboratories because of changes in analytical methods, sensitivity of laboratory equipment, or dilutions during laboratory analysis. Censored values are an important consideration in statistical analysis, especially for trends and loads analysis (Helsel and others, 2020). For comparability of data and consistent statistical analysis, constituents with multiple censoring levels were recensored to a common value, and the newly censored dataset was used for all analyses. When choosing the common censoring level, the censoring level that was most consistently observed, or most recently observed, and was considered the most likely to represent an actual measured concentration was selected. When values were censored at a value greater than the common censoring level, they were left unchanged because R–QWTREND (Vecchia and Nustad, 2020) and R–LOADEST (Runkel and others, 2004; Runkel, 2013) can handle multiple censoring levels. The remaining censored values were recoded to the common censoring level, and uncensored values less than the common censoring level were recoded as censored values at the common censoring level. For most constituents, a higher censoring level was chosen because the lower censor levels were in the earlier period of the data and likely did not represent an actual measured concentration. For example, chloride data had censoring levels ranging from 0.1 to 30 milligrams per liter (mg/L), but 3 mg/L was the most frequently and recently observed censoring level. The laboratory analysis diluted the samples, causing the samples to have a censored level greater than 3 mg/L, and therefore a higher censored level was not used to recensor the data (table 2).

Selected constituents and sites varied depending on the analysis because of different data requirements for the various models and analyses. R–QWTREND was used for trend analysis, which requires at least 60 water-quality samples distributed among seasons, a complete daily streamflow record, and preferably no more than 25 percent of the dataset containing censored values (Vecchia and Nustad, 2020). Two main-stem sites (sites 1 and 5; fig. 1) and two tributary sites (sites 10 and 22; fig. 1 and table 1) had sufficient TDS, sulfate, sodium, chloride, potassium, calcium, magnesium, and SAR data for trend analysis related to salinity. Two trend periods were evaluated based on data availability: a recent period (1999–2019) and a historical period (1974–2019). All four sites were used for the recent period and only sites 1, 5, and 22 had sufficient data for the historical period. For example, site 2 appears to have met the requirements for water-quality data availability, but a complete streamflow record was not available, so site 2 was not selected for trend analysis (fig. 1 and table 1). Only two main-stem sites (sites 5 and 22) had sufficient data for trend analysis of nitrate plus nitrite and total phosphorus (fig. 1 and table 1). Based on data availability, nitrate plus nitrite and total phosphorus could only be analyzed for the recent period (1999–2019).

R–LOADEST (Runkel and others, 2004; Runkel, 2013) was used for computing loads and yields for a constituent mass balance in the lower Heart River Basin below Lake Tschida. R–LOADEST has different data requirements than R–QWTREND and a different period (2013–20) was used for the mass balance; therefore, different sites were selected for analysis. Like R–QWTREND, R–LOADEST requires a complete daily streamflow record, so site selection was dependent on availability of water-quality data and streamflow data. Sites

Table 2. Selected water-quality constituents for sites in the Heart River Basin, 1970–2020.

[WQP, Water Quality Portal (National Water Quality Monitoring Council, 2020); mg/L, milligram per liter; --, no data; SO_4, sulfate; SiO_2, silicon dioxide; Na, sodium; Ca, calcium; Mg, magnesium; N, nitrogen; P, phosphorus, µS/cm, microsiemen per centimeter at 25 degrees Celsius; µohms/cm, microohm per centimeter]

Constituent name	Units	WQP descriptions	Reporting levels in raw data	Recensored reporting level used
		Major ions		
Total dissolved solids	mg/L	Total dissolved solids, dissolved, mg/L	--	--
		Total dissolved solids, total, mg/L		
Sulfate	mg/L	Sulfate, dissolved, mg/L	--	--
		Sulfate, total, mg/L		
		Sulfate as SO_4, dissolved, mg/L		
Sodium	mg/L	Sodium, dissolved, mg/L	--	--
		Sodium total recoverable, mg/L		
Chloride	mg/L	Chloride, dissolved, mg/L	0.1, 3, 10, 15, 30	3
Potassium	mg/L	Potassium, dissolved, mg/L	--	--
		Potassium, total recoverable, mg/L		
Calcium	mg/L	Calcium, dissolved, mg/L	--	--
		Calcium, total recoverable, mg/L		
Magnesium	mg/L	Magnesium, dissolved, mg/L	--	--
Bicarbonate	mg/L	Bicarbonate, total, mg/L	--	--
		Bicarbonate, dissolved, mg/L		
Silica	mg/L	Silica, water, filtered, mg/L as SiO_2	--	--
		Silica, water, unfiltered, mg/L as SiO_2		
		Calculated constituents		
Sodium adsorption ratio	unitless	Sodium adsorption ratio [(Na)/(square root of 1/2 Ca+Mg)], total recoverable	--	--
		Sodium adsorption ratio [(Na)/(square root of 1/2 Ca+Mg)]	--	--
		Nutrients		
Total ammonia	mg/L as N	Ammonia and ammonium, total, mg/L as N	0.01, 0.03, 0.17	0.03
		Ammonia-nitrogen, supernate, mg/L	--	--
		Ammonia-nitrogen as N, supernate, mg/L	--	--

Table 2. Selected water-quality constituents for sites in the Heart River Basin, 1970–2020.—Continued

[WQP, Water Quality Portal (National Water Quality Monitoring Council, 2020); mg/L, milligram per liter; --, no data; SO_4, sulfate; SiO_2, silicon dioxide; Na, sodium; Ca, calcium; Mg, magnesium; N, nitrogen; P, phosphorus, µS/cm, microsiemen per centimeter at 25 degrees Celsius; µohms/cm, microohm per centimeter]

Constituent name	Units	WQP descriptions	Reporting levels in raw data	Recensored reporting level used
		Nutrients—Continued		
Nitrate plus nitrite	mg/L as N	Inorganic nitrogen (nitrate and nitrite), dissolved, mg/L	0.005, 0.01, 0.02, 0.03, 0.04, 0.05, 0.08, 0.09,0.1	0.03
		Inorganic nitrogen (nitrate and nitrite), dissolved, mg/L as N		
		Inorganic nitrogen (nitrate and nitrite), supernate, mg/L		
		Inorganic nitrogen (nitrate and nitrite), total, mg/L		
		Inorganic nitrogen (nitrate and nitrite), total, mg/L as N		
		Inorganic nitrogen (nitrate and nitrite) as N, dissolved, mg/L		
		Inorganic nitrogen (nitrate and nitrite) as N, supernate, mg/L		
		Inorganic nitrogen (nitrate and nitrite) as N, total, mg/L		
		Nitrate, dissolved, mg/L as N		
		Nitrate, total, mg/L as N		
Dissolved phosphorus	mg/L as P	Phosphorus, dissolved, mg/L as P	0.004, 0.01, 0.02	0.02
		Phosphate-phosphorus, dissolved, mg/L		
Total phosphorus	mg/L as P	Phosphorus, total, mg/L as P	0.004, 0.01, 0.018, 0.02, 0.031	0.02
		Phosphate-phosphorus as P, total, mg/L		
		Phosphate-phosphorus, total, mg/L		
		Physical measurements		
Specific conductance	µS/cm	Specific conductance, µS/cm	--	--
		Specific conductance, µmho/cm		
		Specific conductance, µS/cm		
		Specific conductance		
		Conductivity, µS/cm		
		Conductivity, µmho/cm		
pH	Standard units	pH	--	--

selected for load estimation and mass balance included site 5, Heart River above Lake Tschida near Glen Ullin, N. Dak. [site 7], and site 20 on the main-stem Heart River and sites 10, 18, and 21 on Antelope, Big Muddy, and Sweetbriar Creeks, respectively, that are tributaries to the Heart River (fig. 1 and table 1). Loads were estimated for TDS, sulfate, sodium, chloride, and total phosphorus at the selected sites. High variability and prevalence of censored data prevented the estimation of loads for nitrate plus nitrite.

PHREEQC was used for inverse geochemical modeling on two selected reaches of the Heart River based on locations of sites with available data. One reach (model zone 1) included site 5 and Heart River above Lake Tschida near Glen Ullin, N. Dak. [site 6] and another reach (model zone 2) included sites 20, 21, and 22 (fig. 1 and table 1). Constituents selected for use in the PHREEQC model included sulfate, sodium, chloride, potassium, calcium, magnesium, bicarbonate, silica, pH, and water temperature to model geochemical reactions. Although inclusion of iron and aluminum data would have resulted in more accurate geochemical models, too few data were available for those constituents at the selected sites.

Descriptive Statistics

Descriptive statistics were computed for all sites in the Heart River Basin with at least 10 samples collected between 1970 and 2020 to describe the spatial variability of concentrations in the basin. Although 10 or more samples were collected at the sites, the number of values for specific constituents varied by site because samples were collected by various agencies or groups for different purposes. Statistics included minimum, maximum, and the 10th, 25th, 50th (median), 75th, and 90th percentiles of values for individual constituents at each site. Median concentrations for selected constituents were plotted on a map of the Heart River Basin to show spatial patterns in concentration across the basin.

Trend Analysis

R–QWTREND, a publicly available software package developed by USGS for analyzing trends in stream water quality, was used to evaluate water-quality trends (Vecchia and Nustad, 2020). R–QWTREND is a parametric time-series model for streamflow and concentration data (Vecchia and Nustad, 2020). The theory and parameter estimation for the time-series model are described in detail in several publications (Vecchia, 2003, 2005; Vecchia and Nustad, 2020). R–QWTREND can run the time-series model, determine model fit, verify trend models, and produce an output for interpreting and evaluating the results (Vecchia and Nustad, 2020). One of the model's variables, *FRVAR,* was designed to capture as much natural flow-related variability in logarithmically transformed concentrations as possible. *FRVAR* is a function of variables called flow anomalies that depend on concurrent and antecedent streamflow (Vecchia and Nustad, 2020). Flow anomalies address the relation between a constituent concentration and concurrent and lagged streamflow at annual, seasonal, and daily time scales. In addition, the periodic functions of sine and cosine are used to capture the seasonal variation in concentration that is not captured by the flow anomalies (Vecchia and Nustad, 2020). Because of the variable hydroclimate in the basin, characterizing flow-related variability in concentrations at multiple time scales is important because concentrations of water-quality constituents interact with the streamflow in complex ways that cannot be captured using a simple regression between concentration and concurrent streamflow. By accounting for the natural flow-related variability, the ability to detect trends in concentration that are independent of streamflow and climate variability is greatly increased (Vecchia, 2003).

The trends detected by R–QWTREND indicate long-term (10 or more years) changes in annual "flow-averaged" geometric mean concentrations (FAGMCs) that are unrelated to streamflow changes from year to year (Vecchia and Nustad, 2020). To determine the significance of the trend results, the generalized likelihood ratio test statistic was used and is described in Vecchia and Nustad (2020). Three levels of significance were used for this study: a probability (p) value of less than or equal to 0.01 was considered significant; a p-value between 0.01 and 0.05 was considered mildly significant; and a p-value greater than 0.05 was considered nonsignificant. A small p-value indicates that a real trend was detected by R–QWTREND. For example, for a trend with a p-value less than 0.05, the chance that this trend could have occurred given the null (no trend) model that the flow-adjusted concentrations were trend free would be less than 5 percent. A nonsignificant trend indicates that a trend was inconclusive given the available data (Helsel and others, 2020), which does not mean the data have no trend, but that the data may have a trend that is too small to be detected in relation to the natural variability of the data.

Censored values, or values less than the method detection limit for which an exact value is not known (Oblinger Childress and others, 1999), need to be considered during trend analysis (Helsel and other, 2020). R–QWTREND handles censored values and will estimate a value, but it is recommended that no more than 25 percent of the data set be censored values. For the current (2022) study, to include as many sites and constituents as possible in the analysis, sites with constituents having as much as 55 percent censored data were analyzed for trends. Results for sites and constituents analyzed with more censored data than recommended should be interpreted with caution. Chloride, nitrate plus nitrite, and total phosphorus all had censored values with multiple censoring levels and were recensored to a common censoring level (table 2). After recensoring, some sites had more than 50-percent data censored and were not analyzed. Censoring levels for chloride ranged from 0.1 to 30 mg/L (table 2). A higher censoring level of 3 mg/L was used to recensor chloride data with the lower censoring level of 0.1 mg/L to a common censoring level of 3 mg/L. Values with censoring limits higher

than 3 mg/L were left as is for R–QWTREND. After recensoring the chloride data, site 10 had more than 50 percent censored data, and therefore chloride trends were not analyzed for this site. For nitrate plus nitrite, censoring levels ranged from 0.005 to 0.1 mg/L (table 2). Nitrate plus nitrite concentrations were recensored to 0.03 mg/L for trend analysis. After recensoring the nitrate plus nitrite data, site 22 had about 50 percent of the data censored and site 5 had about 55 percent of the data censored, but trends were analyzed because of the lack of sites with available data for nitrate plus nitrite trend analysis. For total phosphorus, censoring levels ranged from 0.004 to 0.031 mg/L. Total phosphorus concentrations were recensored to 0.02 mg/L for trend analysis. After recensoring the total phosphorus data, sites 5 and 22 had less than 50 percent of the data censored, but trends were analyzed because of the lack of sites with available data for total phosphorus trend analysis.

Two trend periods were evaluated in this report: a historical period (1974–2019) and a recent period (1999–2019). Streamflow and water-quality data from 1995 to 2020 were used for the recent period and data from 1970 to 2020 were used for the historical period. Data were available for evaluating historical trends at sites 1, 5, and 22 and for recent trends at sites 1, 5, 10, and 22. Historical and recent trends were analyzed for selected constituents including TDS, sodium, sulfate, chloride, potassium, calcium, magnesium, and SAR. Only recent trends were analyzed for nitrate plus nitrite and total phosphorus owing to data availability.

Geochemical Modeling

Inverse geochemical modeling was performed using PHREEQC to simulate geochemical reactions related to increasing salinity (for example, dissolution of calcite [$CaCO_3$] or gypsum [$CaSO_4 \cdot 2H_2O$]; Parkhurst, 1995; Parkhurst and Appelo, 1999). PHREEQC inverse modeling is a mole-balance formulation that solves a set of linear equalities that account for the changes in the number of moles for each ion based on the expected minerals present in the system (Parkhurst, 1995; Parkhurst and Appelo, 1999, 2013). The calculations of the mole-balance formulas are based on the stoichiometry of the potential chemical reactions that have been identified as reacting along the selected flow path (Parkhurst and Appelo, 1999). PHREEQC uses several equations and inequality constraints that allow for uncertainty in the data to calculate the mole transfers (Parkhurst and Appelo, 1999). Specific equations and inequalities used within the PHREEQC program are detailed in several publications (Parkhurst, 1995; Parkhurst and Appelo, 1999). The inverse modeling approach determined the chemical reactions that had occurred in the basin by working backwards from current conditions to historical conditions. Parkhurst and Appelo (1999) contains additional information regarding the PHREEQC inverse model.

Uncertainty terms were included in the model for each aqueous solution and could also be used for each element in the suite of aqueous solutions. These uncertainty terms were related to the charge balance of a solution and adjust the analytical data by the defined percentage to create a charge balance or were related to the analytical uncertainty of a particular constituent (Parkhurst and Appelo, 1999). For example, if an aqueous solution had a charge balance of plus or minus 20 percent, the uncertainty term for this solution cannot be less than 0.2, meaning the analytical data are adjusted within 20 percent for each constituent to reach a suitable charge balance. These uncertainty terms manifest in the model results as residuals. The PHREEQC inverse model produced a residual value that indicated how many parameters and how much the model adjusted the input concentrations to create the balance (Parkhurst and Appelo, 1999). For example, a lower sum of residuals indicated that the data were adjusted less than a model with a higher sum of residuals.

PHREEQC requires a thermodynamic and mineral database for comparison to chemical reactions. The phreeqc.dat database (Parkhurst and Appelo, 1999) was used for the Heart River Basin. Many of the minerals previously identified to be present in the Heart River Basin were already included in the phreeqc.dat database, but the minerals of mirabilite, thenardite, konyaite, biotite, and sodium montmorillonite (Na-montmorillonite) were added (table 3). Inverse modeling only used the stoichiometry of the minerals dissolution reaction, but thermodynamic calculations were performed on thenardite and mirabilite to obtain accurate saturation index (SI) values for these phases. Balanced dissolution reactions were required for all the added minerals.

A list of minerals used for the models were identified from natural sources such as soil and geologic formations, and from anthropogenic sources such as fertilizers used in agricultural practices (table 3). Although cation exchange processes were likely occurring owing to the high cation exchange capacity of clays in the local geology (Langmuir, 1997), these processes were not simulated in the PHREEQC model because the models would not converge when cation exchange processes were included. Minerals present in the Ludlow, Cannonball, and the Bullion Creek Formations, located in the lower Heart River Basin, were identified through previous mineralogical and chemical analyses (Fenner, 1974; Jacob, 1975; Brekke, 1979). Previous soil chemistry studies outlined the possible minerals that could be present in soils across North Dakota (Keller and others, 1986a). A necessary mineral input was to assume mineral precipitation or dissolution, and this assumption was made based on other geochemistry information at each site. To determine whether individual minerals were most likely precipitating or dissolving at a site, a dissolution plot was used in which paired constituent concentrations in millimole per liter were plotted against one another and compared against a dissolution line. The dissolution line was based on the stoichiometry of the dissolution reaction for a given mineral, which is the ideal dissolution of the given mineral. For example, in the dissolution of calcite ($CaCO_3 + 2H^+ = Ca^{2+} + 2HCO_3^-$), the ratio of moles [$Ca^{2+}$] to [$HCO_3^-$] is 1:2. The ratio of 1:2 represents the expected slope of 0.5 for the dissolution of calcite. If dissolution is occurring, when

Table 3. Minerals included in the PHREEQC inverse modeling for the selected reaches in the Heart River Basin.

[Na, sodium; S, sulfur; O, oxygen; H, hydrogen; Ca, calcium; K, potassium; Cl, chloride; Mg, magnesium; C, carbon; Si, silicon; Al, aluminum; Fe, iron; F, fluorine]

Mineral	Chemical equation	Source	Available in the phreeqc.dat mineral database?	Reference
Mirabilite	$Na_2SO_4 \cdot 10H_2O$	Soil	No	Keller and others (1986a)
Thenardite	Na_2SO_4	Soil	No	Keller and others (1986a)
Konyaite	$Na_2Mg(SO_4)_2 \cdot 5H_2O$	Soil	No	Keller and others (1986a)
Gypsum	$CaSO_4 \cdot 2H_2O$	Anthropogenic/geology	Yes	Brekke (1979); Fenner (1974); Keller and others (1986a)
Sylvite	KCl	Anthropogenic	Yes	Granato and others (2015)
Calcite	$CaCO_3$	Geology	Yes	Brekke (1979); Fenner (1974)
Dolomite	$CaMg(CO_3)_2$	Geology	Yes	Brekke (1979); Fenner (1974); Jacob (1975)
Quartz	SiO_2	Geology	Yes	Brekke (1979); Fenner (1974); Jacob (1975)
K-feldspar	$KAlSi_3O_8$	Geology	Yes	Brekke (1979)
Biotite	$K(Mg,Fe)_3(AlSi_3O_{10})(F,OH)_2$	Geology	No	Fenner (1974)
Na-Montmorillonite	$(Na)_{0.33}(Al,Mg)_2(Si_4O_{10})(OH)_2 \cdot nH_2O$	Geology/soil	No	Brekke (1979)
Ca-Montmorillonite	$(Ca)_{0.33}(Al,Mg)_2(Si_4O_{10})(OH)_2 \cdot nH_2O$	Geology/soil	Yes	Fenner (1974)
Illite	$(Al,Mg,Fe)_2(Si,Al)_4O_{10}[(OH)_2,(H_2O)]$	Geology/soil	Yes	Brekke (1979); Fenner (1974)

bicarbonate (HCO_3^-) concentrations in millimole per liter are plotted against calcium (Ca^{2+}) concentrations in millimole per liter, the points should fall along the dissolution line. Also, SI values were calculated using PHREEQC to test whether the mineral would be dissolving or precipitating for a given mineral in each model. SI values greater than zero indicated precipitation because the solution was supersaturated with respect to that mineral and SI values less than zero indicated dissolution owing to the solution being undersaturated with respect to the given mineral.

Two model zones were delineated to evaluate geochemical changes in salinity in the Heart River Basin. Each model zone was delineated along bedrock geology to understand the control geology has on geochemical changes in salinity. Two model periods for each model zone were selected based on the trend analysis: period 1 included 1974–99, and period 2 included 1999–2019. Model zone 1 was delineated as the reach between site 5 and site 6 upstream from Lake Tschida, and model zone 2 was delineated for the reach between site 20 and site 22 that includes Sweetbriar Creek (site 21; table 1). Model zone 1 was the farthest upstream reach and is underlain by the Bullion Creek Formation (fig. 2*A*), whereas model zone 2 is underlain by the Ludlow and Cannonball Formations (fig. 2*A*).

For each model zone and model period, a single sample from each site that was considered most representative of the water-quality changes from the beginning to the ending of the model period was needed to simulate the geochemistry along the reach. Several considerations were made when selecting a representative sample for each site and model period. The most important consideration for selecting a representative sample was the suite of constituents collected for a given sample. For a sample to be included it needed to have results for sulfate, sodium, calcium, magnesium, chloride, potassium, and bicarbonate. Ideally, each sample would also have results for dissolved silica. Another consideration was selecting two samples that closely resemble the results from the trend analysis. Trend analysis results from sites 5 and 22 were used to select samples for model zones 1 and 2, respectively, that showed similar trends for each constituent used in trend analysis. For example, if the trend results at site 22 showed a 45-percent increase in sulfate and a 46-percent increase in chloride between 1999 and 2019, selected samples from sites 21 and 22 might have a 60-percent increase in sulfate and a 50-percent increase in chloride. Although the percentages of each individual constituent did not exactly match the trend result, the sample was overall considered to be representative of the trends observed in the basin. To eliminate seasonal effects, samples for the two sites were selected from the same season. The model periods determined the range of samples from which to select, but the selected samples did not need to come from the specified years at the beginning and end of the model periods but needed to have changes similar to the trend analysis results. Groundwater water-quality data were not considered for the PHREEQC modeling because there were not enough data for the aquifers of interest. This selection method limited the bias in the sample selection process and did not induce an artificial trend when providing representative samples.

Results of the PHREEQC inverse modeling produces multiple models for each model zone and period. Because PHREEQC inverse modeling produces multiple models, a criterion was needed to determine which models were reasonable and unreasonable. Comparison of mole transfers among models was used to ensure that the model was converging on a reliable solution. Models with mole transfer results that were one or more order of magnitude greater than the others were deemed unreasonable. These unreasonable models fit the solution but do not provide accurate information about the model zone and period.

Load Estimation and Mass Balance Analysis

To evaluate what portions of the basin contribute to the mass of selected constituents in the Heart River downstream from Lake Tschida (fig. 1), a mass-balance was computed from estimated loads (mass per time) at selected sites. Constituent load (L) is a function of the volumetric rate of water passing a point in the stream, known as streamflow (Q), and the constituent concentration within the water (C). Constituent yield is a function of constituent load and the drainage area contributing to flow at the site.

The program R–LOADEST (Runkel and others, 2004; Runkel, 2013) was used to estimate constituent loads using regression methods. These methods use natural logarithm (ln)-transformed relations between Q and C to estimate daily C (or L) for a particular constituent at a site (Cohn and others, 1989; Cohn and others, 1992; Cohn, 1995). The regression method can account for non-normal data distributions, seasonal and long-term cycles, censored data, biases associated with using logarithmic transformations, and serial correlations of the residuals (Cohn, 1995). Regression methods use discrete water-quality samples often collected during several years and a daily streamflow hydrograph. A regression model for estimating constituent load can be expressed as the following equation:

$$\ln(L) = \beta_0 + \beta_1 \ln(Q_d) + \beta_2 T + \beta_3 \sin(2\pi T) + \beta_4 \cos(2\pi T) + E \quad (1)$$

where,

ln ( ) represents the natural logarithm function;

L is the constituent load;

β_0, β_1, β_2, β_3, and β_4 are the coefficients of the model;

Q_d is the daily mean streamflow, in cubic feet per second;

T is decimal time, in years; and

E is the model error.

In this model, relations between streamflow and load are identified by the β_1 coefficient, temporal trends are identified by β_2, and seasonal effects are identified by β_3 and β_4. Transforming the results of the model from logarithmic space to linear space was accomplished using an adjusted maximum likelihood estimator (AMLE) (Cohn and others, 1992). The AMLE method can also handle censored values. For this application, the variables included in the load model (eq. 1) were selected by using various diagnostic statistics provided by R–LOADEST to evaluate the significance of the variables to include in the model for each site and constituent combination. The explanatory variables were considered statistically significant if the *p*-value was less than 0.05 for the *t*-statistic. In using the AMLE method, normal distribution (normality) of the dataset is assumed. The validity of the normality assumption for the residuals was examined using the Turnbull-Weiss likelihood ratio normality statistic (Turnbull and Weiss, 1978). If the *p*-value from the Turnbull-Weiss statistic was less than 0.05, the residual plots were examined for homoscedasticity (equal statistical variances) and normality. There were some cases where the *p*-value was less than 0.05, but the AMLE method was used because the dataset contained censored data. As a measure of how much variability in the dependent variable is explained by the independent variable and the R–LOADEST regression equation, R^2 values were computed and expressed as a percentage. The R^2 value is a number, 0–1, that when multiplied by 100 is interpreted as the percentage of the variability in the dependent variable explained by the independent variable(s) and the regression equation (Helsel and others, 2020). Generally, a larger R^2 value indicates a better relation. For example, an R^2 of 100 percent indicates that all the variability in the dependent variable is explained by the independent variable(s). However, a large R^2 value does not guarantee the relation is useful (Neter and others, 1996). For example, if estimates require extrapolation outside of the observed independent variables, the estimates may not be accurate. Unless constituent concentrations were highly variable, R^2 values were expected to be large for the R–LOADEST models because the dependent variable in the R–LOADEST models (constituent load) is a function of one of the independent variables (streamflow).

As a measure of uncertainty in the load estimates, the standard error of prediction (SEP) was provided in R–LOADEST output (Runkel and others, 2004). To compare uncertainty among sites with large differences in loads, the SEP was expressed as a percentage of the total estimated load during the 7-year period for each site and constituent (table 4).

Loads were estimated for selected dissolved ion constituents related to salinity concerns including TDS, sulfate, sodium, and chloride. Loads also were estimated for total phosphorus to evaluate the mass balance of nutrients. High variability and prevalence of censored data prevented the estimation of loads for nitrate plus nitrite. The selected load models, calibration periods, R^2, and SEP values for each site and constituent are given in table 4.

Loads were computed for sites selected by location and data availability. Site 5 was selected to represent loads in the Heart River Basin upstream from Lake Tschida. For the mass balance analysis, loads were computed for sites 7, 10, 18, 20, 21, and 22. Site 7, located just downstream from Lake Tschida, represents the upper end of the reach for mass balance analysis. Site 22 represents the lower end of the reach for analysis. Sites 10, 18, and 21 represent tributary inputs to the Heart River (fig. 4). Loads for site 20 were computed to evaluate the change in constituent mass in the reach of the Heart River between tributaries for TDS, sulfate, sodium, and chloride. Loads were not computed at site 20 for total phosphorus because no data were available for this constituent.

To avoid long-term changes in streamflow, a short period of 2013–20 was used for developing load models for the selected constituents and sites, and estimation of loads was based on concentration data availability. Data from 2004 to 2020 were used for developing load models for site 7 because there were fewer sample data compared to other sites, although loads were only computed for the 2013–20 period. Constituent concentration data were not collected at site 7, so concentration data collected in Lake Tschida (fig. 1) were used with outflow discharge data from Heart Butte Dam (not shown) to build the load models for the site. Water-quality samples at Lake Tschida near Glen Ullin, N. Dak. [site 23] were collected near the outlet structure in the lake at the midpoint of the total reservoir depth. It was assumed that the water quality near the outlet structure in Lake Tschida would be similar to the outflow location at site 7, although no data were available to evaluate the comparison. For total phosphorus, data from 2004 to 2020 were also used for building the load models for all the selected sites because of the high number of censored data. Estimated loads were only computed for the period of 2013–20.

Monthly, annual, and total loads were estimated for selected sites and constituents for the period of 2013–20. Yields in tons per year per square mile were also calculated for each site by dividing the annual loads by the drainage area (in square miles) contributing to flow at the sampling site for each constituent. Total phosphorus yields were computed as pounds per year per square mile.

A simplistic mass balance was computed for the lower Heart River Basin using the reach on the Heart River between site 7 and site 22 (fig. 4) and the total load for the period of 2013–20. The total load at site 22 was assumed to be a sum of the load from sites 7, 10, 18, and 21, and any intervening flow. Intervening flow includes any input of flow not accounted for by measured tributary inflow and could include groundwater inflow, irrigation return flow, local runoff, and smaller unmeasured tributaries. Not all processes that can affect the mass of constituents in the Heart River were accounted for in the mass balance analysis. Although most of the dissolved ions are generally conservative (the mass of a constituent at an upstream site will be transported to a downstream site with minimal loss of mass), nutrients generally are not considered to be conservative because many processes can affect nutrients such as biological activity and atmospheric exchange (Hem, 1985).

Table 4. Load model and characteristics used to determine loads at the selected sites in the Heart River Basin.

[Q, streamflow; ln(), natural logarithm function; T, decimal time; π, pi]

Site number (fig. 1)	Site description	Number of values used in calibration (number of censored values)	Model calibration period	Load model	Coefficient of determination (percent)	Standard error of prediction, as a percent of annual load during 2013–20
			Total dissolved solids			
5	Heart River near Richardton	64 (0)	2013–20	12.5+0.86lnQ−0.032T	96.0	5.4
7	Heart River below Heart Butte Dam	49 (0)	2004–20	7.55+0.99lnQ	99.3	8.7
10	Antelope Creek near Carson	112 (0)	2013–20	8.73+1.03lnQ−0.032T	97.8	6.1
18	Big Muddy Creek	38 (0)	2013–20	8.3+0.99lnQ	99.1	8.3
20	Heart River at Stark Bridge near Judson	15 (0)	2013–20	12.4+0.89lnQ	95.4	10.0
21	Sweetbriar Creek	38 (0)	2013–20	7.57+0.95lnQ−0.04(2π)sin−0.18(2π)cos	99.0	8.8
22	Heart River at Mandan	76 (0)	2013–20	13.1+0.86lnQ-0.031T	96.1	3.7
			Sulfate			
5	Heart River near Richardton	64 (0)	2013–20	12+0.86lnQ−0.044T	93.0	7.1
7	Heart River below Heart Butte Dam	50 (0)	2004–20	6.83+0.99lnQ	98.9	9.9
10	Antelope Creek near Carson	112 (0)	2013–20	7.91+1.06lnQ−0.051T	96.6	7.9
18	Big Muddy Creek	38 (0)	2013–20	7.55+1.01lnQ	98.5	11.3
20	Heart River at Stark Bridge near Judson	15 (0)	2013–20	11.7+0.91lnQ	92.5	13.8
21	Sweetbriar Creek	38 (0)	2013–20	7.0+0.97lnQ	98.6	9.3
22	Heart River at Mandan	76 (0)	2013–20	12.6+0.87lnQ−0.054T	93.1	5.2
			Sodium			
5	Heart River near Richardton	64 (0)	2013–20	10.9+0.81lnQ−0.040T	94.3	5.7
7	Heart River below Heart Butte Dam	50 (0)	2004–20	5.93+0.98lnQ	99.2	9.2
10	Antelope Creek near Carson	112 (0)	2013–20	6.78+1.04lnQ	97.1	6.1
18	Big Muddy Creek	38 (0)	2013–20	6.88+0.97lnQ	99.2	7.8
20	Heart River at Stark Bridge near Judson	15 (0)	2013–20	10.8+0.84lnQ	93.8	10.7
21	Sweetbriar Creek	38 (0)	2013–20	5.934+0.94lnQ−0.10(2π)sin−0.22(2π)cos	99.1	8.8
22	Heart River at Mandan	76 (0)	2013–20	11.6+0.81lnQ−0.042T	94.0	4.2
			Chloride			
5	Heart River near Richardton	64 (0)	2013–20	8.57+0.75lnQ	91.1	5.8
7	Heart River below Heart Butte Dam	50 (0)	2004–20	3.25+0.98lnQ	99.2	7.8
10	Antelope Creek near Carson	112 (0)	2013–20	4.4+1.01lnQ−0.073T	98.5	4.6

Table 4. Load model and characteristics used to determine loads at the selected sites in the Heart River Basin.—Continued

[Q, streamflow; ln(), natural logarithm function; T, decimal time; π, pi]

Site number (fig. 1)	Site description	Number of values used in calibration (number of censored values)	Model calibration period	Load model	Coefficient of determination (percent)	Standard error of prediction, as a percent of annual load during 2013–20
			Chloride—Continued			
18	Big Muddy Creek	38 (0)	2013–20	3.35+0.98lnQ	97.8	13.3
20	Heart River at Stark Bridge near Judson	15 (0)	2013–20	8.15+0.88lnQ	95.7	9.6
21	Sweetbriar Creek	38 (0)	2013–20	3.07+0.97lnQ	99.5	5.8
22	Heart River at Mandan	76 (0)	2013–20	8.91+0.84lnQ	96.0	3.4
			Total phosphorus			
5	Heart River near Richardton	64 (5)	2013–20	2.9+1.5lnQ	94.0	20
7	Heart River below Heart Butte Dam	18 (0)	2004–20	−2.5+1.03lnQ	98.5	19
10	Antelope Creek near Carson	229 (84)	2013–20	−2.67+1.47lnQ−0.055T	91.2	19
18	Big Muddy Creek	150 (0)	2013–20	−1.75+1.16lnQ+0.047(2π)sin−0.004(2π)cos	99.7	10
21	Sweetbriar Creek	31 (1)	2013–20	−2.4+1.13lnQ	96.2	31
22	Heart River at Mandan	64 (26)	2013–20	2.62+1.8lnQ	90.7	23

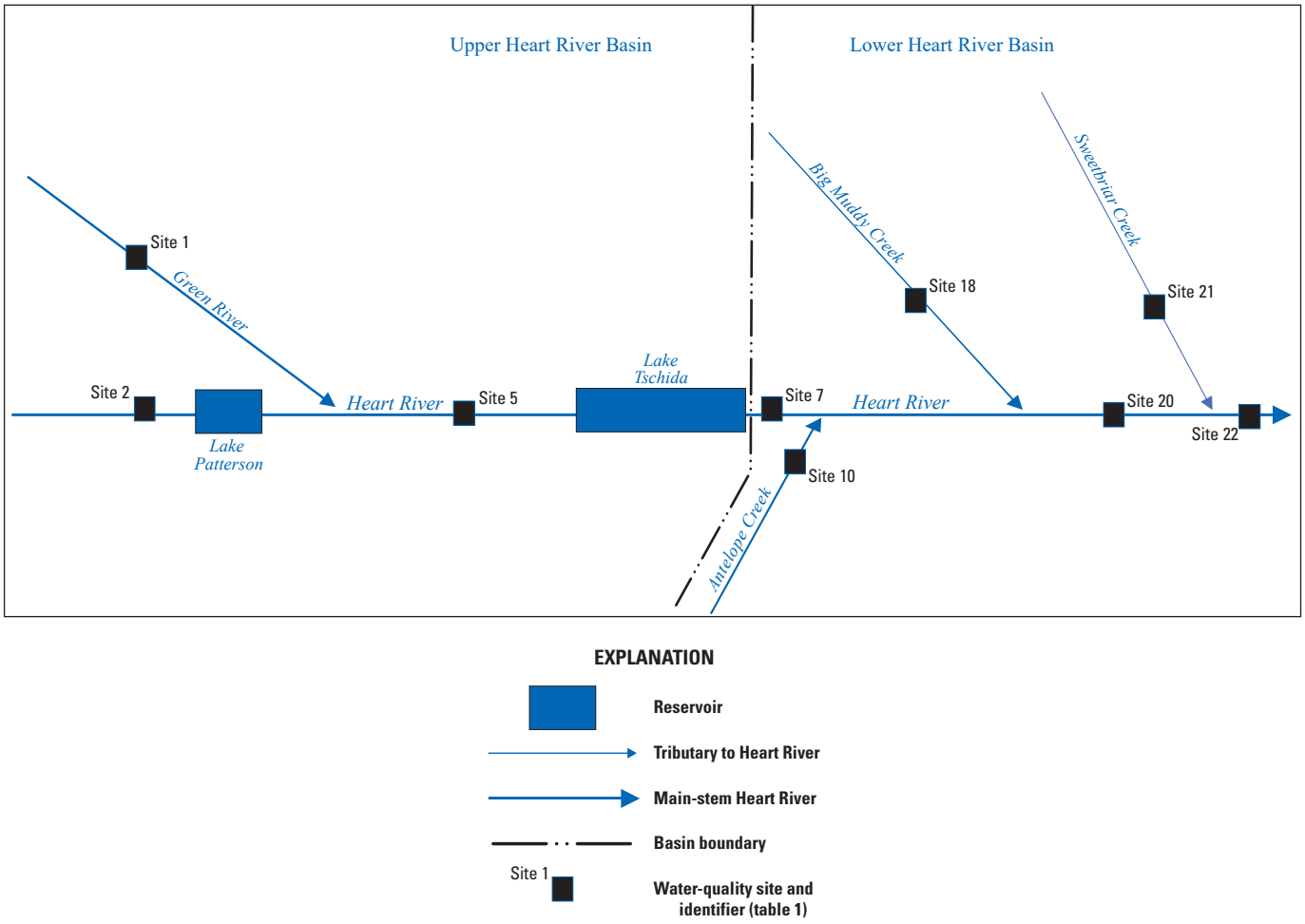

Figure 4. Schematic of sites used for mass balance analysis in the lower Heart River Basin.

Streamflow Characteristics

A shift from a dry to wet climatic period in the late 1980s to early 1990s has been documented in some North Dakota basins, including the Heart River Basin, which has resulted in increasing streamflow. The hydroclimatic pattern in North Dakota is characterized by highly variable precipitation from year to year resulting in highly variable streamflow (Vecchia, 2003; Kolars and others, 2015; Ryberg and others, 2016). Studies in North Dakota basins near the Heart River Basin have shown that precipitation alternates between wet and dry climatic periods, with the wet or dry climatic period lasting for decades and then abruptly shifting from one type of climatic period to the other. These studies identified a shift from a dry to a wet climatic period in the 1980s, which resulted in an abrupt increase in streamflow in the early 1990s, and the wet climatic period has persisted to the present (2022) (Vecchia, 2003, 2008; Kolars and others, 2015; Ryberg and others, 2016). A shift from a dry to a wet climatic period during the late 1980s into the early 1990s has also been documented for the Heart River Basin (Williams-Sether, 1999). Changes in streamflow characteristics were investigated at sites 1, 5, and 22 from 1970 to 2020 using EGRET (Hirsch and De Cicco, 2015). Any changes in streamflow were likely not attributed to the installation of the dams because the Dickinson Dam and Heart Butte Dam were in operation prior to 1970 (Linenberger, 1996; Simonds, 1996).

Visual observation of streamflow trends at sites 1, 5, and 22 (figs. 5–7, respectively) indicated decreasing streamflow for maximum daily, mean daily, and 7-day minimum flows from 1970 until the late 1990s followed by increasing flow through 2020. No formal significance value was calculated for these trends, so interpretations should be made with caution. Except for site 22 (fig. 7), the annual maximum daily streamflow, the annual mean daily streamflow, and the 7-day minimum streamflow for all sites demonstrated decreasing streamflow from 1970 into the late 1990s and increasing streamflow from the late 1990s through 2020. For site 22, the annual maximum daily streamflow was generally unchanged during the entire period (fig. 7*A*), but all other statistics showed the same shift from decreasing to increasing in the late 1990s (figs. 7B and 7*C*). Although the shift to a wet climatic period happened in the late 1980s, streamflow lagged the increase in precipitation likely because of the filling up of surface water depressions,

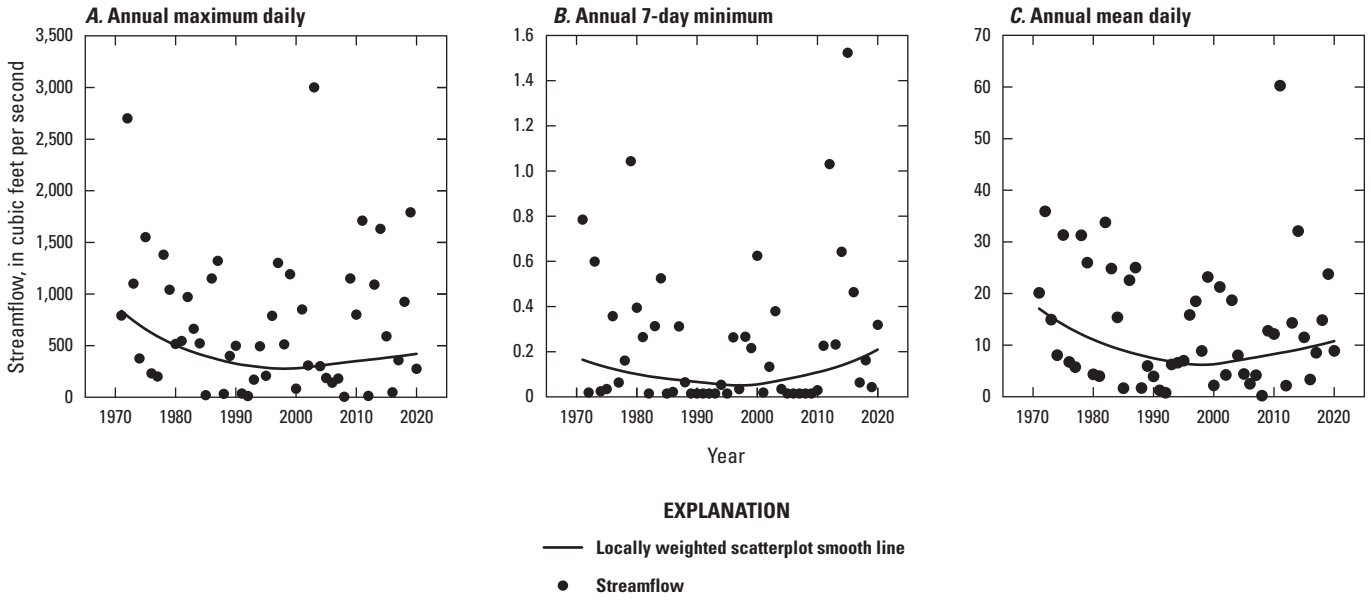

Figure 5. Streamflow analysis for the Green River near New Hradec, North Dakota (site 1), 1970–2020. *A*, annual maximum daily; *B*, annual 7-day minimum; and *C*, annual mean daily.

soil storage, and groundwater storage. Since the late 1990s, the 7-day minimum streamflow exhibited the largest increase for all sites, and the annual maximum daily streamflow had the smallest increase. For sites on the main stem (sites 5 and 22), the smaller increase in maximum streamflow was likely because dams upstream from these sites are operated for flood control. For the current study, the patterns in the 7-day minimum flows were assumed to represent changes in base-flow conditions, and most of the natural gains to streamflow during base flow conditions are discharge from groundwater storage (Smakhtin, 2001; Brutsaert, 2008). Increasing base-flow conditions increases the connectivity of the stream with the groundwater and soil, which can affect water-quality conditions in the stream. The pattern of decreasing streamflow since 1970 followed by increasing streamflow since the late 1990s through 2020 is consistent with hydroclimate conditions that have been observed in other North Dakota basins (Williams-Sether, 1999; Vecchia, 2003, 2008; Kolars and others, 2015; Ryberg and others, 2016).

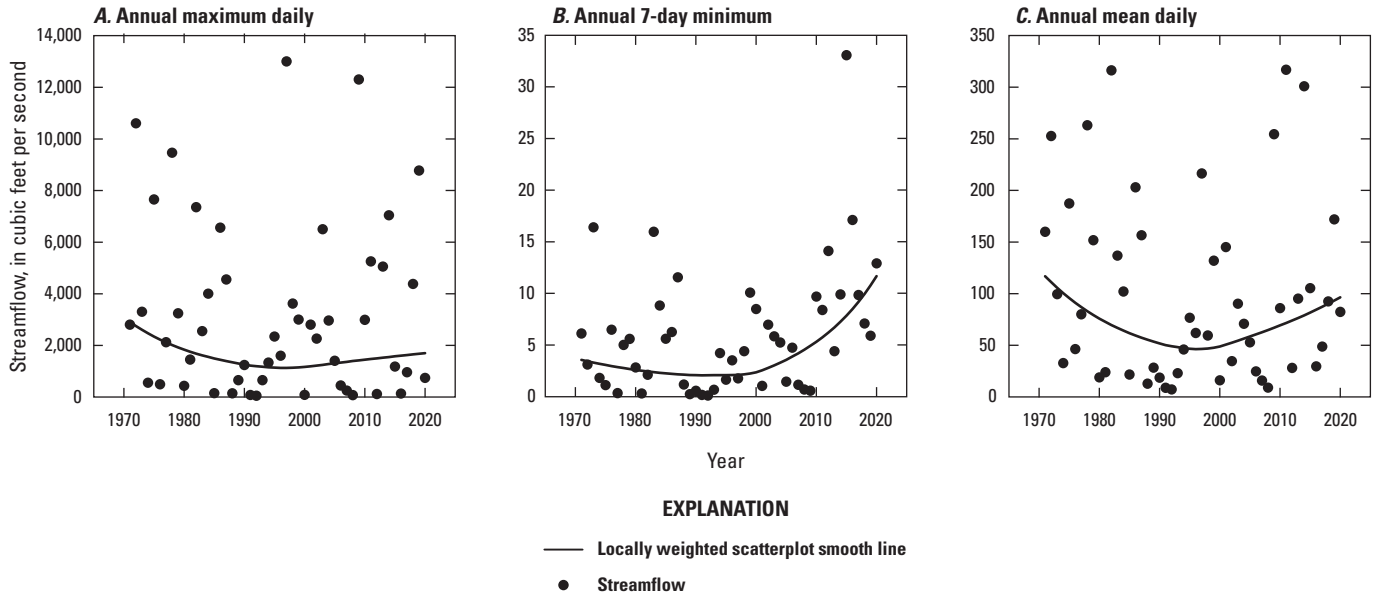

Figure 6. Streamflow analysis for the Heart River near Richardton, North Dakota (site 5) 1970–2020. *A*, annual maximum daily; *B*, annual 7-day minimum; and *C*, annual mean daily.

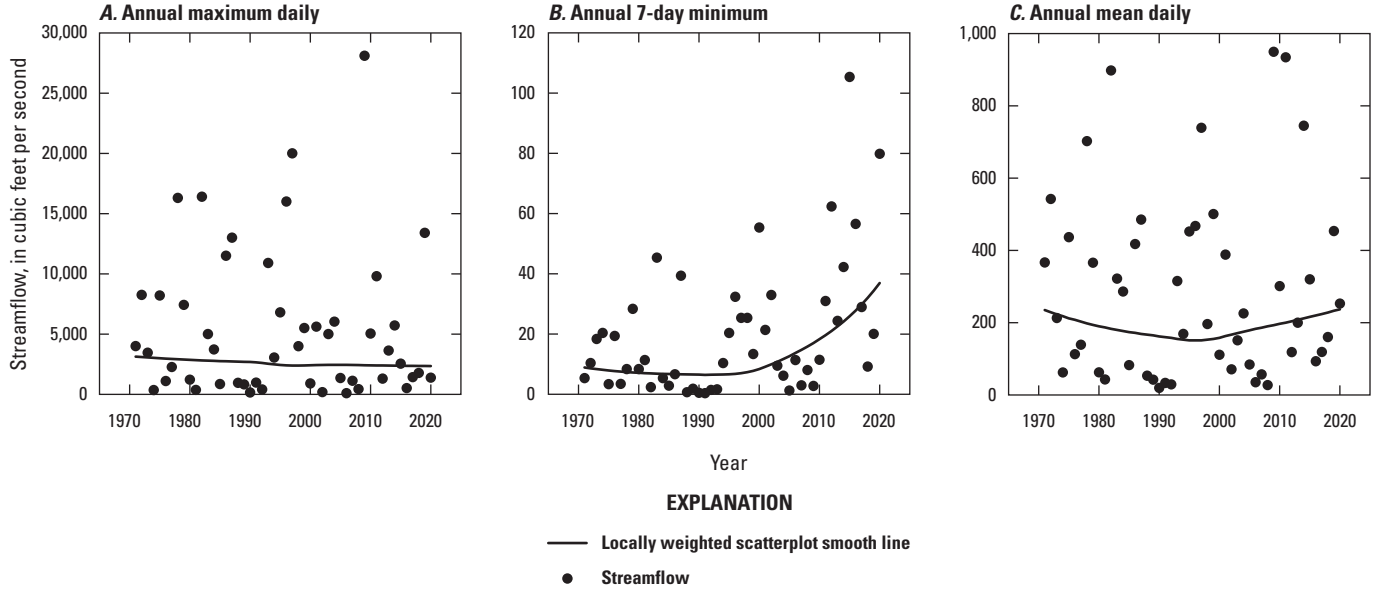

Figure 7. Streamflow analysis for the Heart River near Mandan, North Dakota (site 22) 1970–2020. *A*, annual maximum daily; *B*, annual 7-day minimum; and *C*, annual mean daily.

Spatial Water-Quality Patterns

Water-quality data from 1970 to 2020 were compiled for 22 sites within the Heart River Basin (table 1). These sites have different periods of record between 1970 and 2020 ranging from 1 to 49 years. An additional site on Lake Tschida (USGS site number 06346000; U.S. Geological Survey, 2020) was used for the load and yield calculations; however, a statistical summary was not included for that site. A statistical summary is provided in appendix 1 for TDS, dissolved ions, SAR, silica, nutrients, and physical properties (tables 1.1, 1.2, and 1.3). The chloride and nutrient data contained many censored values with the percentage of censored values at sites ranging from 0 to 100 percent of the data (tables 1.1 and 1.2).

Total Dissolved Solids, Dissolved Ions, Sodium Adsorption Ratio, and Silica

In the Heart River Basin, TDS is more likely to reflect patterns in sulfate, sodium, and bicarbonate because these generally represent a majority portion of the dissolved constituents in a water sample. In contrast, changes in chloride and potassium, which are present in smaller concentrations, have less effect on TDS concentrations. Total dissolved solids, a measure of the sum of all dissolved constituents such as sulfate, sodium, chloride, calcium, magnesium, potassium, bicarbonate, and many other constituents present in small amounts, can be used as an indication of salinity. Most sites had median sulfate and sodium concentrations greater than about 400 and 200 mg/L respectively, compared with most sites having median concentrations of chloride and potassium less than about 30 and about 12 mg/L, respectively (figs. 8 and 9; table 1.1).

The spatial patterns of median concentrations in the basin tended to be similar among TDS, sulfate, sodium, chloride, and bicarbonate with the lowest median concentrations in the South Branch Heart River near South Heart, N. Dak. (site 4) and the highest median concentrations at one of three sites, Heart River near South Heart, N. Dak. (site 2), Hailstone Creek (site 17), or site 18 (table 1.1; figs. 8 and 9). Median TDS concentrations ranged from 510 mg/L at site 4 to 2,150 mg/L at site 17, sulfate concentrations ranged from 170 mg/L at site 4 to 1,160 mg/L at site 17, median sodium concentrations ranged from 120 mg/L at site 4 to 485 mg/L at site 2; median chloride concentrations ranged from 4.8 mg/L at site 4 to 30 mg/L at site 17; and median bicarbonate concentrations ranged from 199 mg/L at site 4 to 606 mg/L at site 18. Spatial patterns among calcium, magnesium, and potassium concentrations were similar; some of the highest concentrations were also observed at site 17 and some of the lowest concentrations at site 4 (fig. 9). At many of the sites, the median concentrations are less representative because fewer observations or years of data are available compared to other sites. Hailstone Creek (sites 12 and 13), Sims Creek (site 14), Big Muddy Creek (site 15), and Wilson Creek (site 16) are located on smaller tributaries and had too few data for a statistical summary.

For one-third of the selected sites in the Heart River Basin with SAR data, median values were relatively high in relation to usability for irrigation water. The SAR is a relation between concentrations of sodium, calcium, and magnesium in the sample and is indicative of the suitability of irrigation water (Richards, 1954; Hem, 1985). In North Dakota, it is recommended that water for continuous irrigation should have SAR values less than 6, and some sites in the Heart River Basin had SAR values greater than 6 (Scherer and others, 2017). Five sites out of 15 had median values for SAR that were greater than 6 (table 1.1), meaning that for these five sites, about one-half of the measured SAR values were less than 6 and the other one-half were greater than 6. Of the five sites, two were in the lower basin in the Big Muddy Creek Basin (sites 17 and 18) and the other three sites were in the upper basin, with one on the Heart River (site 2) and two on tributaries (sites 3 and 4) upstream from E.A. Patterson Lake. The SAR values exceeded 6 in 25 percent of the measured values (the 75th percentile) from 1970 to 2020 at seven sites (sites 2, 3, 4, 17, 18, 21, and 22; table 1.1) in the basin, of which three were in the upper basin and four in the lower basin. At 11 sites (sites 1, 2, 3, 4, 5, 6, 17, 18, 20, 21, and 22), 10 percent of the SAR values (the 90th percentile) exceeded 6, with six in the upper basin and five in the lower basin.

Median silica concentrations were low compared to other constituents, ranging from 3.2 mg/L at site 11 to 9.1 mg/L at site 4 (table 1.1). Silica data were not available for sites 12–17. Generally, main-stem sites had lower concentrations of silica than tributaries.

Spatial patterns in TDS and dissolved ions in the basin may be related to evaporation, groundwater effects from geology, and lake processes in Lake Tschida. The process of evaporation may contribute to higher concentrations within the basin, particularly in tributaries and upper basin sites that have lower volumes of water. The concentration of a constituent is determined by dividing its mass by the volume of water. Evaporation reduces the volume of water and, therefore, produces higher concentrations. Differing bedrock across the basin may contribute to the spatial water-quality patterns observed in the Heart River Basin. The Ludlow and Cannonball, Bullion Creek, and Sentinel Butte Formations have aquifers that contribute flow to streams in the Heart River Basin. The Ludlow and Cannonball Formations and Bullion Creek aquifer systems have been defined as sodium-bicarbonate dominated water (Naplin and Shaver, 1978; Randich, 1979; Ackerman, 1980), whereas the Sentinel Butte aquifer system has been defined as a sodium-sulfate type water (Trapp and Croft, 1975). Comparing these aquifer systems, the Sentinel Butte system has higher dissolved ion concentrations than the Ludlow and Cannonball and Bullion Creek systems (Naplin and Shaver, 1978; Randich, 1979; Ackerman 1980). Groundwater can have a major effect on a stream's water quality during low flow or base-flow conditions (Smakhtin, 2001; Brutsaert, 2008). Site 7, downstream from Lake Tschida, generally had lower dissolved ion concentrations than site 5, upstream from Lake Tschida, which indicates that processes within the lake are reducing dissolved ion concentrations (figs. 8 and 9). Using the average storage volume for Lake Tschida (60,737 acre-feet) and average discharge (12 cubic feet per second) between 1999 and 2019 (Bureau of Reclamation, 2020), residence time of Lake Tschida was estimated to be 253 days. This residence time is sufficient to allow the lake processes to have some effect on the concentration disparity in dissolved ion concentrations between upstream and downstream sites. A potential process could be the settling of negatively charged clay particles, which occurs because the water does not turn over as frequently, and this allows the adsorption of positively charged cations to these clay particles (Langmuir, 1997). Reservoirs have been observed elsewhere in the United States to reduce concentrations in dissolved ion concentrations between upstream and downstream sections and reduce the variability in concentrations in the downstream section (Hem, 1985).

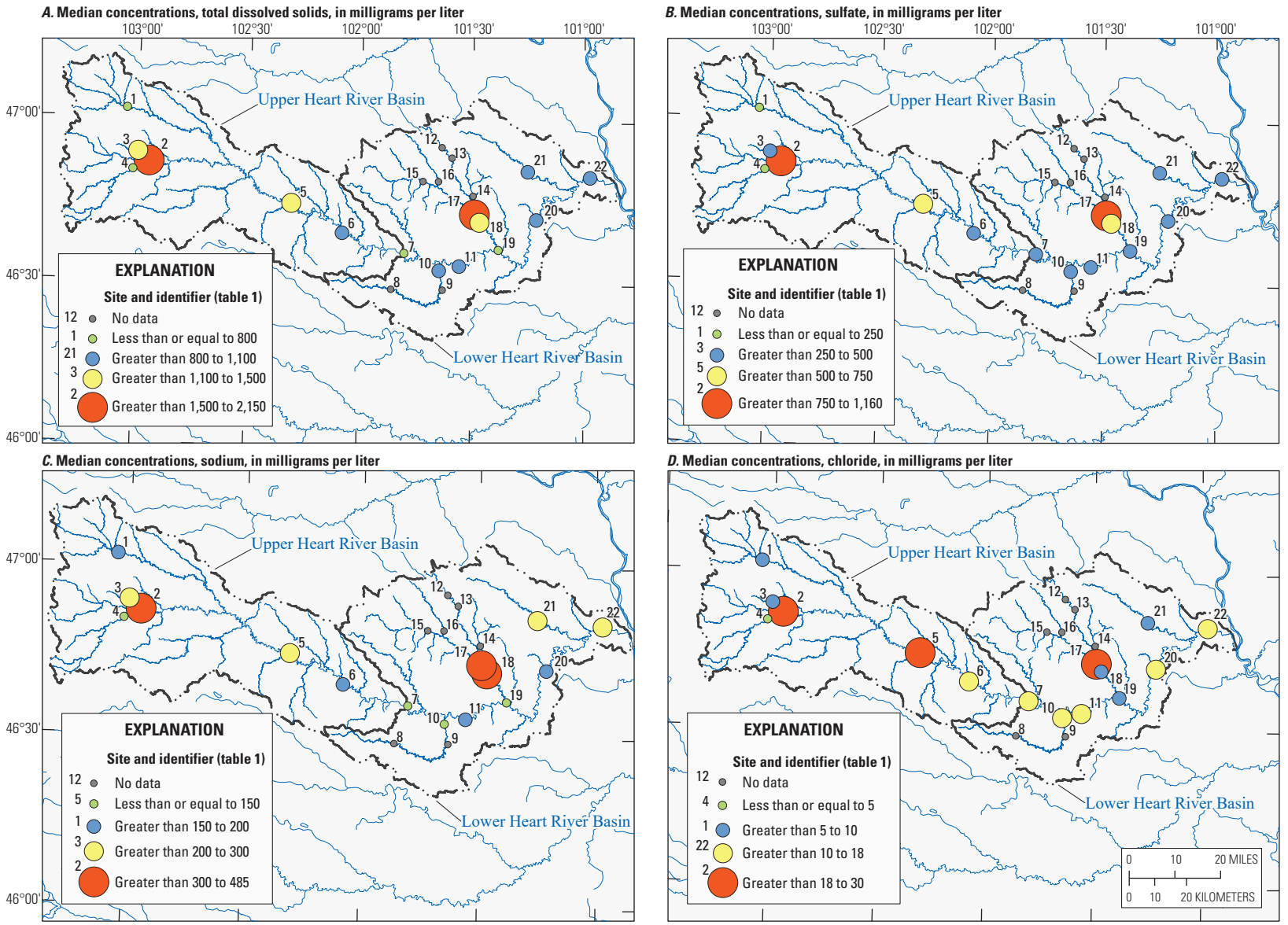

Figure 8. Median concentrations in the Heart River Basin, 1970–2020. *A*, total dissolved solids; *B*, sulfate; *C*, sodium; and *D*, chloride.

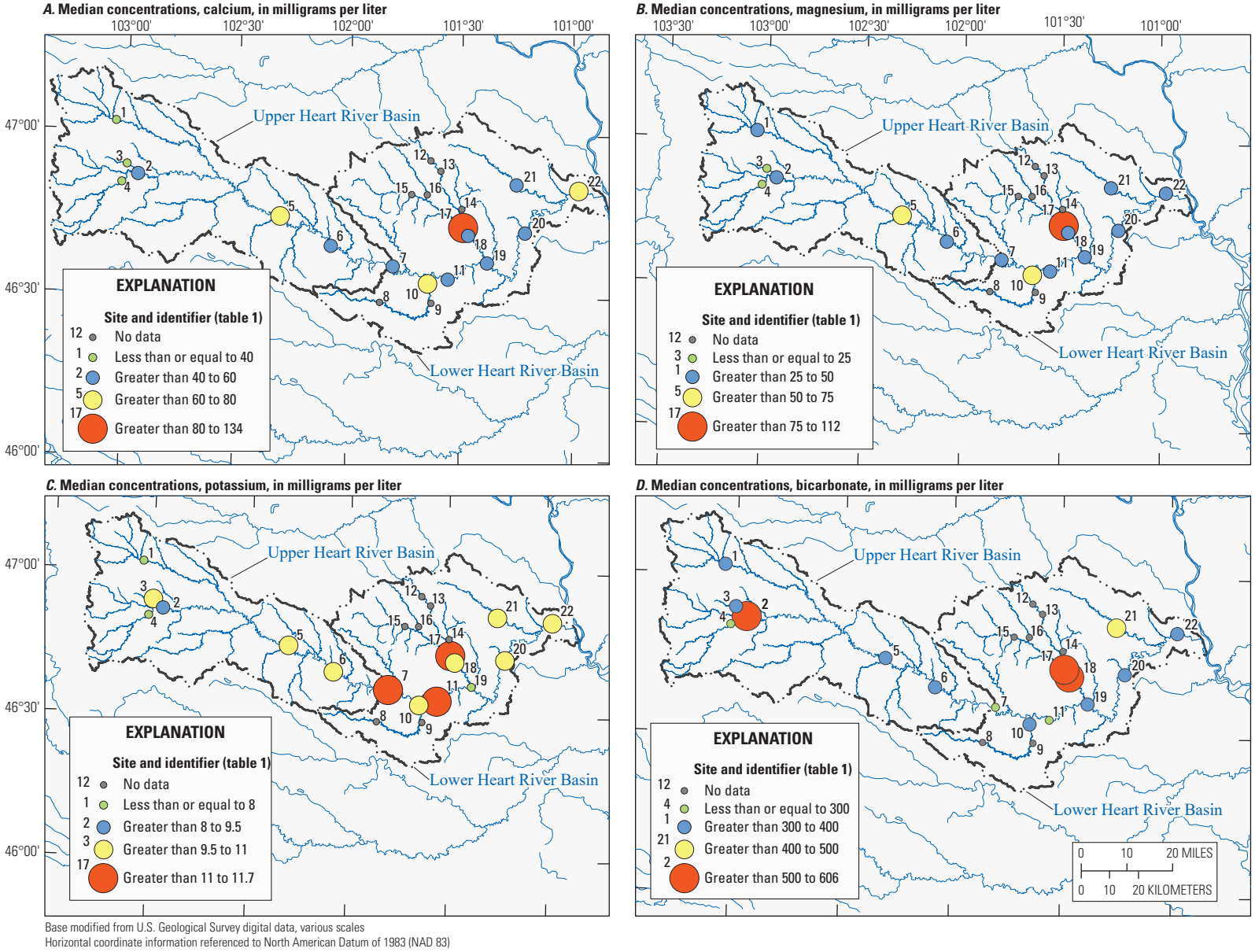

Base modified from U.S. Geological Survey digital data, various scales
Horizontal coordinate information referenced to North American Datum of 1983 (NAD 83)

Figure 9. Median concentrations in the Heart River Basin, 1970–2020. *A*, calcium; *B*, magnesium; *C*, potassium; and *D*, bicarbonate.

Nutrients

Spatial patterns for median concentrations of nitrate plus nitrite differed from the other nutrient constituents. The lowest median nitrate plus nitrite concentrations were below the recensored reporting level of 0.03 mg/L at multiple sites, and the highest median concentration was 0.8 mg/L at Antelope Creek (site 8; fig. 10 and table 1.2). Spatial patterns for median concentrations in total ammonia, dissolved phosphorus, and total phosphorus were similar with the lowest median concentrations at site 11 and the highest median concentrations at site 4 and site 15. Median concentrations of total ammonia ranged from less than 0.03 mg/L at many sites to 0.09 mg/L at site 4; median dissolved phosphorus concentrations ranged from less than 0.02 mg/L at four sites (sites 5, 10, 11, and 22) to 0.1 mg/L at site 4; and median total phosphorus concentrations ranged from less than 0.02 mg/L at sites 11 and 20 to 0.51 mg/L at site 15 (fig. 10 and table 1.2). At many of the sites, the median concentrations were less representative because fewer observations or years of data were available to compare to other sites, such as North Creek near South Heart, N. Dak. (site 3) or site 11. Sites 6, 7, and 20 had too few data for a statistical summary.

A large percentage of censored values in the nutrient data, in many cases 50 percent or more, made it difficult to compare concentrations spatially. Many of the median values in the statistical summaries for the four nutrient constituents of ammonia, nitrate plus nitrite, dissolved phosphorus, and total phosphorus were censored values. Dissolved phosphorus had the least amount of data of the selected nutrient constituents.

Nutrient patterns in the Heart River Basin may be related to land use differences, energy production, and lake processes in Lake Tschida. Land use differences in the basin can contribute to the higher median nutrient concentrations because of different practices on the landscape that can contribute nutrients to streams. Some sources of nutrients include runoff from agricultural areas, where fertilizers are applied or livestock production occurs, and runoff from urban areas, where fertilizers are applied to lawns, shrubs, and trees (Hem, 1985). As described above, the upper basin has higher land use of cultivated crops and hay/pasture than the lower basin (fig. 2*B*). The Antelope Creek Basin and Big Muddy Creek Basin (not shown) both had sites with the highest median concentrations for some of the nutrients (fig. 10), and these basins have 63 and 36 percent land use for cultivated crops and hay/pasture, respectively (fig. 2*B*). Energy production in North Dakota has increased dramatically since about 2008 (U.S. Energy Information Administration, 2013). Energy production in the Heart River Basin is generally only in the upper basin near Dickinson, N. Dak. The burning of fossil fuels is a source of nitrogen in the atmosphere (Hem, 1985), which could be an atmospheric source of nitrogen in the basin.

Like dissolved ions, processes in Lake Tschida can reduce the concentrations of nutrients in the basin. Lake processes such as eutrophication and adsorption of nutrients can decrease nutrient concentrations in the basin. Algal blooms, a result of eutrophication, have been observed in Lake Tschida. Algae use the nitrogen and phosphorus as a nutrient source, which can result in reduced the concentrations dissolved in the water column (North Dakota Department of Environmental Quality, 2021b). The adsorption of positively charged nutrients to negatively charged clay particles can occur because the particles settle out of suspension when they reach the lake (Langmuir, 1997). Reservoirs elsewhere in the United States were observed to reduce nutrient concentrations between upstream and downstream sections and reduce the variability in concentrations in the downstream section (Hem, 1985). Because many of the sites had censored data, it was difficult to observe the effects Lake Tschida had on the spatial pattern of nutrient concentrations in the Heart River Basin.

Physical Properties

The spatial pattern of specific conductance was similar to TDS, and the median specific conductance values ranged in the Heart River Basin from 641 microsiemens per centimeter at 25 degrees Celsius (µS/cm) at site 4 to 2,320 µS/cm at site 2 on the Heart River (table 1.3). Specific conductance is an indirect measure of the collective concentration of dissolved ions in solution (U.S. Geological Survey, variously dated), and can be used to evaluate the salinity hazard of irrigation water (Wilcox, 1955). Many of the same processes that can affect TDS and dissolved ion concentrations will also affect the specific conductance of a sample. Basinwide median specific conductance values were greater than 1,000 µS/cm at all sites except site 4.

No spatial pattern for pH was evident in the basin, and the median pH value in the basin ranged from 8.1 at site 4 to 8.4 at three sites (sites 11, 18, and 20; table 1.3). The pH of water is defined as the negative base-10 logarithm of the hydrogen ion activity and is used as an indicator of the health of any given aquatic system (U.S. Geological Survey, variously dated). River waters generally have a pH range between 6.5 and 8.5 and median values for pH in the Heart River Basin fall in this range (Hem, 1985).

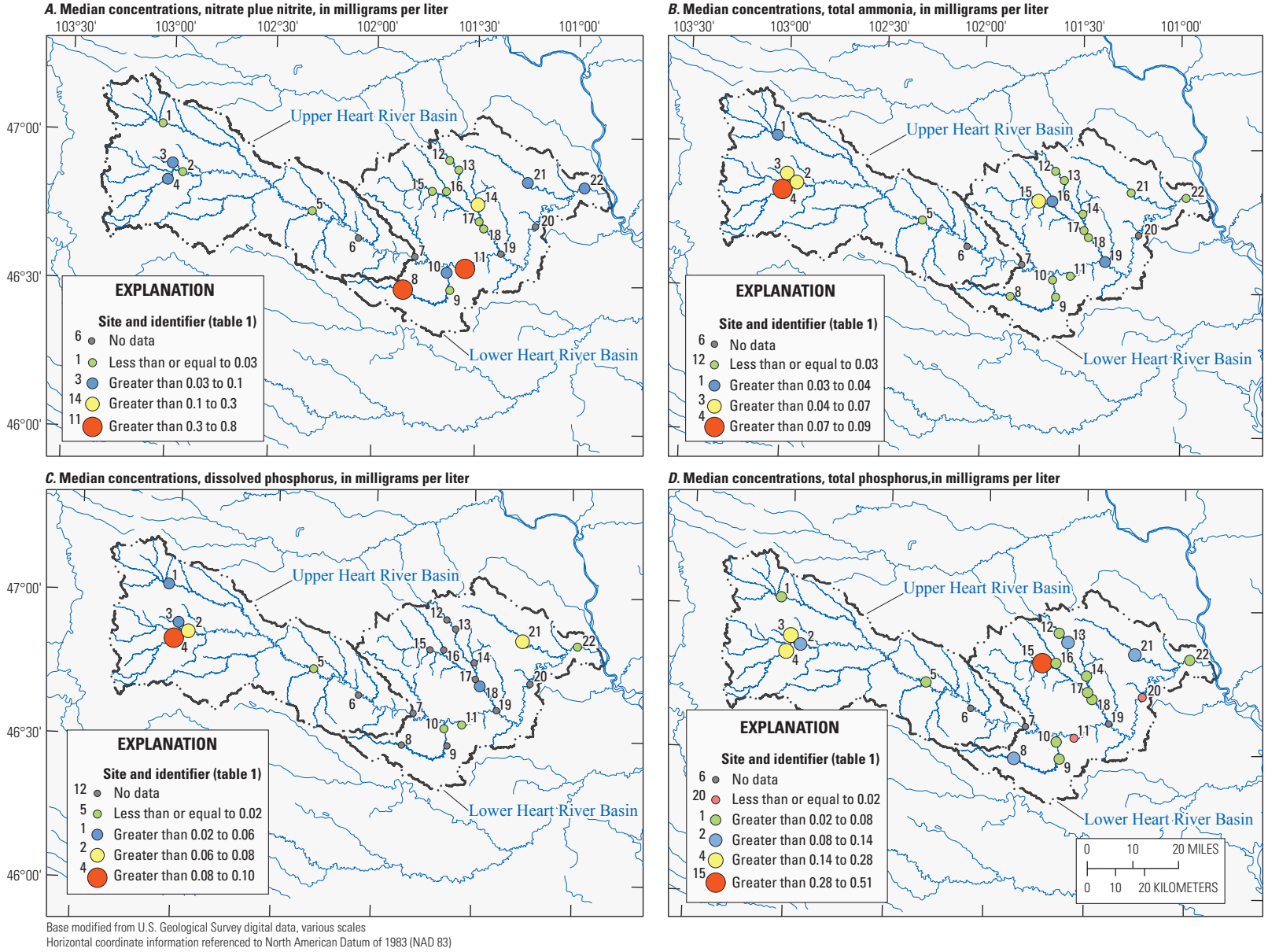

Figure 10. Median concentrations in the Heart River Basin, 1970–2020. *A*, nitrate plus nitrite; *B*, total ammonia; *C*, dissolved phosphorus; and D, total phosphorus.

Water-Quality Trends for Selected Sites

Water-quality trends were analyzed for a historical trend period (1974–2019) for one tributary site (site 1) and two main-stem Heart River sites (sites 5 and 22) and for a recent trend period (1999–2019) at two tributary sites (1 and 10) and two main-stem Heart River sites (sites 5 and 22). Increasing or decreasing trends are only discussed herein if they are significant (p-value less than 0.01) or mildly significant (p-value is less than 0.05 and greater than 0.01; see "Trend Analysis" section). Historical trends were analyzed for TDS, selected dissolved ions, and SAR. Recent trends were analyzed for TDS, selected dissolved ions, SAR, and the nutrient constituents including total phosphorus and nitrate plus nitrite. Only two main-stem sites (sites 5 and 22) had sufficient data for analysis of nutrient trends for the recent trend period. Depending on the data available for a given site, a one-, two-, or three-trend model was used. One-trend models spanned the entire historical period of 1974–2019 and consisted of a single monotonic trend. The one-trend model was used at site 1 for sodium, sulfate, calcium, magnesium, and chloride. The one-trend model was also used at all sites for the TDS trends. Two-trend models consisted of two piecewise monotonic trends between 1974 and 1999 and between 1999 and 2019. The two-trend model was used at site 1 for potassium, site 5 for all constituents except potassium and TDS, and site 22 for all constituents except TDS. Three-trend models consisted of three piecewise monotonic trends between 1974 and 1984, 1984 and 1999, and 1999 and 2019, and were only used at site 5 for potassium. The use of different trend models was based on the best fit model for a given constituent at a given site. The one-trend model was used for the recent trend period for all constituents and sites. Results from water-quality analysis of the historical trend period and the recent trend period provide insight into temporal and spatial water-quality changes in the basin. Results for the historical and recent trend period are displayed in table 5 and table 6.

Total Dissolved Solids, Dissolved Ions, and Sodium Adsorption Ratio

During the historical trend period, TDS concentrations have increased since the mid-1970s through 2019 (fig. 11, table 5). For all sites, a one-trend model was used. For site 1, a significant 22-percent increase in FAGMC was detected between 1974 and 2019 where the FAGMC increased from 590 to 723 mg/L (table 5). The significant trend detected at site 5 was a 23-percent increase where the FAGMC increased from 1,100 to 1,350 mg/L (table 5). Finally, at site 22 a significant 44-percent increase was detected in which the FAGMC increased from 830 to 1,200 mg/L (table 5).

During the recent trend period, increasing concentrations in TDS were observed across the Heart River Basin, and the magnitude of the increases was smaller at tributary sites compared to main-stem sites (table 5). All sites had similar percentage changes in FAGMC of TDS except for site 10, which had a nonsignificant 0.5-percent increase with a FAGMC increase in TDS of 3 mg/L. Percentage changes at the other sites ranged between 15 (site 5) and 26 percent (site 1), but the FAGMC increases were larger in the main-stem sites (sites 5 and 22). Both increases in FAGMC on the main-stem sites were greater than 150 mg/L, whereas the tributary sites had increases less than 150 mg/L (table 5).

During the historical trend period, sulfate and sodium concentrations have increased since the mid-1970s at all sites, but the increase was greater on main-stem sites from 1999 to 2019 than from 1974 to 1999 (table 5, figs. 12–13). For site 1, a one-trend model was used for sulfate and sodium and significant 46- and 30-percent increases, respectively, were detected from 1974 to 2019 (table 5). For site 5, a two-trend model was used for sulfate and sodium and a nonsignificant 4-percent increase for sulfate and a 16-percent mildly significant increase for sodium was detected from 1974 to 1999, but a larger significant increase of 37 percent for sulfate and 30 percent for sodium was detected from 1999 to 2019 (table 5). Sulfate and sodium at site 22 had a mildly significant 27- and significant 34-percent increase detected from 1974 to 1999, respectively (table 5). A larger significant increase in sulfate and sodium of 44 and 36 percent, respectively, was detected during 1999–2019 (figs. 12 and 13, table 5). For sulfate and sodium, the percentage increases on the main-stem sites for the 20-year period between 1999 and 2019 were nearly equivalent to the increase for site 1 during the 45-year period. Taking the 45-year period into account, during 1974–2019, the FAGMC nearly doubled at site 22 for sulfate (351 to 641 mg/L) and sodium (161 to 293 mg/L) (table 5).

During the recent trend period, increases in sulfate and sodium concentrations were detected basinwide, and sulfate trends had larger increases in concentration compared to sodium (table 5). For sulfate and sodium, the largest increases in magnitude and percentage change occurred on the main-stem sites (sites 5 and 22). Site 10 had the smallest increases in magnitude and percentage change for sulfate and sodium, but site 1 had a similar percentage change to the main-stem sites (table 5). However, the FAGMC increase in sulfate and sodium at site 1 was smaller than the changes on the main-stem sites. The FAGMC increases for sulfate and sodium at sites 5 and 22 were nearly identical, but site 5 had a higher starting and ending concentration compared to site 22. The large disparity in concentrations between site 1 and site 5 in the upper basin indicated that increases in both constituents were likely occurring in other Heart River tributaries upstream from site 5.

Land use, agricultural practices, and hydroclimatic changes in the Heart River Basin, combined with naturally occurring and readily available sulfate and sodium in geologic

Table 5. Summary of trend results for total dissolved solids, dissolved ions, and sodium adsorption ratio at selected sites in the Heart River Basin.

[USGS, U.S. Geological Survey; *p*-value, probability value; FAGMC, flow-averaged geometric mean concentration; N. Dak., North Dakota; --, no data]

Site number (fig. 1)	USGS site number	Site name	Trend model	Trend period	Trend period description	*p*-value	Significance level	Annual FAGMC for first year in trend period	Annual FAGMC for last year in trend period	Change, in percent, from first to last year[1]
				Total dissolved solids, in milligrams per liter						
1	06344600	Green River near New Hradec, N. Dak.	One	1974–2019	Historical	0.0014	Significant increase	590	723	22
5	06345500	Heart River near Richardton, N. Dak.	One	1974–2019	Historical	0.0017	Significant increase	1,100	1,350	23
22	06349000	Heart River near Mandan, N. Dak.	One	1974–2019	Historical	0.0000	Significant increase	830	1,200	44
1	06344600	Green River near New Hradec, N. Dak.	One	1999–2019	Recent	0.0467	Mildly significant increase	492	618	26
5	06345500	Heart River near Richardton, N. Dak.	One	1999–2019	Recent	0.0260	Mildly significant increase	1,200	1,380	15
10	--	Antelope Creek near Carson, N. Dak.	One	1999–2019	Recent	0.9663	Nonsignificant increase	693	696	0.4
22	06349000	Heart River near Mandan, N. Dak.	One	1999–2019	Recent	0.0006	Significant increase	1,020	1,250	22
				Sulfate, in milligrams per liter						
1	06344600	Green River near New Hradec, N. Dak.	One	1974–2019	Historical	0.0002	Significant increase	203	296	46
5	06345500	Heart River near Richardton, N. Dak.	Two	1974–99	Historical	0.6436	Nonsignificant increase	536	561	4
5	06345500	Heart River near Richardton, N. Dak.	Two	1999–2019	Historical	0.0053	Significant increase	561	767	37
22	06349000	Heart River near Mandan, N. Dak.	Two	1974–99	Historical	0.0166	Mildly significant increase	351	447	27
22	06349000	Heart River near Mandan, N. Dak.	Two	1999–2019	Historical	0.0009	Significant increase	447	641	44
1	06344600	Green River near New Hradec, N. Dak.	One	1999–2019	Recent	0.0287	Mildly significant increase	168	243	45
5	06345500	Heart River near Richardton, N. Dak.	One	1999–2019	Recent	0.0011	Significant increase	586	803	37
10	--	Antelope Creek near Carson, N. Dak.	One	1999–2019	Recent	0.3297	Nonsignificant increase	270	312	15
22	06349000	Heart River near Mandan, N. Dak.	One	1999–2019	Recent	0.0006	Significant increase	440	653	48
				Sodium, in milligrams per liter						
1	06344600	Green River near New Hradec, N. Dak.	One	1974–2019	Historical	0.0012	Significant increase	130	168	30
5	06345500	Heart River near Richardton, N. Dak.	Two	1974–99	Historical	0.0216	Mildly significant increase	209	244	16
5	06345500	Heart River near Richardton, N. Dak.	Two	1999–2019	Historical	0.0007	Significant increase	244	317	30
22	06349000	Heart River near Mandan, N. Dak.	Two	1974–99	Historical	0.0004	Significant increase	161	216	34
22	06349000	Heart River near Mandan, N. Dak.	Two	1999–2019	Historical	0.0002	Significant increase	216	293	36
1	06344600	Green River near New Hradec, N. Dak.	One	1999–2019	Recent	0.0856	Nonsignificant increase	109	140	28
5	06345500	Heart River near Richardton, N. Dak.	One	1999–2019	Recent	0.0004	Significant increase	238	311	31
10	--	Antelope Creek near Carson, N. Dak.	One	1999–2019	Recent	0.8204	Nonsignificant increase	95	97	3
22	06349000	Heart River near Mandan, N. Dak.	One	1999–2019	Recent	0.0001	Significant increase	213	284	33

Table 5. Summary of trend results for total dissolved solids, dissolved ions, and sodium adsorption ratio at selected sites in the Heart River Basin.—Continued

[USGS, U.S. Geological Survey; *p*-value, probability value; FAGMC, flow-averaged geometric mean concentration; N. Dak., North Dakota; --, no data]

Site number (fig. 1)	USGS site number	Site name	Trend model	Trend period	Trend period description	*p*-value	Significance level	Annual FAGMC for first year in trend period	Annual FAGMC for last year in trend period	Change, in percent, from first to last year[1]
Chloride, in milligrams per liter										
1	06344600	Green River near New Hradec, N. Dak.	One	1974–2019	Historical	0.0000	Significant increase	5.6	10	84
5	06345500	Heart River near Richardton, N. Dak.	Two	1974–99	Historical	0.0019	Significant increase	13	17	30
5	06345500	Heart River near Richardton, N. Dak.	Two	1999–2019	Historical	0.0000	Significant increase	17	32	87
22	06349000	Heart River near Mandan, N. Dak.	Two	1974–99	Historical	0.0001	Significant increase	10	14	41
22	06349000	Heart River near Mandan, N. Dak.	Two	1999–2019	Historical	0.0001	Significant increase	14	19	41
1	06344600	Green River near New Hradec, N. Dak.	One	1999–2019	Recent	0.0029	Significant increase	7.1	10	46
5	06345500	Heart River near Richardton, N. Dak.	One	1999–2019	Recent	0.0000	Significant increase	17	31	78
10	--	Antelope Creek near Carson, N. Dak.	--	--	--	--	--	--	--	--
22	06349000	Heart River near Mandan, N. Dak.	One	1999–2019	Recent	0.0000	Significant increase	13	18	44
Potassium, in milligrams per liter										
1	06344600	Green River near New Hradec, N. Dak.	Two	1974–99	Historical	0.0014	Significant increase	5.6	7.4	32
1	06344600	Green River near New Hradec, N. Dak.	Two	1999–2019	Historical	0.0468	Mildly significant decrease	7.4	6.3	−15
5	06345500	Heart River near Richardton, N. Dak.	Three	1974–84	Historical	0.0001	Significant increase	7.9	11	40
5	06345500	Heart River near Richardton, N. Dak.	Three	1984–99	Historical	0.0345	Mildly significant decrease	11	9.8	−11
5	06345500	Heart River near Richardton, N. Dak.	Three	1999–2019	Historical	0.0078	Significant increase	9.8	11	12
22	06349000	Heart River near Mandan, N. Dak.	Two	1974–99	Historical	0.0012	Significant increase	8.2	9.4	15
22	06349000	Heart River near Mandan, N. Dak.	Two	1999–2019	Historical	0.0011	Significant increase	9.4	11	14
1	06344600	Green River near New Hradec, N. Dak.	One	1999–2019	Recent	0.1797	Nonsignificant decrease	7.1	6.2	−12
5	06345500	Heart River near Richardton, N. Dak.	One	1999–2019	Recent	0.0027	Significant increase	9.7	11	14
10	--	Antelope Creek near Carson, N. Dak.	One	1999–2019	Recent	0.8172	Nonsignificant decrease	8.7	8.6	–2
22	06349000	Heart River near Mandan, N. Dak.	One	1999–2019	Recent	0.0027	Significant increase	9.2	10.0	14
Calcium, in milligrams per liter										
1	06344600	Green River near New Hradec, N. Dak.	One	1974–2019	Historical	0.4790	Nonsignificant increase	39	40	4
5	06345500	Heart River near Richardton, N. Dak.	Two	1974–99	Historical	0.0956	Nonsignificant decrease	80	71	−11

Table 5. Summary of trend results for total dissolved solids, dissolved ions, and sodium adsorption ratio at selected sites in the Heart River Basin.—Continued

[USGS, U.S. Geological Survey; *p*-value, probability value; FAGMC, flow-averaged geometric mean concentration; N. Dak., North Dakota; --, no data]

Site number (fig. 1)	USGS site number	Site name	Trend model	Trend period	Trend period description	*p*-value	Significance level	Annual FAGMC for first year in trend period	Annual FAGMC for last year in trend period	Change, in percent, from first to last year[1]
Calcium, in milligrams per liter—Continued										
5	06345500	Heart River near Richardton, N. Dak.	Two	1999–2019	Historical	0.0005	Significant increase	71	95	34
22	06349000	Heart River near Mandan, N. Dak.	Two	1974–99	Historical	0.2400	Nonsignificant increase	58	63	8
22	06349000	Heart River near Mandan, N. Dak.	Two	1999–2019	Historical	0.0028	Significant increase	63	78	24
1	06344600	Green River near New Hradec, N. Dak.	One	1999–2019	Recent	0.2245	Nonsignificant increase	28	32	13
5	06345500	Heart River near Richardton, N. Dak.	One	1999–2019	Recent	0.0001	Significant increase	74	97	32
10	--	Antelope Creek near Carson, N. Dak.	One	1999–2019	Recent	0.1828	Nonsignificant increase	58	69	17
22	06349000	Heart River near Mandan, N. Dak.	One	1999–2019	Recent	0.0046	Significant increase	67	76	14
Magnesium, in milligrams per liter										
1	06344600	Green River near New Hradec, N. Dak.	One	1974–2019	Historical	0.0005	Significant increase	22	29	29
5	06345500	Heart River near Richardton, N. Dak.	Two	1974–99	Historical	0.5828	Nonsignificant decrease	50	48	−5
5	06345500	Heart River near Richardton, N. Dak.	Two	1999–2019	Historical	0.0008	Significant increase	48	73	54
22	06349000	Heart River near Mandan, N. Dak.	Two	1974–99	Historical	0.0144	Mildly significant increase	36	44	22
22	06349000	Heart River near Mandan, N. Dak.	Two	1999–2019	Historical	0.0001	Significant increase	44	66	49
1	06344600	Green River near New Hradec, N. Dak.	One	1999–2019	Recent	0.0072	Significant increase	17	23	39
5	06345500	Heart River near Richardton, N. Dak.	One	1999–2019	Recent	0.0002	Significant increase	50	76	52
10	--	Antelope Creek near Carson, N. Dak.	One	1999–2019	Recent	0.2469	Nonsignificant increase	53	60	13
22	06349000	Heart River near Mandan, N. Dak.	One	1999–2019	Recent	0.0003	Significant increase	43	64	46
Sodium adsorption ratio, unitless										
1	06344600	Green River near New Hradec, N. Dak.	One	1974–2019	Historical	0.0076	Significant increase	4.1	4.9	19
5	06345500	Heart River near Richardton, N. Dak.	One	1974–2019	Historical	0.0000	Significant increase	4.6	5.8	25
22	06349000	Heart River near Mandan, N. Dak.	One	1974–2019	Historical	0.0000	Significant increase	4.3	5.8	35
1	06344600	Green River near New Hradec, N. Dak.	One	1999–2019	Recent	0.2434	Nonsignificant increase	4.1	4.6	13
5	06345500	Heart River near Richardton, N. Dak.	One	1999–2019	Recent	0.0150	Mildly significant increase	5.1	5.6	10
10	--	Antelope Creek near Carson, N. Dak.	One	1999–2019	Recent	0.5212	Nonsignificant increase	2.1	2.2	4
22	06349000	Heart River near Mandan, N. Dak.	One	1999–2019	Recent	0.0048	Significant increase	4.9	5.7	17

[1]Percentage change values are directly calculated from R–QWTREND. Starting and ending concentrations in table are rounded and may not produce the exact percentage change.

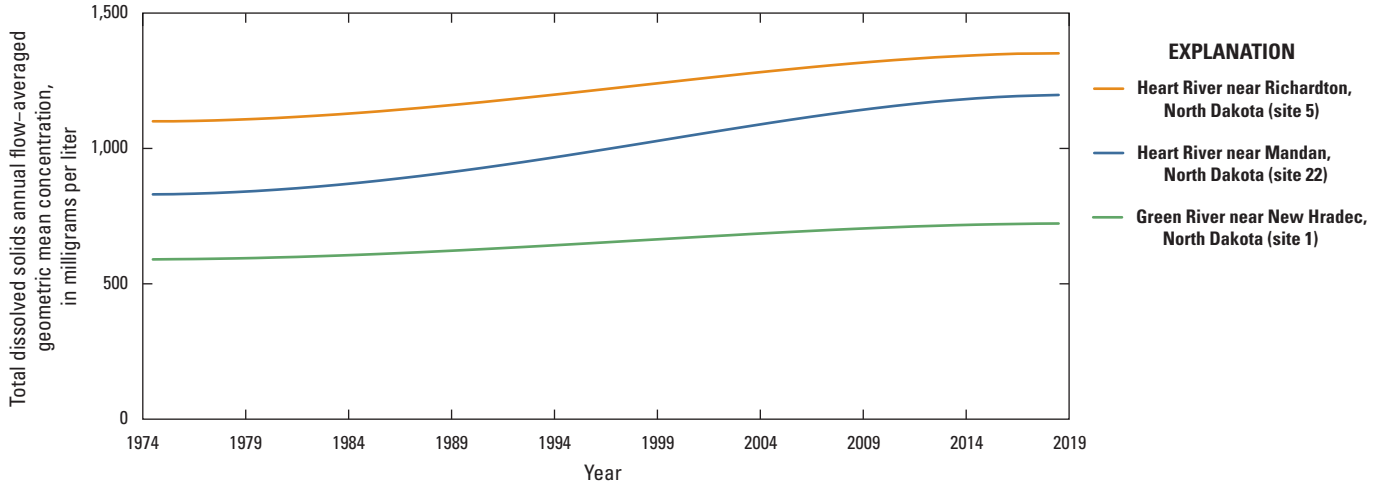

Figure 11. Fitted trends for total dissolved solids in annual flow-averaged geometric mean concentration of total dissolved solids at three sites in the Heart River Basin for the historical trend period (1974–2019).

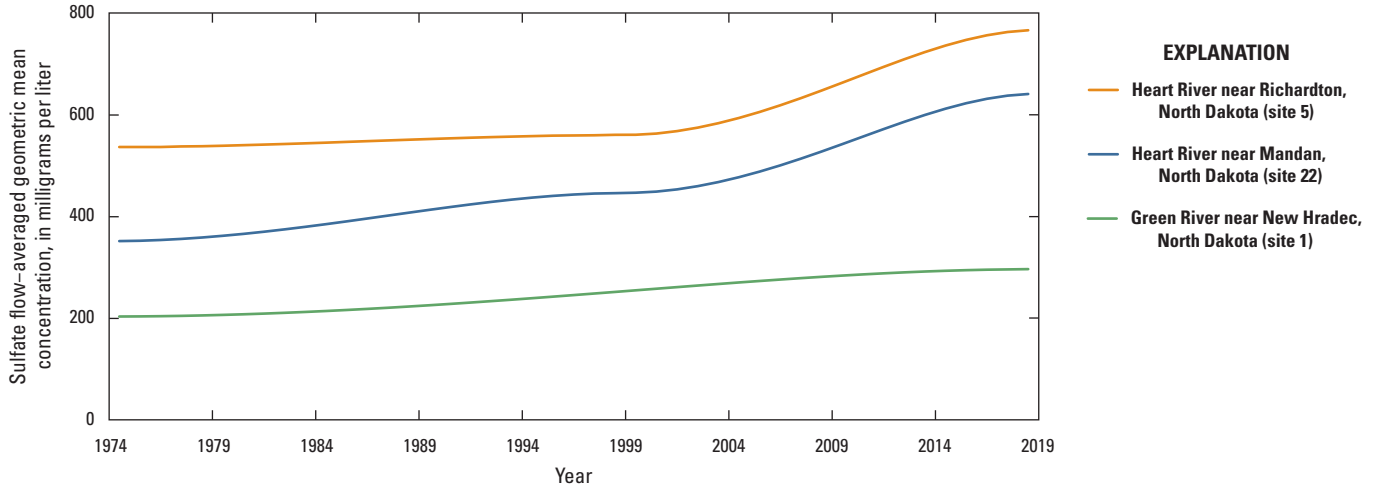

Figure 12. Fitted trend for sulfate in annual flow-averaged geometric mean concentration of sulfate at three sites in the Heart River Basin for the historical trend period (1974–2019).

formations, soils, and aquifers, likely contributed to the moderate to large increases of sulfate and sodium concentrations. A primary land-use change in the basin during the recent trend period was the conversion of "considerable acreage" from flood to pivot irrigation (Chad Skretteburg, Western Heart River Irrigation District, written commun., 2021). Pivot irrigation can cause increases in soil salinity because there is not a large enough volume of water applied to leach the salts through the soil column (Al-Ghobari, 2011; Shahid, 2013). The salts that form in the Heart River Basin are sodium-sulfate evaporites (Keller and others, 1986a), and during runoff events these evaporites dissolve and flow into the Heart River owing to the high solubility of the sodium-sulfate evaporites (Keller and others, 1986b). Hydroclimate changes from a dry to wet climatic period around 1995 in the basin likely contributed to the increasing concentrations of sulfate and sodium because increases in base flows were observed basinwide (figs. 5–7). Although R–QWTREND does remove streamflow variability when computing the trends, it may not fully capture these streamflow changes in the basin (Nustad and Vecchia, 2020). Increases in base flow correspond to increases in groundwater discharge, and sulfate and sodium are naturally occurring in the geology of the basin (Trapp and Croft, 1975; Naplin and Shaver, 1978; Randich, 1979; Ackerman, 1980). Concentrations of sulfate and sodium likely increase in the streams owing to the increasing discharge from the aquifers. With the change to a wet climatic period, increasing groundwater levels will have more contact with sodium-sulfate evaporites that were in the previously unsaturated zone, increasing the concentrations in the groundwater. The NRCS has implemented conservation practices on about 300 acres for salinity and sodicity management in the basin for saline or sodic soils

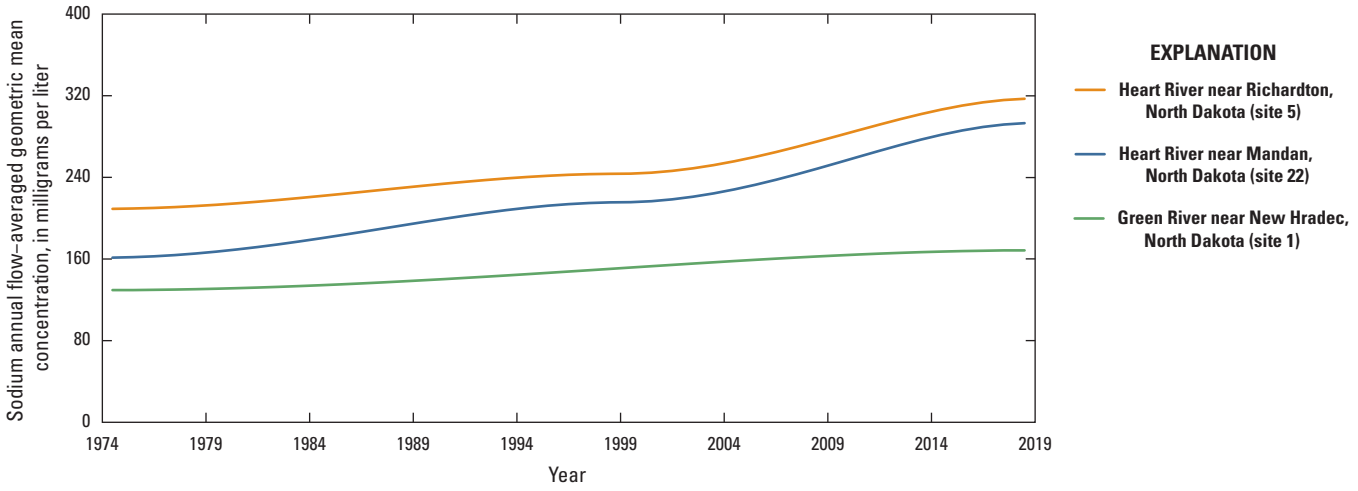

Figure 13. Fitted trend for sodium in annual flow-averaged geometric mean concentration of sodium at three sites in the Heart River Basin for the historical trend period (1974–2019).

since 2006 (Rita Sveen, NRCS, written commun., 2021). Two common methods are used to treat saline and sodic soils: one is the application of elemental sulfur to form gypsum and the other is the direct application of gypsum (Franzen and others, 2014; Diaz and Presley, 2017). In both methods, the dissolution of the gypsum is used to replace the sodium ions that have adsorbed to the soil particles and flush the system of sodium ions (Franzen and others, 2014; Diaz and Presley, 2017).

Chloride concentrations showed large, consistent, and significant increases starting in the mid-1970s through 2019, whereas potassium concentrations remained mostly constant with some small fluctuations over the same period (figs. 14 and 15, respectively; table 5). From the one-trend chloride model at site 1, a significant 84 percent increase was detected from 1974 to 2019, where the FAGMC increased from 5.6 to 10 mg/L. From the two-trend potassium model at site 1, a significant 32 percent increase was detected from 1974 to 1999 and a mildly significant 15 percent decrease was detected from 1999 to 2019. Considering both trend periods for potassium at site 1, the FAGMC remained largely unchanged (5.6 to 6.3 mg/L; table 5). At site 5, the two-trend chloride model detected a significant 30 percent increase in chloride concentrations from 1974 to 1999 and a significant 87 percent increase from 1999 to 2019. Considering both trend periods for chloride at site 5, the FAGMC more than doubled from 13 to 32 mg/L during 1974–2019 (fig. 14; table 5). At site 5, the three-trend potassium model detected fluctuating concentrations with a significant 40 percent increase from 1974 to 1984, a mildly significant 11 percent decrease from 1984 to 1999, followed by a significant 12 percent increase from 1999 to 2019 (table 5). Considering the three trend periods for potassium at site 5, overall, the FAGMC slightly increased from 7.9 to 11 mg/L. At site 22, the same significant increase of 41 percent was detected for chloride for both trend periods, and the FAGMC of chloride nearly doubled between 1974 and 2019 from 10 to 19 mg/L (table 5).

During the recent period, large increases (greater than 40 percent) in chloride concentrations were detected, and potassium concentrations were mostly constant, although small (0.9 mg/L or less) decreases on tributaries and small (1.3 mg/L) increases on the main-stem sites were detected (table 5). Although percentage increases in chloride were large, actual changes in concentration seem small because FAGMCs of chloride were less than about 30 mg/L (table 5). For site 10, recent trends for chloride were not analyzed because of too many censored values. Site 1 and 22 had similar percentage changes for chloride (46 and 44 percent, respectively) and FAGMC increases (2.9 and 5 mg/L, respectively, table 5). The increase in chloride for the main-stem site upstream from Lake Tschida (site 5) was substantially larger (14 mg/L) than the increase at the most downstream main-stem site (5 mg/L; site 22), which indicates larger increases in chloride in the upper basin tributaries compared to the lower basin tributaries (table 5). The FAGMC of potassium generally hovered around 10 mg/L at all sites, and the tributary sites had small nonsignificant decreasing concentrations (15 percent or smaller) compared to the main-stem sites that had small significant (15 percent or smaller) increasing concentrations (table 5). Overall, the FAGMC changes in potassium at all sites ranged from −1.2 to 1.3 mg/L and the percentage changes ranged from −12 to 14 percent. The small FAGMC and percentage changes were indicative that the potassium concentrations were remaining mostly constant basinwide.

Chloride concentrations had larger increases between 1999 and 2019 compared to 1974–99, which were likely a result of sources such as deicing and dust-control chemicals, agricultural management and practices, and energy production (Granato and others, 2015). Many roadways are located within the basin, notably Interstate 94 (fig. 1), that may have had deicing chemicals applied to road surfaces during the winter, which may have contributed to increased trends in chloride (Granato and others, 2015). Dust-control chemicals, such as

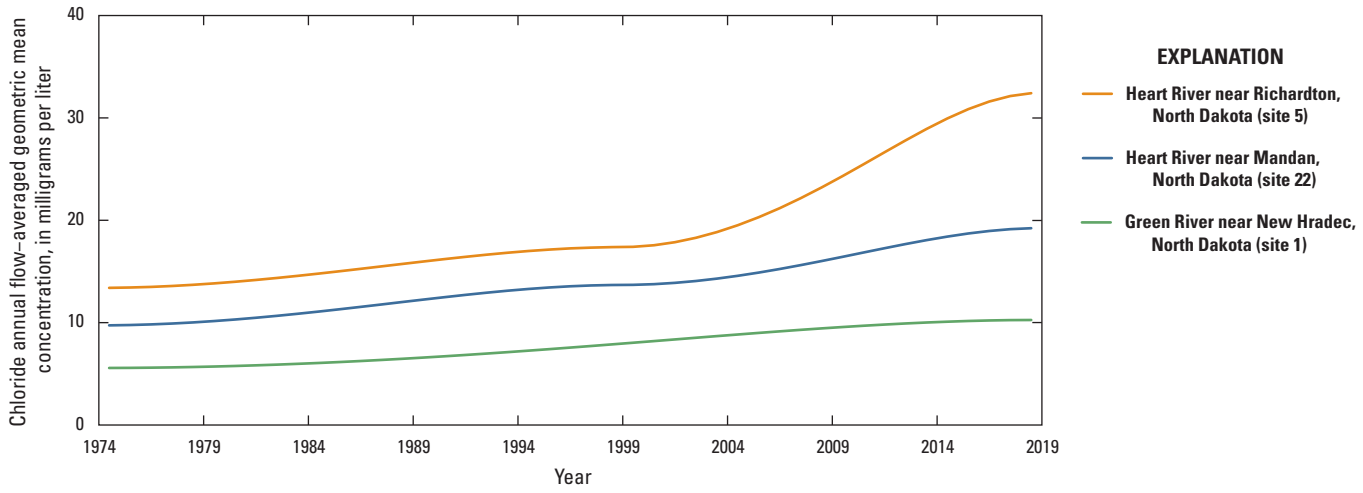

Figure 14. Fitted trend for chloride in annual flow-averaged geometric mean concentration of chloride at three sites in the Heart River Basin for the historical trend period (1974–2019).

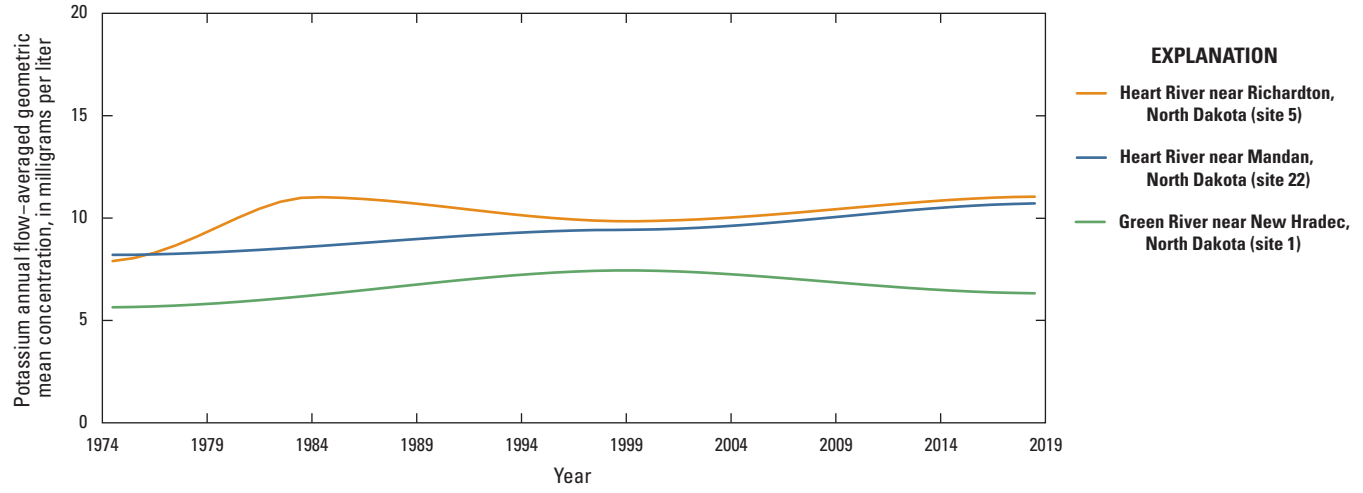

Figure 15. Fitted trend for potassium in annual flow-averaged geometric mean concentration of potassium at three sites in the Heart River Basin for the historical trend period (1974–2019).

calcium and magnesium chloride, used for gravel and oil field roads likely affected the chloride concentration increases in the basin. Agricultural fertilizers with potash (potassium chloride) are used in North Dakota, and an average of 40 percent of wheat, corn, and soybean fields in the State have potash applied (U.S. Department of Agriculture, 2019). Runoff from hay/pasture lands in the Heart River Basin also likely contributed to the increasing chloride concentrations from animal waste (fig. 2*B*; Granato and others, 2015). Documentation from the Western Heart River Irrigation District stated that conversion from flood to pivot irrigation has been occurring in the Heart River Basin (Chad Skretteburg, Western Heart River Irrigation District, written commun., 2021). These practices may produce more salts on the soil surfaces, which can include chloride salts (Al-Ghobari, 2011; Shahid, 2013). Many of the salts that would be precipitated on the surface are highly soluble when in contact with water and would likely be dissolved and transported during runoff events. Energy production in North Dakota has increased dramatically since about 2008 and could be a possible source for increasing chloride concentrations (U.S. Energy Information Administration, 2013). Energy production in Heart River Basin is generally only in the upper portion of the basin, mostly in Stark and Dunn Counties. Saline waters or brines are produced as part of the extraction process. Historically, production water was disposed of using evaporation pits until 2011 when it was mandated that all production waters either be disposed of in deep injection wells or be recycled (North Dakota Administrative Code, 2020). Releases of brines into the environment can occur from the transport of the brines to disposal sites, pipeline breaks, vehicle accidents, and leakage from historic evaporation pits.

Potassium concentrations did not follow the trends observed with other constituents and remained mostly constant from 1974 to 2019, likely because of stable processes during the trend periods. These processes include, but are not limited to, agricultural fertilizer application, weathering of biotite and potassium feldspars into clays, and possible biological processes (Langmuir, 1997; Franzen and Bu, 2018). The Heart River Basin is a predominantly agricultural basin, and 40 percent of wheat, soybean, and corn fields in North Dakota have potash applied (U.S. Department of Agriculture, 2019). Naturally occurring potassium is present in the geologic formations but is likely a minor contributor to the potassium concentrations (Langmuir, 1997).

Calcium and magnesium concentrations increased since the mid-1970s at all sites (table 5, figs. 16–17, respectively), except for a decrease at site 5 between 1974 and 1999. At site 1, one-trend models were used for calcium and magnesium and a nonsignificant 4-percent increase in calcium and a significant 29-percent increase in magnesium was detected from 1974 to 2019. A two-trend model was used for site 5, and nonsignificant decreases in calcium and magnesium concentrations of 11 and 5 percent, respectively, were detected from 1974 to 1999 (table 5). At site 5 during 1999–2019, a significant 34-percent increase in calcium and a significant 54-percent increase in magnesium was detected (figs. 16 and 17, respectively, table 5). At site 22, a two-trend model was used for calcium and magnesium and increases in concentrations were detected for both trend periods. For calcium, a nonsignificant 8-percent increase was detected from 1974 to 1999, and a significant 24-percent increase was detected from 1999 to 2019 (table 5, fig. 16). For magnesium, a mildly significant 22-percent increase was detected from 1974 to 1999, and a significant 49-percent increase was detected from 1999 to 2019 was detected (table 5, fig. 17).

During the recent period, calcium and magnesium concentrations increased basinwide (table 5). Sites 1, 10, and 22 all had similar percentage increases (13, 17, and 14 percent, respectively) for calcium concentrations, whereas the percentage change at site 5 was nearly double (32 percent) compared to the other three sites (table 5). FAGMC from the first to last year of calcium started and ended at similar concentrations at sites 5, 10, and 22. The FAGMC at site 1 was one-half that of the other three sites. Site 5 had the largest percentage change and FAGMC increase in calcium in the basin, which indicates that the upper basin tributaries had larger increases compared to the lower basin tributaries. At the Heart River sites (sites 5 and 22), the magnesium percentage increases (52 and 46 percent, respectively) were larger than on the tributary sites (sites 1 and 10), with the increases of 39 and 13 percent, respectively (table 5). The FAGMC magnesium increases at sites 1 and 10 were similar (6 and 7 mg/L, respectively; table 5), however site 10 has starting and ending concentrations that were more than double the concentrations at site 1 (table 5). Main-stem sites (sites 5 and 22) had similar starting and ending magnesium concentrations and similar FAGMC increases (26 and 21 mg/L, respectively; table 5).

Overall, increasing concentrations of calcium and magnesium were consistent between the upper and lower basin and are likely related to anthropogenic effects and naturally occurring geologic effects. Anthropogenic effects in the basin include dust-control measures on gravel roads or agricultural practice changes. Calcium and magnesium chloride chemicals are used to control dust on gravel and oil field roads and can be a source of increased concentrations in streams (Granato and others, 2015). The conversion from flood to pivot irrigation is the major agricultural change in the basin and can cause the accumulation of salts on the surface and in the shallow subsurface (Al-Ghobari, 2011; Shahid, 2013). Changing climatic conditions in the basin include the increase in base flow that was observed across the basin (figs. 5–7). The increasing

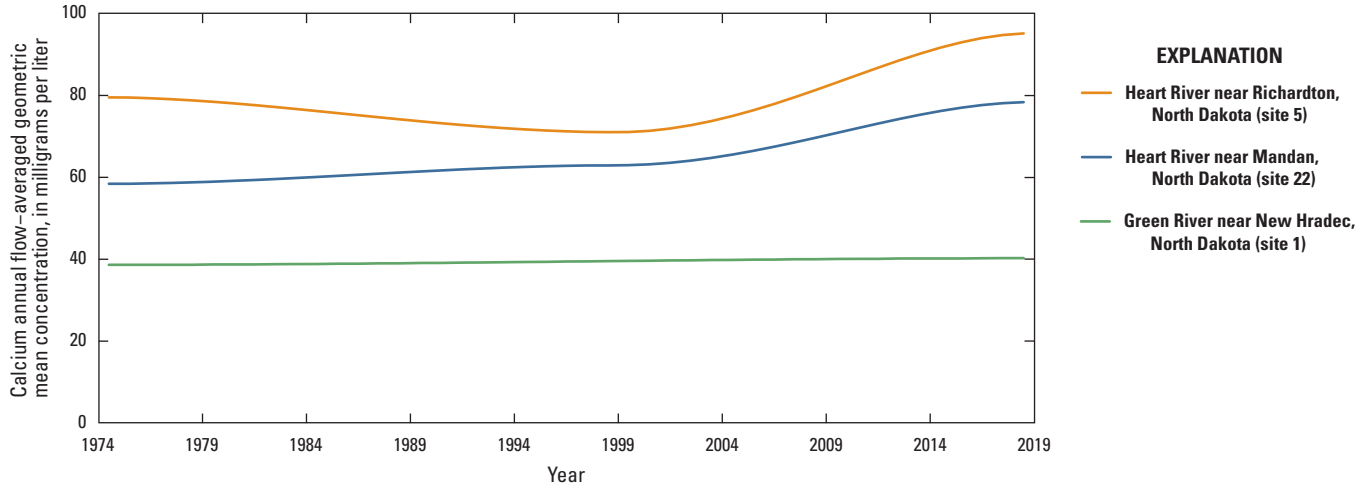

Figure 16. Fitted trend for calcium in annual flow-averaged geometric mean concentration of calcium at three sites in the Heart River Basin for the historical trend period (1974–2019).

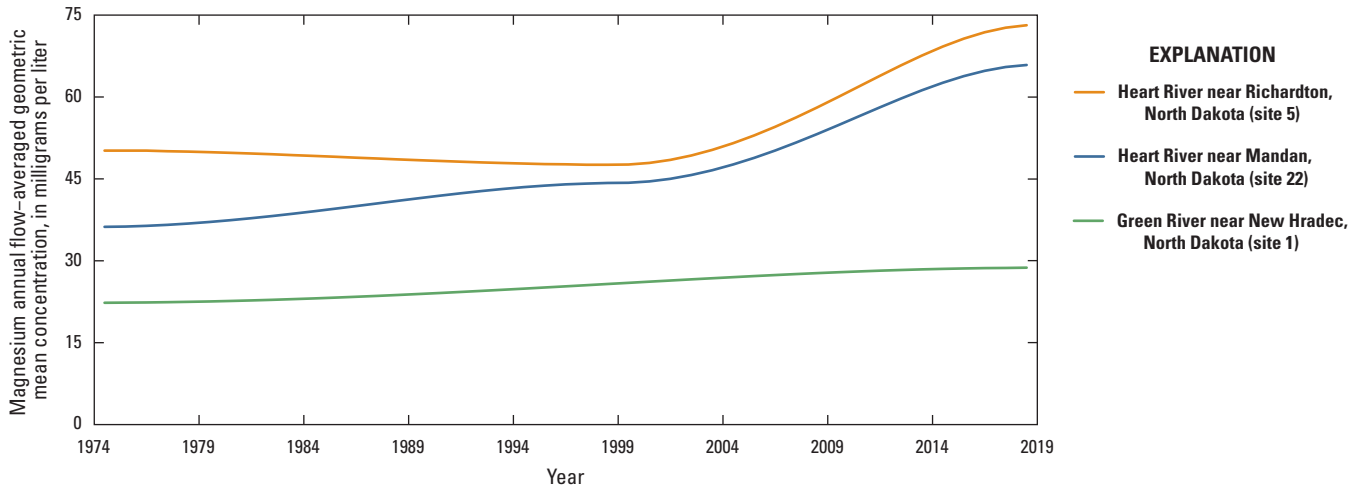

Figure 17. Fitted trend for magnesium in annual flow-averaged geometric mean concentration of magnesium at three sites in the Heart River Basin for the historical trend period (1974–2019).

base flow likely affects the increasing concentrations in calcium and magnesium because both are present in the aquifer materials (Trapp and Croft, 1975; Naplin and Shaver, 1978; Randich, 1979; Ackerman, 1980). The most common soluble salts in soils in the basin were sodium-, calcium-, and magnesium-sulfates (Keller and others, 1986a). Dissolution of these calcium- and magnesium-sulfates owing to wetter conditions was likely contributing to the increasing concentrations.

Results of the historical trend analysis of SAR values detected significant increases basinwide since the mid-1970s (fig. 18, table 5). Site 1 had a significant 19-percent increase where the FAGMC increased from 4.1 to 4.9 from 1974 to 2019 (table 5). Site 5 had a significant 25-percent increase where the FAGMC increased from 4.6 to 5.8 from 1974 to 2019 (table 5). Site 22, the farthest downstream site on the Heart River, had a significant 35-percent increase in SAR, where the FAGMC increased from 4.3 to 5.8 from 1974 to 2019 (table 5). The magnitude of the increases in SAR was greater in the lower basin at site 22 (35 percent) compared to the upper basin at site 1 (19 percent) (table 5).

Increasing values of SAR were observed basinwide during the recent trend periods (table 5). Both tributary sites (sites 1 and 10) had nonsignificant increases and both Heart River sites (site 5 and 22) had significant increases. The percentage change of the increases was similar at sites 1, 5, and 22 (13, 10, and 17 percent, respectively) and site 10 had a smaller percentage increase (4 percent). The smallest increase occurred at site 10 on Antelope Creek, but overall by the end of the trend period the tributary sites (sites 1 and 10) had lower SAR values than main-stem sites (sites 5 and 22) and Heart River sites had values approaching the recommended SAR value threshold of 6 (Scherer and others, 2017).

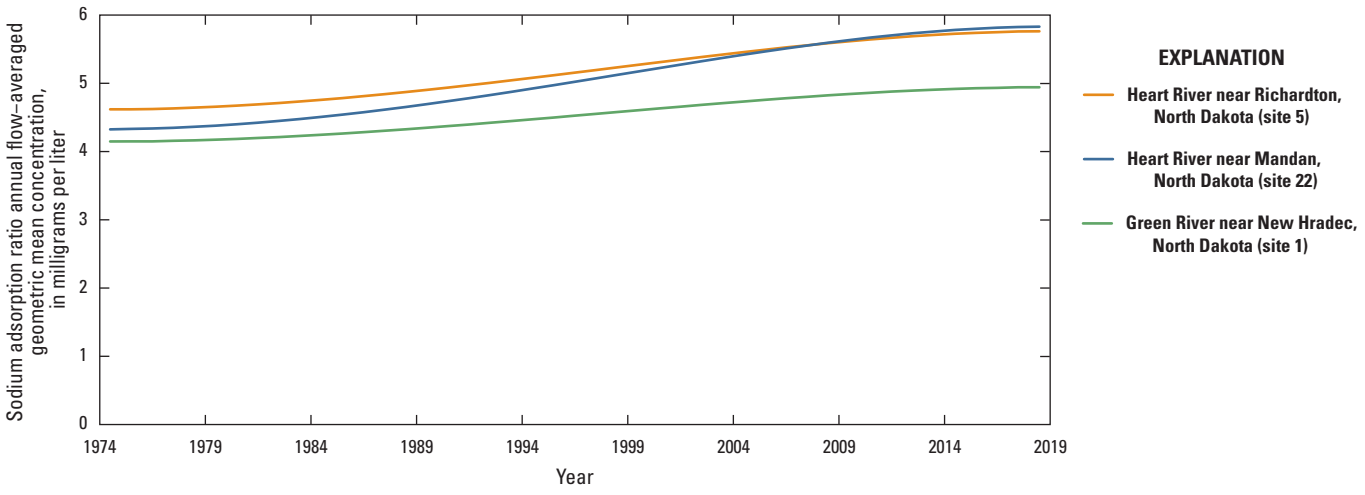

Figure 18. Fitted trend for sodium adsorption ratio in annual flow-averaged geometric mean value of sodium adsorption ratio at three sites in the Heart River Basin for the historical trend period (1974–2019).

Because SAR is computed as the ratio of sodium to calcium and magnesium in the soil water, increasing concentrations in these constituents resulted in increasing SAR values. SAR is an indicator used in the management of irrigation water along with TDS and specific conductance. In North Dakota, the recommendation is that for continuous irrigation SAR should remain below 6 mg/L (Scherer and others, 2017). Poorer quality water may be used for irrigation on land that is irrigated sporadically, which is defined as 1 year out of every 3 or more years (Scherer and others, 2017). The small to moderate trends observed in SAR were a function of sodium, magnesium, and calcium each having positive trends. SAR is related to all of those constituents and with each having a different positive trend, the effect on the overall SAR was reduced. If the changes occurred in only one or two of the constituents, it would have a greater effect on the SAR trend. A difference in the SAR trends compared to the other constituents was that site 22 had the largest magnitude increase. Site 5 consistently had the largest increases with the other constituents, but not the largest increase in SAR. Results of the trend analysis at site 5 and 22 were similar for sodium, calcium, and magnesium (table 5). Sodium concentrations were similar at sites 5 and 22, but site 22 had lower concentrations for calcium and magnesium, which corresponded to larger SAR values.

Nutrients

Unlike TDS and dissolved ion concentrations, significant increases in nutrient concentrations were not detected from 1999 to 2019, and nitrate plus nitrite concentrations most likely decreased upstream from Lake Tschida (table 6). Because of limited data availability, only nitrate plus nitrite and total phosphorus at two sites for the recent trend period could be analyzed. Additionally, because 55 percent of the nitrate plus nitrite data for site 5 were censored and 41 percent of the nitrate plus nitrite data were censored for site 22, results should be interpreted with caution (table 1.2). No significant changes in nutrient concentrations were detected in the Heart River Basin during the recent trend period (table 6). Site 5, upstream from Lake Tschida, had a 47-percent decrease in nitrate plus nitrite concentrations (table 6). From visual inspection of the nitrate plus nitrite data for site 5 (not shown), most of the censored values occurred toward the end of the trend period, supporting the trend result of decreasing concentrations. Nonsignificant changes do not necessarily mean that a trend is not present, but variability in the data combined with a small trend can make a trend undetectable. Results from site 22, the most downstream site, indicate that the nutrient concentrations did not have significant changes in the lower basin.

Trend results did not indicate increasing concentrations of nitrate plus nitrite and total phosphorus concentrations on the two Heart River sites (sites 5 and 22), but anthropogenic changes, conservation practices, and land use can affect nutrients in the basin. When nutrients become overabundant in lakes and reservoirs, harmful algal blooms can form (Paerl and others, 2001). Anthropogenic changes in nutrient concentrations can be related to crop management, livestock, fertilizers, land-use changes, geology, and industrial or municipal effluents (Hem, 1985; Tornes and Brigham, 1993; Dubrovsky and others, 2010). Crop and livestock management practices can also affect nutrient concentrations through the application of fertilizer and runoff from feed lots (Hem, 1985; Tornes and Brigham, 1993). Conservation practices are implemented to limit the amount of nutrients being transported to streams and lakes. Between 2006 and 2020, conservation practices to reduce nutrients were applied to about 128,000 acres throughout the Heart River Basin (Rita Sveen, NRCS, written commun., 2021). The upper basin has a higher percentage of agricultural land use than the lower basin does (fig. 2*B*), which likely corresponds to more acres in the upper basin with conservation practices being implemented. Site 5, located in the upper basin, had decreasing nitrate plus nitrite concentrations, which may be related to conservation practices implemented in the upper basin. Nutrient dynamics are complex and may vary over time and location. Increased energy production in the western portion of the basin may contribute to the nitrate plus nitrite concentrations in the basin (U.S. Energy Information Administration, 2013) because the burning of fossil fuels, such as coal or petroleum products, release nitrogen into the atmosphere (Hem, 1985).

Table 6. Summary of recent (1999–2019) trend results for nitrate plus nitrite and total phosphorus at selected sites in the Heart River Basin.

[USGS, U.S. Geological Survey; *p*-value, probability value; FAGMC, flow-averaged geometric mean concentration, in milligrams per liter]

Site number (fig. 1)	USGS site number	Site name	Trend model	Trend period	*p*-value	Significance level	Annual FAGMC for first year in trend period	Annual FAGMC for last year in trend period	Change, in percent from first to last year[1]
Nitrate plus nitrite, in milligrams per liter									
5	06345500	Heart River near Richardton, N. Dak.	One	1999–2019	0.0507	Nonsignificant decrease	0.11	0.059	−47
22	06349000	Heart River near Mandan, N. Dak.	One	1999–2019	0.7150	Nonsignificant increase	0.099	0.107	8
Total phosphorus, in milligrams per liter									
5	06345500	Heart River near Richardton, N. Dak.	One	1999–2019	0.1785	Nonsignificant decrease	0.051	0.043	−16
22	06349000	Heart River near Mandan, N. Dak.	One	1999–2019	0.7744	Nonsignificant increase	0.027	0.028	3

[1]Percentage change values are directly calculated from R–QWTREND. Starting and ending concentrations in table are rounded and may not produce the exact percentage change.

Geochemical Changes in Salinity

Increasing dissolved ion concentrations (except potassium) were detected in the Heart River Basin during the last several decades. The major concern for agricultural producers and water-resource managers in the basin is increasing salinity. Possible geochemical controls on these water-quality trends could be from minerals present in soils, bedrock geology, or agricultural products (table 3). Four sulfate evaporite minerals (mirabilite, thenardite, konyaite, and gypsum) are present in the basin soils (Keller and others, 1986a); minerals present in bedrock geology include calcite, dolomite, quartz, potassium feldspar (K-feldspar), biotite, Na-montmorillonite, calcium montmorillonite (Ca-montmorillonite), and illite. Sylvite was used to model the agricultural practices because sylvite is an additive in many fertilizers in the basin (Franzen and Bu, 2018). Sylvite is the only mineral that has chloride in its composition, and although there are likely other sources in the basin, these contribute small amounts owing to small chloride concentrations basinwide. Using the inverse modeling function in PHREEQC, the chemical reactions controlling geochemistry in the Heart River Basin were evaluated.

Results of the PHREEQC inverse modeling are presented in tables 7–9, showing all reasonable models explaining geochemical reactions controlling concentrations of dissolved ions in the Heart River Basin. Positive values of mole transfers indicate dissolution of the mineral and negative values of mole transfers indicate precipitation of the mineral. Clay minerals, K-feldspar, and biotite cannot dissolve or precipitate in the same way as other minerals with total dissociation, but these minerals can gain or lose potassium as the mineral changes. These minerals were examined in pairs such that positive mole transfers of K-feldspar or biotite and negative mole transfers of illite or montmorillonite would indicate the hydrolysis of those minerals.

Model Zone 1

Inputs for the PHREEQC inverse model for model zone 1 (Heart River reach from site 5 to site 6; fig. 1) included minerals, dissolution or precipitation assumptions, and uncertainty terms. The 11 minerals included in model zone 1 for both model periods were mirabilite, thenardite, konyaite, gypsum, sylvite, calcite, dolomite, quartz, K-feldspar, Na-montmorillonite, and illite (Keller and others, 1986a; Fenner, 1974; Jacob, 1975; Brekke, 1979; Granato and others, 2015). Within the shales and sandstones of Bullion Creek Formation that underlies model zone 1, gypsum, calcite, dolomite, quartz, K-feldspar, Na-montmorillonite, and illite are present (Brekke, 1979). From the dissolution plots at site 5, it was determined that mirabilite, thenardite, konyaite, sylvite, calcite, and dolomite were most likely dissolving (fig. 19*A–F*). The SI values for mirabilite and thenardite from PHREEQC of approximately −5 and −7, respectively, indicated dissolution of these minerals. The SI values for sylvite were less than zero, indicating dissolution, and the dissolution plot for sylvite also indicates dissolution as the data plots close to the line (fig. 19*D*). The sample selection for model zone 1 was determined by the trend analysis completed at site 5. Two samples were selected for sites 5 and 6 for each model period (table 7). The uncertainty term specified for period 1 was 2.5 percent and for period 2 was 10 percent. The uncertainty terms for each model were low, reflecting the quality of the methods used to collect the data.

From PHREEQC inverse modeling for period 1 (1974–99) and model zone 1, eight reasonable models indicated that the clay mineral-water interactions and dissolution of evaporites control the geochemistry (table 8); however, some models have lower residuals (for example, model 5 has a model residual of 2.6), indicating less adjustment of selected water-quality samples, so all eight models were taken into consideration when interpreting geochemical changes. Hydrolysis of K-feldspar to clays in the Bullion Creek Formation was determined to be a control on potassium concentrations as seen in the positive mole transfers of K-feldspar in five models and the negative mole transfers of illite, which occurred in all eight models (table 8). The dissolution of sylvite, as seen in every model with 0.18 millimole per kilogram of water (mmol/kg H_2O) of sylvite dissolving, indicates that agricultural fertilizers were another source of potassium and likely the main source of chloride in the system. The amount of konyaite, mirabilite, and thenardite dissolving during this period ranged from 0.50 to 1.16 mmol/kg H_2O. Dissolution of konyaite, mirabilite, and thenardite was the major source of sodium, sulfate, and magnesium in the system because one of these minerals was dissolving in 7 of 8 models. Dolomite and calcite were sources of magnesium, calcium, and dissolution of these minerals, which occurred in 4 out of 5 models, accounting for the increases in concentrations of magnesium and calcium in the Heart River. The amount of gypsum precipitating ranged from 0.81 to 2.2 mmol/kg H_2O, and precipitation occurred in 7 of 8 models (table 8). From trend analysis, the sulfate concentration was unchanging and calcium concentrations were slightly decreasing during this period, which was most likely caused by the precipitation of gypsum.

Results of the inverse modeling for period 2 (1999–2019) for model zone 1 had eight reasonable models that indicated that the dissolution of evaporites was the major geochemical control (table 8). Three major differences were observed in period 2 compared to period 1: (1) gypsum was dissolving in five models, (2) dissolution of sylvite was the dominant source of potassium over hydrolysis of K-feldspar (reduction of approximately 98 percent in K-feldspar mole transfers), and (3) evaporite (konyaite, mirabilite, and thenardite) dissolution was 50 percent greater compared to period 1. Dissolution of gypsum, konyaite, mirabilite, and thenardite increased from an average of about 0.9 mmol/kg H_2O in period 1 to about 1.45 mmol/kg H_2O in period 2 and was the major source of calcium, sodium, sulfate, and magnesium (table 8). Dissolution of dolomite, ranging from 0.67 to 1.72 mmol/kg H_2O, was another major source of magnesium in the system

Table 7. Summary of water-quality samples used for model zone 1 and 2 for each PHREEQC modeling period.

[°C, degree Celsius; mg/L, milligram per liter; --, no data]

Model zone	Model period	Date	Site	pH (standard units)	Temperature (°C)	Concentration (mg/L)								Saturation indices					
						Sodium	Potassium	Calcium	Magnesium	Chloride	Bicarbonate	Silica	Sulfate	Mirabilite	Thenardite	Gypsum	Sylvite	Calcite	Dolomite
1	1974–99	3/21/1975	5	8.2	0	160	6.8	64	36	9.8	299	4.3	400	−4.60	−6.81	−1.13	−8.20	0.47	0.62
1	1974–99	4/13/1992	6	8.4	0.5	210	7.6	55	35	16	386	2.1	410	−4.39	−6.57	−1.20	−7.95	0.71	1.15
2	1974–99	4/11/1989	20	8.5	4	150	7	47	28	6.5	335	4.7	280	−7.27	−7.27	−1.39	−8.38	0.77	1.33
2	1974–99	8/29/1979	21	8.4	21	150	5.1	40	19	6	370	4.5	180	−7.45	−7.45	−1.67	−8.64	0.92	1.82
2	1974–99	9/30/1997	22	8.42	14	209	7.8	58	41	17.6	428	--	470	−6.83	−6.83	−1.21	−7.98	0.97	1.99
1	1999–2019	4/7/1998	5	7.9	4	148	7.6	61	31	10.3	244	--	490	−4.80	−6.79	−1.09	−8.16	0.12	−0.04
1	1999–2019	8/29/2011	6	8.5	23.3	234	9.6	95	70.8	17.5	377	4.79	717	−5.32	−6.31	−0.94	−7.96	1.26	2.71
2	1999–2019	8/27/2003	20	8.6	24	203	11.8	58	42.1	11.3	309	5.47	420	−6.90	−6.90	−1.28	−8.04	1.14	2.46
2	1999–2019	8/18/2005	21	8.8	24	266	9.6	38	35.8	9.1	398	6.47	475	−6.62	−6.61	−1.44	−8.23	1.21	2.73
2	1999–2019	7/23/2019	22	8.5	24.2	319	15.3	67	55.4	13.5	432	9.64	753	−6.33	−6.33	−1.08	−7.88	1.17	2.58

Table 8. Summary of PHREEQC inverse model results for model zone 1, periods 1 (1974–99) and 2 (1999–2019).

[Negative values indicate precipitation of the given mineral and positive values indicate dissolution of that mineral. mmol/kg H_2O, millimole per kilogram of water; --, no data; Na, sodium; K, potassium; CO_2, carbon dioxide; g, gaseous]

Mineral	Assumption	Model							
		1	2	3	4	5	6	7	8
Model zone 1, period 1—Mole transfers (mmol/kg H_2O)									
Mirabilite	Dissolution	1.2	--	0.89	--	--	--	--	--
Thenardite	Dissolution	--	--	--	--	--	--	1.2	0.89
Konyaite	Dissolution	--	--	--	0.79	1.2	0.50	--	--
Gypsum	--	−1.0	--	−0.81	−1.4	−2.2	−0.90	−1.0	−0.81
Sylvite	Dissolution	0.18	0.18	0.18	0.18	0.18	0.18	0.18	0.18
Calcite	--	0.81	−2.1	--	1.2	3.1	--	0.81	--
Dolomite	--	--	1.9	0.58	--	−1.1	0.68	--	0.58
Quartz	--	−0.068	−7.2	−2.3	−3.1	−0.068	−4.6	−0.068	−2.3
K-feldspar	--	--	4.4	1.3	1.8	--	2.8	--	1.3
Na-montmorillonite	--	0.25	5.6	1.9	2.5	0.25	3.6	0.25	1.9
Illite	--	−0.26	−7.6	−2.5	−3.3	−0.26	−4.9	−0.26	−2.5
CO_2(g)	--	0.55	--	--	--	0.55	--	0.55	--
Residuals	--	3.1	10	4.4	3.6	2.7	2.9	3.1	4.4
Uncertainty term, in percent	--	2.5	2.5	2.5	2.5	2.5	2.5	2.5	2.5
Model zone 1, period 2—Mole transfers (mmol/kg H_2O)									
Mirabilite	Dissolution	1.5	--	1.5	--	--	--	--	--
Thenardite	Dissolution	--	--	--	--	--	--	1.5	1.5
Konyaite	Dissolution	--	1.5	--	1.3	1.5	1.3	--	--
Gypsum	--	1.1	--	1.1	--	--	--	1.1	1.1
Sylvite	Dissolution	0.20	0.20	0.20	0.20	0.20	0.20	0.20	0.20
Calcite	--	−2.0	1.1	−2.0	--	1.1	--	−2.0	−2.0
Dolomite	--	1.7	--	1.7	0.67	--	0.67	--	1.7
Quartz	--	0.049	0.049	--	0.49	--	--	0.059	--
K-feldspar	Dissolution	--	--	0.030	--	0.030	0.030	--	0.030
Na-montmorillonite	--	0.25	0.25	0.29	--	0.29	0.29	0.25	0.29
Illite	--	−0.25	--	−0.30	−0.25	−0.30	−0.30	−0.25	−0.30
CO_2(g)	--	--	--	--	--	--	--	--	--
Residuals	--	4.7	7.4	4.7	6.3	7.4	6.3	4.7	4.7
Uncertainty term, in percent	--	10	10	10	10	10	10	10	10

Table 9. Summary of PHREEQC inverse model results for model zone 2, periods 1 (1974–99) and 2 (1999–2019).

[Negative values indicate precipitation of the given mineral and positive values indicate dissolution of that mineral. mmol/kg H_2O, millimole per kilogram of water; --, no data; Ca, calcium; CO_2, carbon dioxide; g, gaseous]

Mineral	Assumption	Model										
		1	2	3	4	5	6	7	8	9	10	11
Model zone 2, period 1—Mole transfers (mmol/kg H_2O)												
Mirabilite	Dissolution	1.6	--	--	1.7	1.7	--	--	--	--	--	--
Thenardite	Dissolution	--	1.6	--	--	--	1.7	1.7	--	--	--	--
Konyaite	--	--	--	1.1	--	--	--	--	--	--	--	--
Gypsum	Dissolution	--	--	0.48	0.91	0.91	0.91	0.91	--	--	--	--
Sylvite	Dissolution	0.31	0.31	0.33	0.33	0.33	0.33	0.33	--	--	--	--
Calcite	Precipitation	--	--	--	--	−0.60	--	−0.60	--	--	--	--
Dolomite	Precipitation	--	--	--	−0.65	--	−0.65	--	--	--	--	--
Quartz	--	−0.55	−0.55	−0.22	−1.2	−0.77	−1.2	−0.77	--	--	--	--
Biotite	Dissolution	0.25	0.25	0.055	0.64	0.39	0.64	0.39	--	--	--	--
Ca-Montmorillonite	--	0.79	0.79	0.49	1.2	0.90	1.2	0.90	--	--	--	--
Illite	--	−0.91	−0.91	−0.52	−1.5	−1.1	−1.5	−1.1	--	--	--	--
CO_2(g)	--	1.5	1.5	--	2.2	1.5	2.2	1.5	--	--	--	--
Residual	--	4.5	4.5	9.3	3.1	3.1	3.1	3.1	--	--	--	--
Uncertainty term, in percent	--	7.5	7.5	7.5	7.5	7.5	7.5	7.5	--	--	--	--
Model zone 2, period 2—Mole transfers (mmol/kg H_2O)												
Mirabilite	Dissolution	--	--	--	--	2.9	--	--	--	2.3	1.6	2.9
Thenardite	Dissolution	2.9	2.9	--	--	--	--	2.3	1.6	--	--	--
Konyaite	--	--	--	0.79	0.81	--	0.79	--	--	--	--	--
Gypsum	Dissolution	0.24	--	0.73	0.73	--	0.73	0.42	0.68	0.42	0.68	0.24
Sylvite	Dissolution	0.0098	0.062	0.12	0.12	0.063	0.12	0.039	0.12	0.039	0.12	0.010
Calcite	Precipitation	--	--	--	--	--	--	--	--	--	--	--
Dolomite	Precipitation	--	--	--	--	--	--	--	--	--	--	--
Quartz	--	−0.18	−0.26	--	0.053	−0.26	--	−0.099	−0.40	−0.099	−0.40	−0.18
Biotite	Dissolution	0.17	0.21	0.036	--	0.21	0.037	0.11	0.28	1.1	0.28	0.17
Ca-Montmorillonite	--	--	0.21	--	--	0.21	−0.016	−0.049	0.30	−0.049	0.30	--
Illite	--	−0.074	−0.30	−0.016	--	−0.30	--	--	−0.43	--	−0.43	−0.074
CO_2(g)	--	2.0	2.0	--	--	2.0	--	1.6	--	1.6	--	2.0
Residual	--	7.9	5.9	4.4	4.9	5.9	4.8	8.8	5.9	8.8	5.9	7.9
Uncertainty term, in percent	--	7.5	7.5	7.5	7.5	7.5	7.5	7.5	7.5	7.5	7.5	7.5

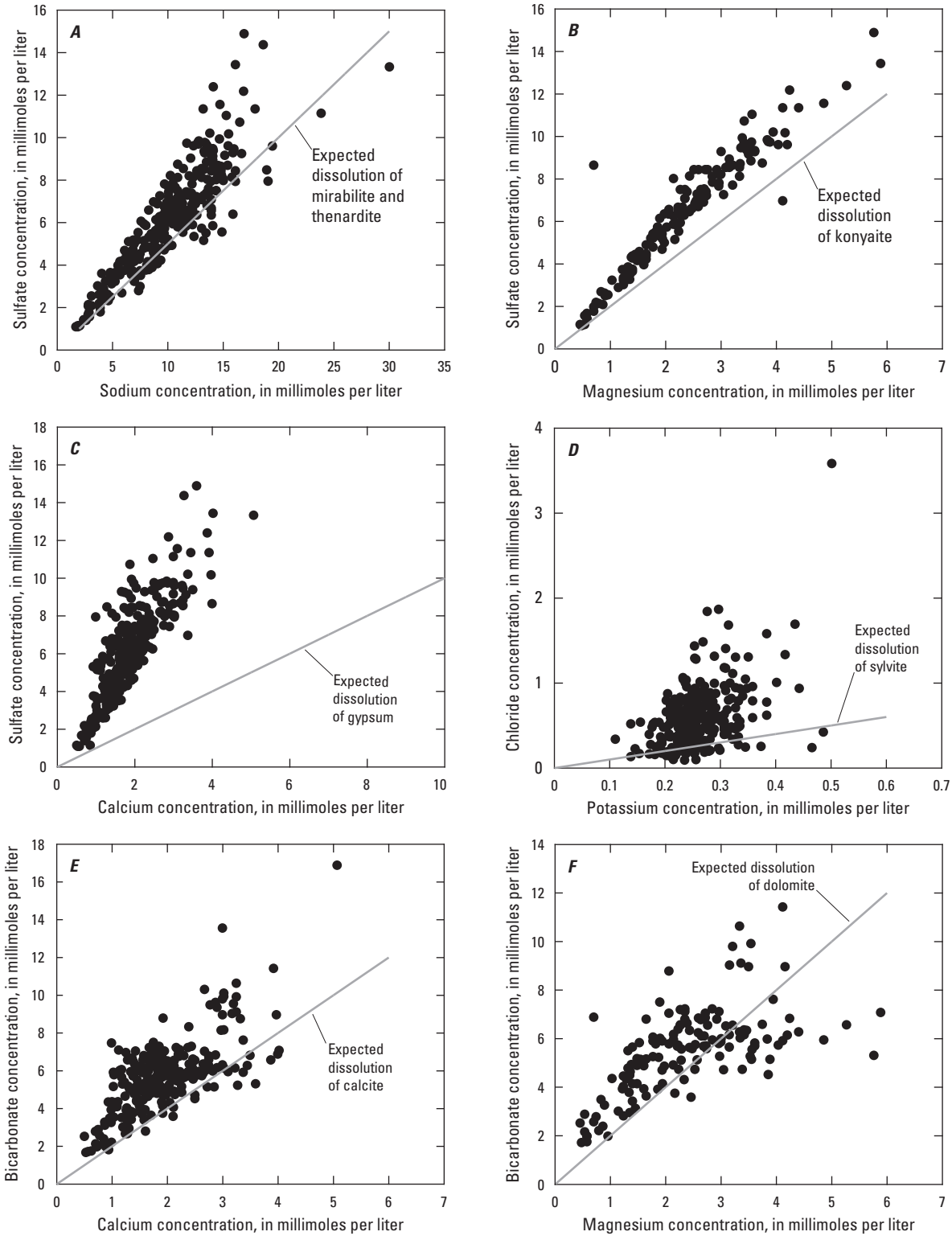

Figure 19. Geochemical plots to determine the minerals that were dissolving at Heart River near Richardton, North Dakota (site 5). *A*, sodium compared to sulfate with expected dissolution of mirabilite and thenardite; *B*, magnesium compared to sulfate with expected dissolution of konyaite; *C*, calcium compared to sulfate with expected dissolution of gypsum; *D*, potassium compared to chloride with expected dissolution of sylvite; *E*, calcium compared to bicarbonate with expected dissolution of calcite; and *F*, magnesium compared to bicarbonate with expected dissolution of dolomite.

and occurred in five of the models (table 8). Precipitation of calcite occurred in four of the models and was in response to the overabundance of bicarbonate and calcium from the dissolution of dolomite and gypsum. Sylvite dissolution increased from 0.18 to 0.20 mmol/kg H_2O and was the major source of potassium and chloride (table 8). Hydrolysis of K-feldspar was no longer a dominant source of potassium, and this explains why the potassium trends discussed in the "Water-Quality Trends for Selected Sites" section decreased during the later periods in the three-trend model at site 5 (fig 15).

Model Zone 2

Inputs to the inverse geochemical model for model zone 2 required inputs for minerals, precipitation or dissolution assumptions, and uncertainty terms. The 11 minerals included in model zone 2 for both periods were mirabilite, thenardite, konyaite, gypsum, sylvite, calcite, dolomite, quartz, biotite, Ca-montmorillonite, and illite (Keller and others, 1986a, 1986b; Fenner, 1974). The Ludlow and Cannonball Formations underlies model zone 2, and calcite, dolomite, quartz, biotite, Ca-montmorillonite, and illite are present in these formations (Fenner, 1974). From the dissolution plots at site 22, mirabilite, thenardite, konyaite, and sylvite were most likely dissolving (fig. 20). Additional information supported that thenardite and mirabilite were assumed to be dissolving in these models owing to these minerals having a high solubility and each having a SI value less than zero (table 7). No dissolution or precipitation assumption was made for konyaite owing to the mineral having the ability to be stable under multiple conditions that could be present in this system (Keller and others, 1986b). Further investigation determined that calcite and dolomite were likely precipitating owing to SI values greater than zero for the selected samples (table 7). The PHREEQC SI value for sylvite was less than zero and supports the dissolution plot for sylvite (table 7). Sample selection for this model zone was determined from the trend analysis at site 22; two samples were selected from sites 20, 21, and 22 and were used to develop the PHREEQC inverse models (table 7). The sample selected at site 5 was collected in 1998 but was determined to be the most representative sample for the starting water-quality conditions for this model. Uncertainty terms used for both model periods were 7.5 percent to account for the charge balance of the samples.

Results of the geochemical modeling for period 1 (1974–99) produced seven reasonable models, and the geochemical control of the system was the dissolution of the sulfate evaporite minerals of mirabilite, thenardite, konyaite, and gypsum (table 9). Dissolution of either mirabilite, thenardite, or konyaite occurred in each model with amounts of gypsum dissolution less than the other three evaporites. These sulfate evaporite minerals were the likely sources of sulfate, sodium, calcium, and magnesium in the system and likely contributed to the increasing concentrations. Minor components in this system included the conversion of biotite (positive mole transfers in all models) to illite (negative mole transfers in all models), the dissolution of sylvite (all models), the weathering of Ca-montmorillonite (all models), and precipitation of calcite or dolomite (2 of 7 models; table 9).

Geochemical modeling results for period 2 (1999–2019) produced 11 reasonable models that were also controlled by the dissolution of sulfate evaporite minerals (table 9). Mole transfers increased between period 1 and period 2 for the sulfate evaporites of mirabilite, thenardite, and konyaite. Mole transfers for these three sulfate evaporites ranged from 1.1 to 1.7 mmol/kg H_2O during period 1 with a combined average of about 1.40 mmol/kg H_2O and ranged from 0.79 to 2.9 mmol/kg H_2O during period 2 with a combined average of about 2.00 mmol/kg H_2O (table 9). Mole transfers of gypsum decreased from about 0.80 to about 0.55 mmol/kg H_2O between period 1and period 2. Sulfate evaporites likely contributed to increasing concentrations of sulfate, sodium, calcium, and magnesium. Another difference of note is that the dissolution of sylvite decreased from period 1 to period 2 from about 0.32 mmol/kg H_2O to about 0.08 mmol/kg H_2O (table 9). Minor controls on the system for model zone 2 during period 2 included agricultural fertilizers (dissolution of sylvite), conversion of biotite (positive mole transfers in 10 models) to illite and montmorillonite (negative mole transfers in 10 models), and the physical weathering of clay minerals (four models).

Model Comparison

Differences between models in the upper and lower basin (model zones 1 and 2, respectively) indicated that geology controls some of the water-quality changes in the Heart River Basin. Carbonate dissolution was occurring in the upper basin, whereas these minerals generally precipitated out in the lower basin. The dissolution of carbonates in the upper basin likely oversaturated the river in these minerals, causing the precipitation of carbonates in the lower basin. The varying composition of sandstones produced different chemical reactions between zones in the basin. Hydrolysis of K-feldspar had a larger effect in the upper basin compared to the chemical weathering of biotite in the lower basin. Groundwater was not considered because of too few data; therefore, geochemical evolution through the aquifers was not modeled.

Sulfate evaporite minerals in soils in the Heart River had the most geochemical control over the system. In the upper and lower basin, large mole transfers of sulfate evaporites likely were a result of natural climate variations and irrigation practices. An increase in base flow beginning in the 1990s was likely caused by a water table increase, which changes the geochemical evolution of the water (figs. 5–7). In the unsaturated zone, evaporites and other minerals are precipitated and left behind during the infiltration of water. With a groundwater table rise, these evaporites and other minerals are in contact with water, which can begin to dissolve the minerals, increasing the dissolved ion content of the groundwater (fig. 21).

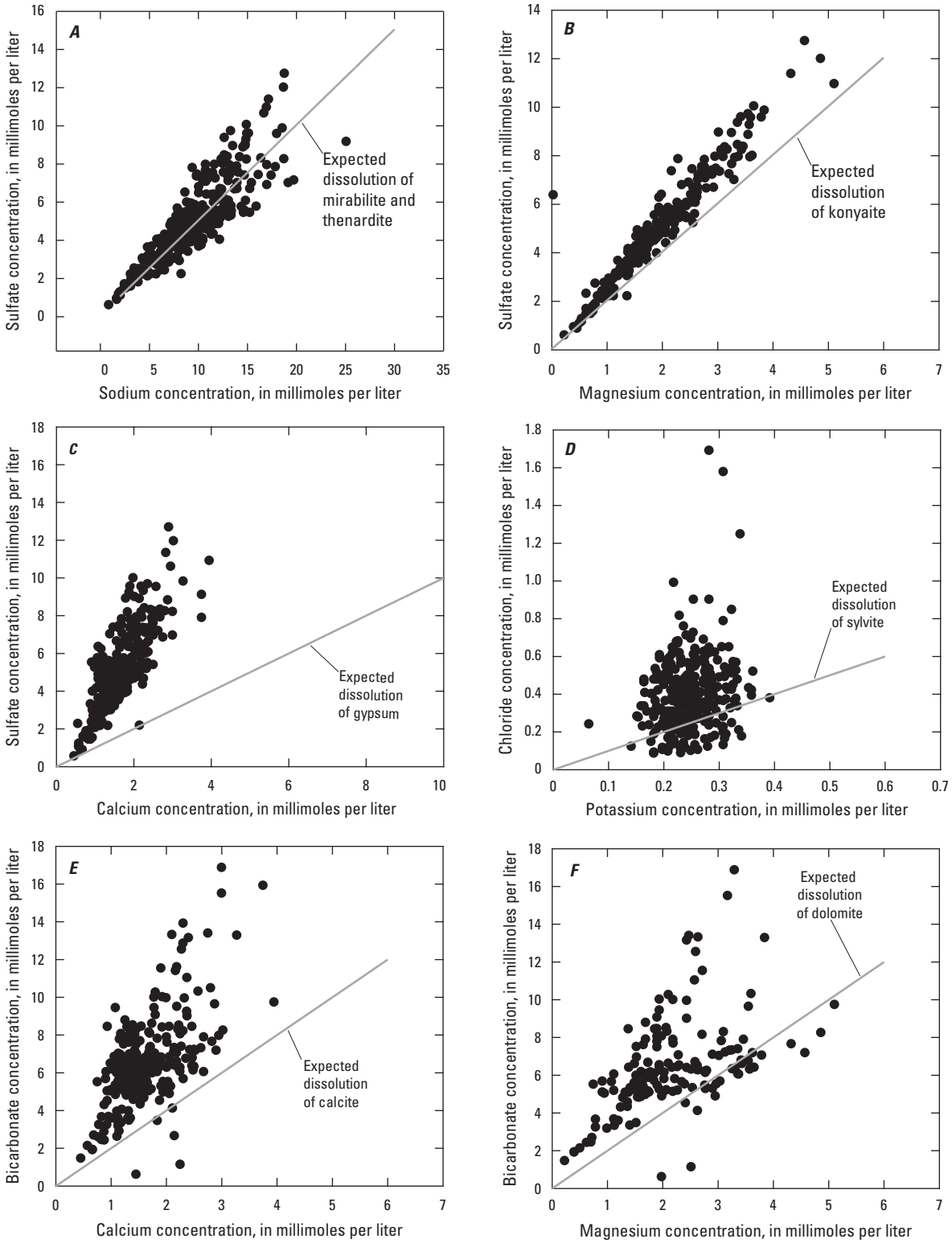

Figure 20. Geochemical plots to determine the minerals that were dissolving at Heart River near Mandan, North Dakota (site 22). *A*, sodium compared to sulfate with expected dissolution of mirabilite and thenardite; *B*, magnesium compared to sulfate with expected dissolution of konyaite; *C*, calcium compared to sulfate with expected dissolution of gypsum; *D*, potassium compared to chloride with expected dissolution of sylvite; *E*, calcium compared to bicarbonate with expected dissolution of calcite; and *F*, magnesium compared to bicarbonate with expected dissolution of dolomite.

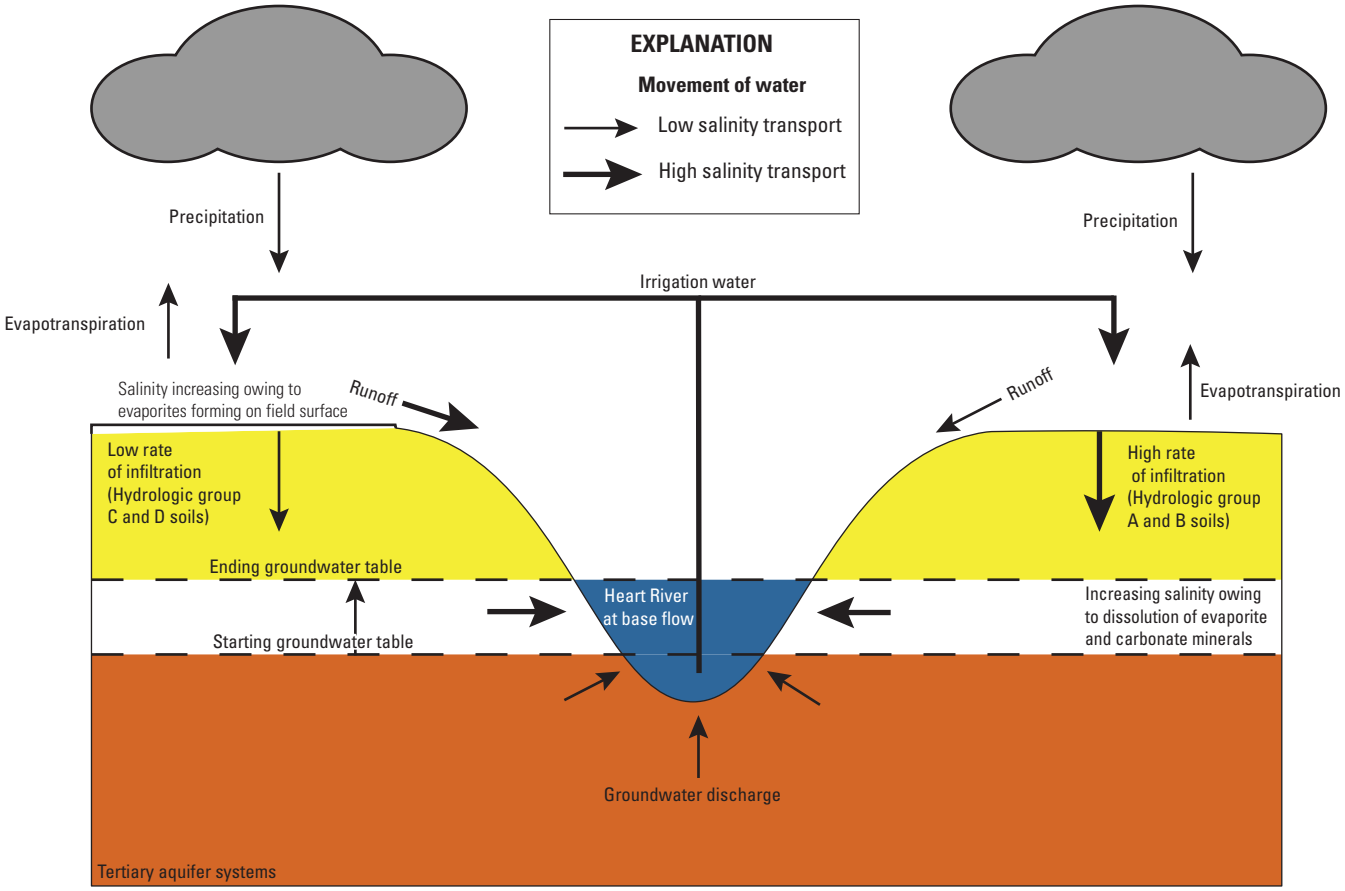

Figure 21. Schematic of processes in a wet climate period that affect the geochemical changes of increasing salinity in the Heart River Basin.

The increase in base flow corresponds to an increase in groundwater discharge into the Heart River Basin, which can increase the loads of the dissolved solids in the streams (fig. 21). The conversion from flood to pivot irrigation can create soil salinity issues at the surface owing to less water infiltrating the soil column (Al-Ghobari, 2011; Shahid, 2013). To manage the development of salts on the surface, more water can be used in irrigation water application to flush the salts below the root zone where accumulation generally happens (Shahid, 2013).

Constituent Loads and Yields

Loads and yields were estimated for selected sites in the Heart River Basin from 2013 to 2020. Loads were estimated for TDS, sulfate, sodium, chloride, and total phosphorus. Monthly, annual, and total loads were computed for each site and constituent, and mean annual yields were computed to normalize loads to the drainage area upstream from the selected sites. Total loads for the period of 2013–20 were used to compute a simplified mass balance in the lower Heart River Basin.

Annual loads estimated for the Heart River from 2013 to 2020 at sites 5 and 22 were generally greatest in 2014 and the least in 2016 for TDS, sulfate, sodium, and chloride (fig. 22 and table 10). Patterns in annual loads were similar to annual streamflow patterns at the two sites. The annual TDS loads for sites 5 and 22 in 2014 were 267,000 and 673,000 tons, respectively, compared to annual loads in 2016 of 36,800 and 102,000 tons, respectively. Similarly, annual sulfate loads for sites 5 and 22 were 168,000 and 415,000 tons in 2014, respectively, and 23,200 and 59,000 tons in 2016, respectively. Annual sodium loads ranged from 8,180 tons (2016) to 51,500 tons (2014) at site 5 and from 23,500 tons (2016) to 140,000 tons (2014) at site 22. Annual chloride loads ranged from 825 tons (2016) to 3,980 tons (2014) at site 5 and from 1,470 tons (2016) to 8,680 tons (2014) at site 22 (fig. 22).

Most of the annual loads of TDS, sulfate, sodium, and chloride are delivered in March through June in the Heart River at sites 5 and 22 likely owing to snowmelt and runoff from rainfall events (fig. 23). Mean monthly TDS ranged from 2,700 tons in December to 26,200 tons in March at site 5 and from 9,090 tons in December to 53,300 tons in March at site 22 (fig. 23*A*). On average, about 58 percent of the annual TDS load moves past sites 5 and 22 on the Heart River in March through June. Mean monthly sulfate, sodium, and chloride loads followed similar patterns as TDS. Monthly sulfate loads ranged from 1,700 tons in December to 15,800 tons in March at site 5 and from 5,180 tons in December to 31,200 tons in April at site 22 (fig. 23*B*). The mean monthly sulfate load at site 22 for March and April was similar at 31,000 tons (fig. 23*B*). Monthly sodium loads ranged from 604 tons in December to 4,790 tons in March at site 5 and from 2,070 tons in December to 10,800 tons in April at site 22 (fig. 23*C*). The mean monthly sodium load at site 22 for March was similar to April at 10,600 tons (fig. 23*C*). Monthly chloride loads ranged from 64 tons in December to 404 tons in March at site 5 and from 132 tons in January to 746 tons in March at site 22 (fig. 23*D*).

The mean annual yields of TDS and sodium between 2013 and 2020 generally were largest in Big Muddy Creek (site 18), whereas yields of sulfate and chloride were largest in Sweetbriar Creek (site 21) compared to the other selected sites in the Heart River Basin (fig. 24 and table 10). Site 18 had a mean annual yield of 124 tons per year per square mile (tons/yr/mi^2) of TDS and 27 tons/yr/mi^2 of sodium (figs. 24*A*, *C* and table 10). The smallest mean annual TDS yields were in the main-stem Heart River (site 20) and Antelope Creek (site 10) at 74 and 79 tons/yr/mi^2, respectively (fig. 24*A* and table 10). The other two main-stem Heart River sites (site 5 and site 22) had mean annual TDS yields of 90 and 87 tons/yr/mi^2, respectively (fig. 24*A* and table 10). The mean annual sodium yield at site 18 was 27 tons/yr/mi^2 compared to Antelope Creek (site 10), which had the smallest mean annual yield among the sites of 12 tons/yr/mi^2 (fig. 24*C* and table 10). The main-stem Heart River sites (site 5, 20, and 22) had mean annual sodium yields of 18, 14, and 18 tons/yr/mi^2, respectively (fig. 24*C* and table 10). The mean annual sulfate yield at site 21 was 87 tons/yr/mi^2 compared to the Heart River (site 20) with the smallest sulfate yield among the sites of 38 tons/yr/mi^2 (fig. 24*B* and table 10). The other two Heart River sites (sites 5 and 22) had mean annual sulfate yields of 56 and 51 tons/yr/mi^2, respectively (fig. 24*B* and table 10). The mean annual chloride yield at site 21 was 1.7 tons/yr/mi^2 compared to Big Muddy Creek (site 18) with the smallest mean annual yield among the sites of 0.9 ton/yr/mi^2 (fig. 24*D* and table 10). In comparison, the main-stem Heart River sites (site 5, 20, and 22) had mean annual chloride yields of 1.6, 1.0 and 1.2 tons/yr/mi^2, respectively (fig. 24*D* and table 10).

Larger yields of TDS, sulfate, sodium, and chloride in sites located on Big Muddy Creek and Sweet Briar Creek in the lower Heart River Basin were likely a result of differences in geology and soils upstream from the selected sites. The presence of the Sentinel Butte Formation in relation to the location of the three major tributaries (Antelope Creek, Big Muddy Creek, and Sweetbriar Creek) in the lower basin may help explain the varying yields among them. Big Muddy Creek and Sweetbriar Creek drain large portions of land overlaying the high sodium-sulfate aquifers of the Sentinel Butte Formation and both sites had larger yields of TDS, sulfate, sodium, and chloride than Antelope Creek (fig. 2*A*). Antelope Creek, which drains a smaller portion of land overlaying Sentinel Butte Formation, had the smallest yields of TDS, sulfate, sodium, and chloride in the lower basin. Antelope Creek, Big Muddy Creek, and Sweetbriar Creek have differences in the hydrologic group soils within each subbasin between well drained A and B group soils and poorly drained C and D soils. Antelope Creek has 46 percent A and B soils and 53 percent C and D soils, whereas Big Muddy and Sweetbriar Creeks have about 20 percent A and B soils and about 80 percent C and D soils (fig. 2*C*; Soil Survey Staff, 2020). Agricultural land use varies within each of the major tributaries, with Antelope Creek, Big Muddy Creek, and Sweetbriar Creek having 63 percent (96,200 acres), 36 percent (110,000 acres), and 50 percent (86,700 acres) agricultural land use, respectively (fig. 2*B*; Homer and others, 2015). Antelope Creek has the most agricultural land use, and the buildup of salts is less likely to occur on the surface owing to well drained soils. In comparison, Big Muddy and Sweetbriar Creeks have less agricultural land compared to Antelope Creek as well as soils that are not drained well, which may lead to a buildup of salts at or near the land surface causing larger yields.

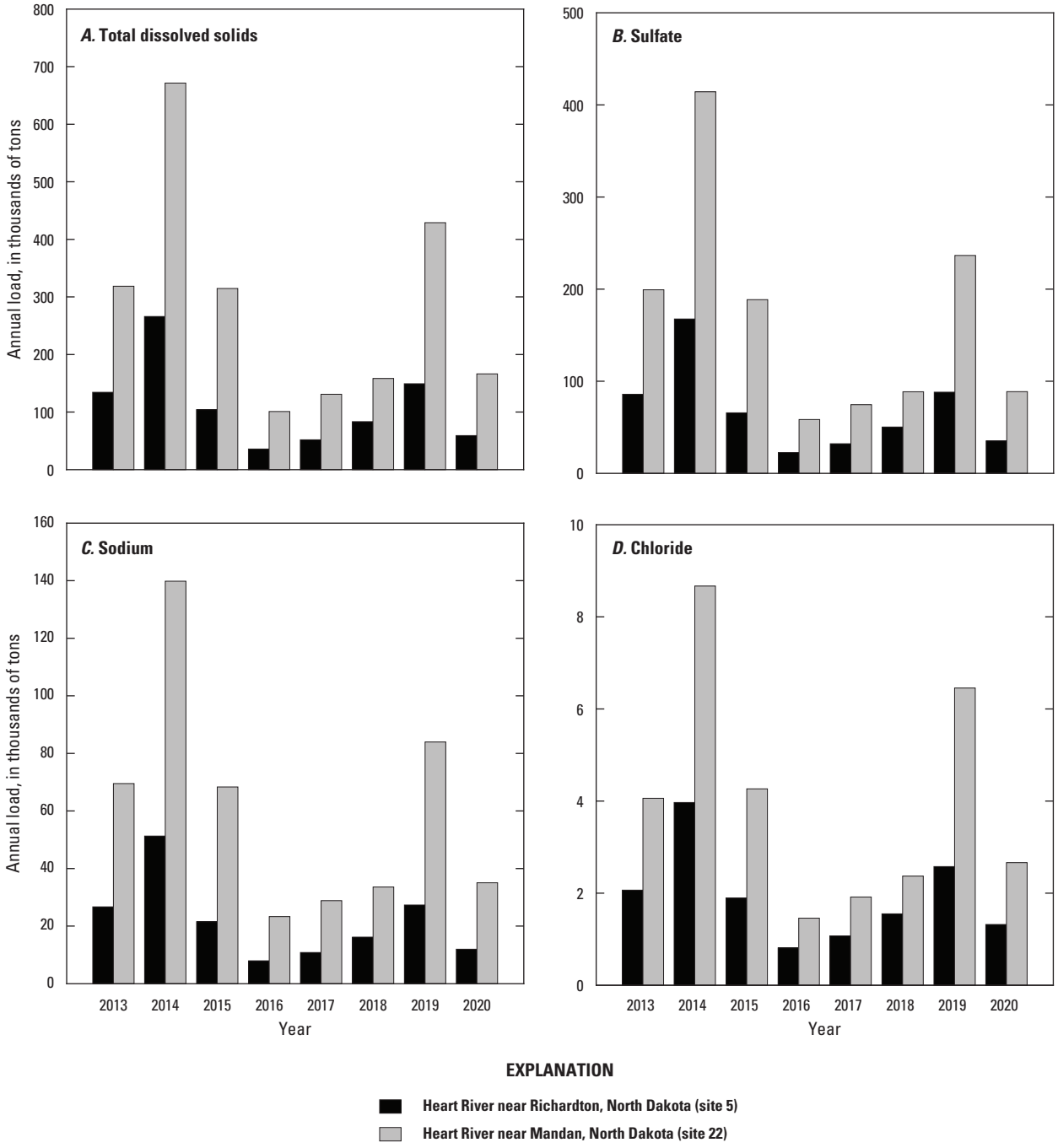

Figure 22. Annual loads for Heart River near Richardton, North Dakota (site 5) and Heart River near Mandan, North Dakota (site 22) between 2013 and 2020. *A*, total dissolved solids; *B*, sulfate; *C*, sodium; and *D*, chloride.

The total loads for TDS, sulfate, sodium, and chloride in the upper Heart River Basin passing site 5 were less than one-half the loads for the entire basin (as measured at site 22, table 10; figs. 22 and 23). The contributing area upstream from site 5 is 1,240 square miles, which is 37 percent of the contributing area for the entire Heart River Basin upstream from site 22. The total loads of TDS, sulfate, sodium, and chloride at site 5 were 39, 41, 36, and 48 percent of the loads at site 22 for 2013–20 (table 10). Loads were reduced from site 5 upstream from Lake Tschida compared to site 7 downstream from the reservoir, likely from processes in the reservoir such as adsorption of cations to suspended and settling sediment in the reservoir owing to the high cation exchange capacity of the bedrock clays in the region (Langmuir, 1997). Total loads between site 5 and site 7 were reduced by 7 percent for TDS, 13 percent for sulfate, 8 percent for sodium, and 19 percent for chloride.

Table 10. Estimated loads and yields in the lower Heart River Basin at selected sites between 2013 and 2020.

[ton/yr/mi^2, ton per year per square mile; lb/yr/mi^2, pound per year per square mile; -- not applicable]

Year	Total dissolved solids		Sulfate		Sodium		Chloride		Total phosphorus	
	Annual load (ton)	Annual yield (ton/yr/mi^2)	Annual load (ton	Annual yield (ton/yr/mi^2)	Annual load (ton)	Annual yield (ton/yr/mi^2)	Annual load (ton)	Annual yield (ton/yr/mi^2)	Annual load (ton)	Annual yield (lb/yr/mi^2)
				Site 5						
2013	135,000	109	86,500	70	26,900	22	2,080	1.7	35	56
2014	267,000	215	168,000	135	51,500	42	3,980	3.2	80	129
2015	105,000	85	66,400	54	21,700	18	1,900	1.5	11	18
2016	36,800	30	23,200	19	8,180	7	825	0.7	1.4	2
2017	53,000	43	32,800	26	11,000	9	1,080	0.9	5.3	8
2018	84,400	68	50,900	41	16,400	13	1,560	1.3	23	37
2019	150,000	121	88,700	72	27,600	22	2,590	2.1	80	129
2020	60,100	48	35,800	29	12,100	10	1,330	1.1	6.6	11
Total	**891,000**	**718**	**552,000**	**445**	**175,000**	**141**	**15,300**	**13**	**242**	**389**
Mean	**111,000**	**90**	**69,000**	**56**	**22,000**	**18**	**1,918**	**1.6**	**30**	**49**
Percentage of total load at site 22	**39**	**--**	**41**	**--**	**36**	**--**	**48**	**--**	**56**	**--**
				Site 7						
2013	57,000	--	29,000	--	10,600	--	730	--	3.2	--
2014	167,000	--	85,400	--	31,000	--	2,130	--	9.7	--
2015	94,900	--	48,400	--	17,700	--	1,220	--	5.4	--
2016	23,900	--	12,100	--	4,540	--	312	--	1.3	--
2017	48,900	--	24,900	--	9,160	--	629	--	2.7	--
2018	67,400	--	34,400	--	12,500	--	857	--	3.9	--
2019	209,000	--	107,000	--	38,200	--	2,620	--	13	--
2020	66,000	--	33,600	--	12,300	--	848	--	3.7	--
Total	**734,000**	**--**	**375,000**	**--**	**136,000**	**--**	**9,350**	**--**	**43**	**--**
Mean	**92,000**	**--**	**47,000**	**--**	**17,000**	**--**	**1,168**	**--**	**5**	**--**
Percentage of total load at site 22	**32**	**--**	**28**	**--**	**28**	**--**	**29**	**--**	**10**	**--**
				Site 10						
2013	21,500	97	11,300	51	2,900	13	291	1.3	3.1	28
2014	41,200	186	21,800	99	5,750	26	529	2.4	7.7	70
2015	15,400	70	7,660	35	2,190	10	198	0.9	1.4	12
2016	4,980	23	2,350	11	721	3	62.9	0.3	0.3	2

Table 10. Estimated loads and yields in the lower Heart River Basin at selected sites between 2013 and 2020.—Continued

[ton/yr/mi², ton per year per square mile; lb/yr/mi², pound per year per square mile; -- not applicable]

Year	Total dissolved solids		Sulfate		Sodium		Chloride		Total phosphorus	
	Annual load (ton)	Annual yield (ton/yr/mi²)	Annual load (ton	Annual yield (ton/yr/mi²)	Annual load (ton)	Annual yield (ton/yr/mi²)	Annual load (ton)	Annual yield (ton/yr/mi²)	Annual load (ton)	Annual yield (lb/yr/mi²)
Site 10—Continued										
2017	3,980	18	1,850	8	596	3	48.3	0.2	0.2	2
2018	8,990	41	4,200	19	1,400	6	102	0.5	0.7	6
2019	31,800	144	15,600	71	5,260	24	328	1.5	7.7	70
2020	11,000	50	5,050	23	1,850	8	115	0.5	1.0	9
Total	**139,000**	**628**	**70,000**	**316**	**21,000**	**94**	**1,670**	**7.6**	**22**	**199**
Mean	**17,000**	**79**	**9,000**	**39**	**3,000**	**12**	**209**	**1.0**	**3**	**25**
Percentage of total load at site 22	**6**	**--**	**5**	**--**	**4**	**--**	**5**	**--**	**5**	**--**
Site 18										
2013	30,400	67	16,400	36	6,850	15	223	0.5	2.2	10
2014	123,000	270	68,900	151	27,000	59	896	2	12	53
2015	59,900	131	32,700	72	13,300	29	439	1	4.9	22
2016	19,100	42	10,100	22	4,350	10	141	0.3	1.2	5
2017	26,600	58	14,300	31	5,990	13	195	0.4	2	9
2018	33,300	73	18,000	39	7,480	16	245	0.5	2.6	11
2019	124,000	272	70,100	154	27,200	60	905	2	13	58
2020	35,100	77	18,900	41	7,900	17	258	0.6	2.6	11
Total	**451,000**	**990**	**249,000**	**547**	**100,000**	**219**	**3,300**	**7.3**	**41**	**178**
Mean annual yield	**56,000**	**124**	**31,000**	**68**	**13,000**	**27**	**413**	**0.9**	**5.1**	**22**
Percentage of total load at site 22	**20**	**--**	**18**	**--**	**21**	**--**	**10**	**--**	**9**	**--**
Site 20										
2013	236,000	81	121,000	41	44,300	15	3,290	1.1	--	--
2014	491,000	168	254,000	87	89,900	31	6,820	2.3	--	--
2015	215,000	73	109,000	37	41,300	14	2,990	1	--	--
2016	69,900	24	34,400	12	14,300	5	981	0.3	--	--
2017	101,000	34	50,700	17	20,100	7	1,420	0.5	--	--
2018	122,000	42	61,500	21	23,600	8	1,700	0.6	--	--
2019	368,000	126	190,000	65	66,600	23	5,100	1.7	--	--
2020	140,000	48	70,600	24	27,400	9	1,960	0.7	--	--

Table 10. Estimated loads and yields in the lower Heart River Basin at selected sites between 2013 and 2020.—Continued

[ton/yr/mi², ton per year per square mile; lb/yr/mi², pound per year per square mile; -- not applicable]

Year	Total dissolved solids		Sulfate		Sodium		Chloride		Total phosphorus	
	Annual load (ton)	Annual yield (ton/yr/mi²)	Annual load (ton	Annual yield (ton/yr/mi²)	Annual load (ton)	Annual yield (ton/yr/mi²)	Annual load (ton)	Annual yield (ton/yr/mi²)	Annual load (ton)	Annual yield (lb/yr/mi²)
Site 20—Continued										
Total	**1,743,000**	**595**	**891,000**	**304**	**328,000**	**112**	**24,300**	**8.2**	**--**	**--**
Mean	**218,000**	**74**	**111,000**	**38**	**41,000**	**14**	**3,030**	**1.0**	**--**	**--**
Percentage of total load at site 22	**76**	**--**	**66**	**--**	**68**	**--**	**76**	**--**	**--**	**--**
Site 21										
2013	28,200	180	16,800	107	5,410	34	323	2.1	4.1	52
2014	47,700	304	28,700	183	8,970	57	554	3.5	8.4	108
2015	25,300	161	14,200	90	4,820	31	274	1.8	4.1	52
2016	8,960	57	5,280	34	1,670	11	102	0.7	1.2	15
2017	11,300	72	7,280	46	2,030	13	140	0.9	1.7	22
2018	11,500	73	7,230	46	2,090	13	139	0.9	1.8	23
2019	33,000	210	20,900	133	6,110	39	404	2.6	6.3	80
2020	13,800	88	9,240	59	2,470	16	178	1.1	2.2	28
Total	**180,000**	**1,145**	**110,000**	**698**	**34,000**	**214**	**2,110**	**14**	**30**	**380**
Mean	**22,000**	**143**	**14,000**	**87**	**4,000**	**27**	**264**	**1.7**	**4**	**48**
Percentage of total load at site 22	**8**	**--**	**8**	**--**	**7**	**--**	**7**	**--**	**7**	**--**
Site 22										
2013	320,000	97	200,000	60	69,700	21	4,070	1.2	37	22
2014	673,000	203	415,000	125	140,000	42	8,680	2.6	140	84
2015	316,000	95	189,000	57	68,500	21	4,280	1.3	24	14
2016	102,000	31	59,000	18	23,500	7	1,470	0.4	1.9	1
2017	132,000	40	75,200	23	29,000	9	1,930	0.6	7.3	4
2018	160,000	48	89,200	27	33,800	10	2,380	0.7	14	9
2019	430,000	130	237,000	72	84,200	25	6,470	2	200	119
2020	168,000	51	89,400	27	35,300	11	2,680	0.8	11	7
Total	**2,301,000**	**695**	**1,354,000**	**409**	**484,000**	**146**	**32,000**	**10**	**435**	**260**
Mean	**288,000**	**87**	**169,000**	**51**	**61,000**	**18**	**4,000**	**1.2**	**54**	**33**

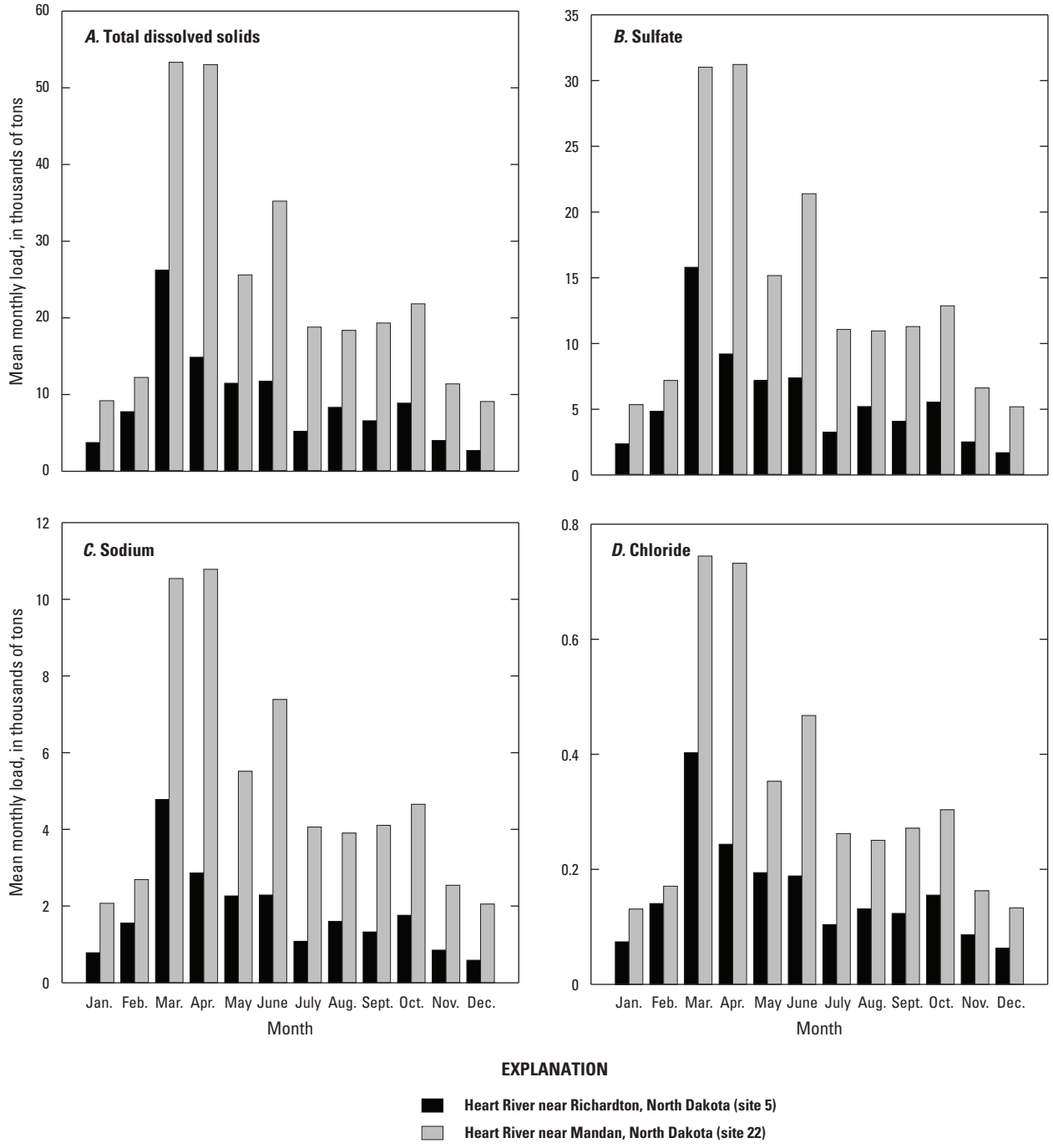

Figure 23. Monthly loads for Heart River near Richardton, North Dakota (site 5) and Heart River near Mandan, North Dakota (site 22) between 2013 and 2020. *A*, total dissolved solids; *B*, sulfate; *C*, sodium; and *D*, chloride.

A mass balance was estimated for TDS, sulfate, sodium, and chloride in the lower basin, specifically the reach on the Heart River from site 7 to site 22 using the total loads computed for 2013–20. Site 7 was selected for the upstream end of the reach to avoid the unknown effects of processes in Lake Tschida that can affect constituent loads. Three major tributaries enter the Heart River in this reach including Antelope Creek (site 10), Big Muddy Creek (site 18), and Sweetbriar Creek (site 21; fig. 4). Many other smaller ephemeral tributaries also enter the reach, but these streams have no data and are included in the intervening load that contributes to the total load calculated at site 22. The intervening load can include groundwater discharge, irrigation return flow, local runoff, and input from smaller ephemeral tributaries. Total loads estimated at sites 7, 10, 18, 21, and 22 were used to determine proportions in each subbasin of TDS, sulfate, sodium, and chloride

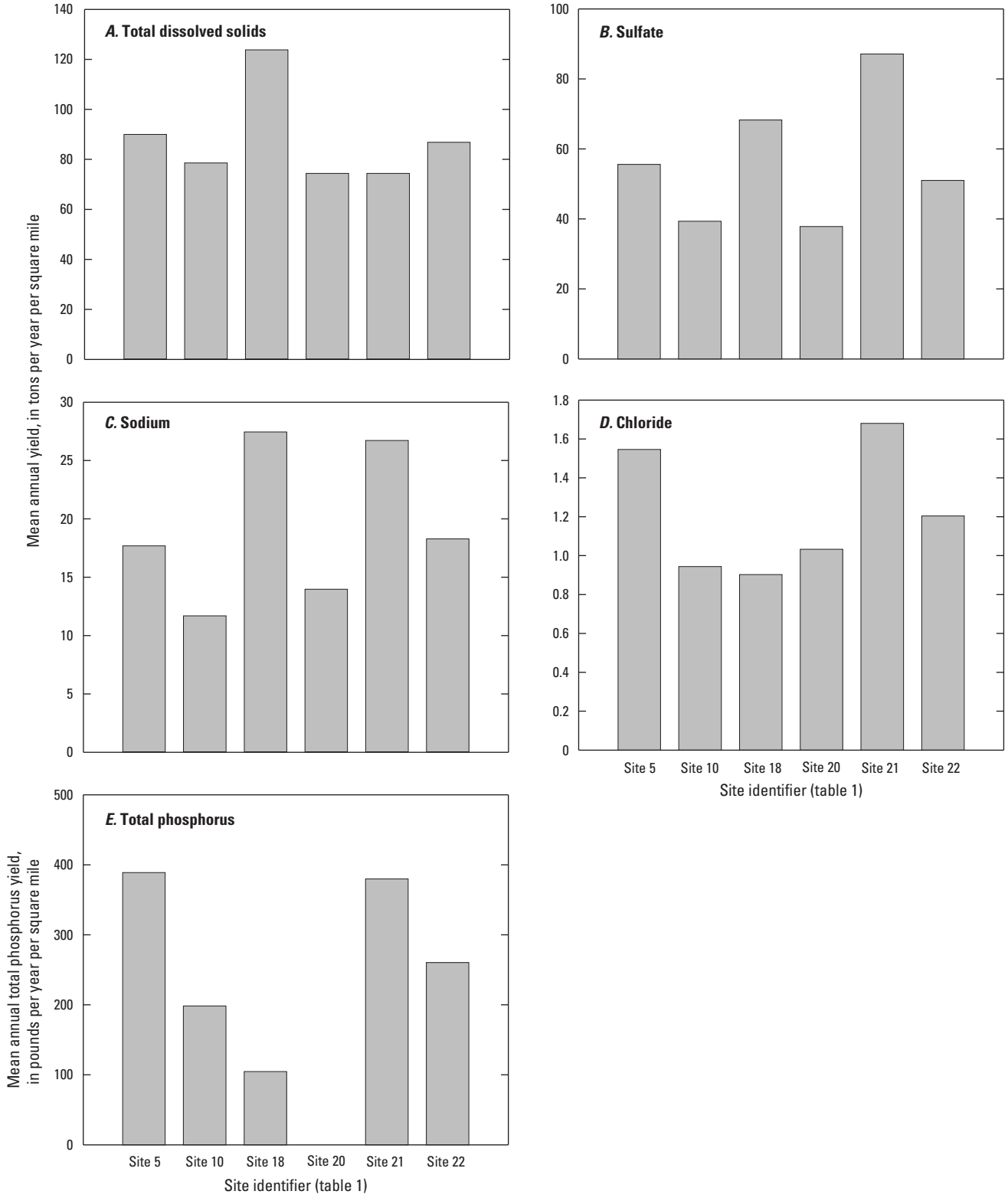

Figure 24. Mean annual yields for the Heart River Basin between 2013 and 2020. *A*, total dissolved solids; *B*, sulfate; *C*, sodium; *D*, chloride; and *E*, total phosphorus.

that contribute to the total load at the downstream end of the Heart River reach (site 22). Total loads were also estimated for the Heart River at site 20 within the reach for comparison to the other sites. Site 20 on the Heart River is located downstream from the confluences of Antelope Creek and Big Muddy Creek with the Heart River and upstream from confluence of Sweetbriar Creek with the Heart River.

In simplified terms, the load is computed as the concentration of a constituent multiplied by the streamflow to determine a mass being transported past a point in the stream represented by the sampling site. Because streamflow delivers the constituent mass in a stream, the percentage of total streamflow volume for the period of 2013–20 was computed for the selected sites from mean annual streamflow values at each site (U.S. Geological Survey, 2020) to compare to the estimated load contributions. Annual contributions of streamflow from various portions of the lower Heart River varied among the years 2013–20, so the total streamflow volume for the entire period was used to look at the contributions of streamflow represented by the selected sites. About 35 percent of the streamflow in the Heart River at site 22 was from the upper Heart River Basin at site 7 (fig. 25; table 11). About 6 percent of the streamflow at site 22 came from Antelope Creek (site 10) and 6 percent from Sweetbriar Creek (site 21) (fig. 25). About 11 percent of the total streamflow at site 22 was from Big Muddy Creek (site 18; fig. 25). About 42 percent of the streamflow in the Heart River at site 22 came from intervening flow such as groundwater discharge, irrigation return flow, local runoff, and smaller unmeasured tributaries (fig. 25). Most of the intervening flow entered the Heart River upstream from site 20 (table 11). The total streamflow volume at site 20 is 86 percent of the streamflow volume at site 22, so 14 percent of the intervening flow entered the Heart River between site 20 and site 22, and 28 percent (42 percent intervening flow at site 22 minus 14 percent intervening flow between site 20 and site 22) of the intervening flow entered the Heart River between site 7 and site 20.

Tributaries in the lower Heart River Basin contributed portions of the total TDS, sulfate, sodium, and chloride loads at the Heart River near Mandan (site 22) that generally were proportional to the streamflow contributions (figs. 25 and 26, table 10). Like the streamflow, 32 percent of the total TDS load in the Heart River at site 22 between 2013 and 2020 came from the upper Heart River Basin at site 7 (figs. 25 and 26). Contributions from Antelope Creek (site 10) and Sweetbriar Creek (site 21) to the total TDS load at site 22 also were similar to the streamflow contributions (figs. 25 and 26, tables 10 and 11). Contributions from Big Muddy Creek (site 18) to the total TDS load were larger than the streamflow contribution at 20 percent compared to 11 percent of the streamflow contributed to site 22 (figs. 25 and 26; tables 10 and 11). About 35 percent of the total TDS load at site 22 came from intervening flows. The Heart River at Stark Bridge (site 20) represented 76 percent of the total TDS load at site 22 (table 10), so 24 percent of the load came into the Heart River downstream from site 20, of which 8 percent was from Sweetbriar Creek (site 21; fig. 26). Sixteen percent of the total TDS load (24 percent of the load downstream from site 20 minus 8 percent of load from site 21) at site 22 came from intervening flow between sites 20 and 22, and the streamflow showed 14 percent of intervening flow in the same reach (figs. 25 and 26, table 10).

Contributions of sulfate, sodium, and chloride loads to the Heart River at the downstream end of the reach (site 22) were similar to the distribution of the TDS loads. Antelope Creek (site 10) represented 5 percent of the sulfate load, 4 percent of the sodium load, and 5 percent of the chloride load in the Heart River at site 22 (fig. 26, table 10). Big Muddy Creek (site 18) represented 18 percent of the sulfate load, 21 percent of the sodium load, and 10 percent of the chloride load in the Heart River at site 22 (fig. 26 and table 10). Sweetbriar Creek (site 21) represented 8 percent of the sulfate load, 7 percent of the sodium load, and 7 percent of the chloride load at site 22. The intervening loads for sulfate and sodium were 41 and 40 percent, respectively, between site 7 and 22. Almost one-half of the total chloride load at site 22 came from intervening

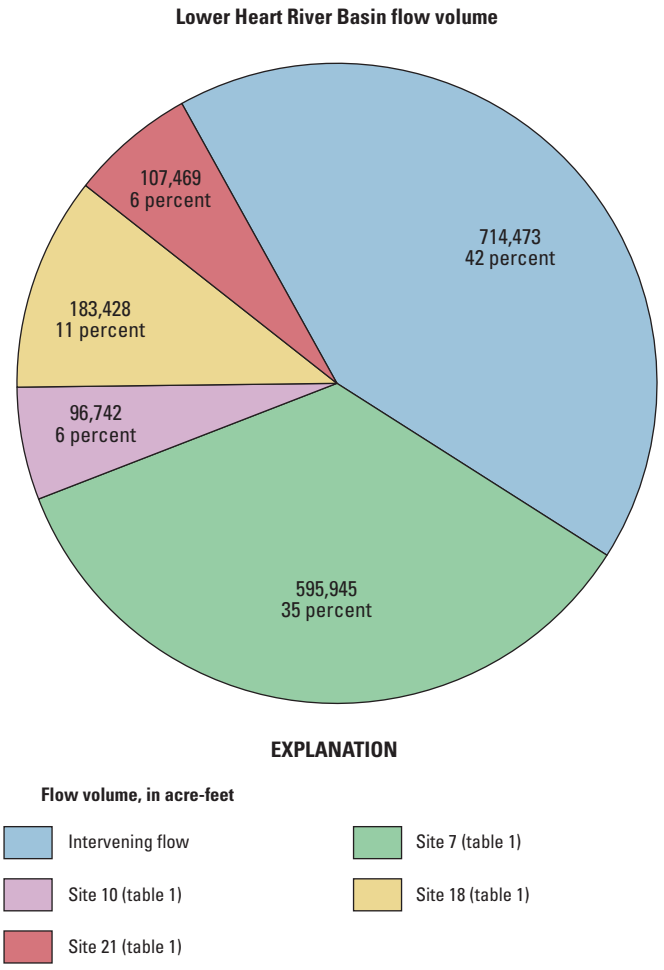

Figure 25. Summary of the flow contributions at Heart River near Mandan, North Dakota (site 22) from the selected sites in the lower Heart River Basin.

Table 11. Summary of streamflow volume calculations used for the mass balance analysis in the lower Heart River Basin.

Year	Annual streamflow volume (acre-feet)	Percentage of streamflow volume at site 22
	Site 7	
2013	45,957	22
2014	135,932	27
2015	76,473	36
2016	18,920	33
2017	39,212	46
2018	54,717	47
2019	171,739	44
2020	52,996	43
Mean	**74,493**	**37**
Total	**595,945**	**35**
	Site 10	
2013	13,710	6
2014	26,379	5
2015	10,675	5
2016	3,684	6
2017	3,041	4
2018	6,917	6
2019	23,422	6
2020	8,914	7
Mean	**12,093**	**6**
Total	**96,742**	**6**
	Site 18	
2013	12,169	6
2014	50,319	10
2015	24,191	11
2016	7,581	13
2017	10,657	12
2018	13,384	12
2019	51,074	13
2020	14,052	11
Mean	**22,928**	**11**
Total	**183,428**	**11**
	Site 20	
2013	197,826	93
2014	437,968	87
2015	165,579	79
2016	45,804	79
2017	73,484	85

Table 11. Summary of streamflow volume calculations used for the mass balance analysis in the lower Heart River Basin.—Continued

Year	Annual streamflow volume (acre-feet)	Percentage of streamflow volume at site 22
Site 20—Continued		
2018	93,818	81
2019	341,879	88
2020	105,395	86
Mean	182,719	85
Total	1,461,755	86
Site 21		
2013	16,154	8
2014	28,601	6
2015	14,051	7
2016	4,990	9
2017	6,934	8
2018	6,988	6
2019	20,895	5
2020	8,855	7
Mean	13,434	7
Total	107,469	6
Intervening flow[1]		
2013	123,660	58
2014	261,726	52
2015	85,213	40
2016	22,594	39
2017	26,227	30
2018	33,437	29
2019	123,391	32
2020	38,226	31
Mean	89,309	39
Total	714,473	42
Site 22		
2013	211,650	211,650
2014	502,956	502,956
2015	210,603	210,603
2016	57,770	57,770
2017	86,071	86,071
2018	115,443	115,443
2019	390,521	390,521
2020	123,043	123,043
Mean	212,257	212,257
Total	1,698,057	1,698,057

[1]Calculated by subtracting the sum of the total annual streamflow at sites 7, 10, 18, and 21 from total annual streamflow at site 22.

Figure 26. Total loads for the lower Heart River Basin as a percentage of the total load for Heart River near Mandan, North Dakota (site 22), 2013–20. *A*, sulfate; *B*, sodium; *C*, chloride; and *D*, total dissolved solids.

sources other than the major tributaries. Generally, the smallest portion of the load for TDS, sulfate, and sodium came from Antelope Creek (site 10).

Intervening flow is a large contributor to dissolved ion loads in the lower Heart River Basin and is an important part of understanding the transport of dissolved ions in the basin. Intervening flow in the basin was defined for this study as groundwater discharge, irrigation return flow, local runoff, and smaller unmeasured tributaries. Intervening flow in the basin between site 7 and site 22 was 42 percent (fig. 25), which is consistent with percentages of intervening loads for TDS, sulfate, sodium, and chloride (fig. 26). Starting around 1993, the climate became wetter (Williams-Sether, 1999), and in response, 7-day minimum streamflow (base flow) increased basinwide starting in the late 1990s (figs. 5–7). Base flow receives most of the streamflow gains from discharge out of the groundwater storage (Smakhtin, 2001; Brutsaert, 2008), which contributes to the intervening flow and ultimately the loads. Increasing concentrations in the basin for TDS, several dissolved ions, and SAR indicated that continuous irrigation in the basin may be increasing the salinity of the surface water through irrigation return flow and local runoff. The combination of increased local runoff owing to the wetter climatic period and conversion from flood to pivot irrigation may contribute to larger loads. With conversion from flood to pivot irrigation, more evaporites are formed on the surface of poorly drained soils, and the increased local runoff can transport more TDS, sulfate, sodium, and chloride to the Heart River. Finally, smaller unmeasured tributaries are usually ephemeral streams and only flow during high-flow conditions, usually in the spring and early summer owing to snowmelt and rainfall events. Because most of the loads are transported during the spring and early summer, these streams are likely contributing to the loads. These small unmeasured tributaries are also subject to groundwater discharge, irrigation return flow, and local runoff.

Annual loads for total phosphorus between 2013 and 2020 at sites 5 and 22 generally were largest in 2019 and smallest in 2016 (fig. 27*A*; table 10). The largest loads for total phosphorus were 80 tons in 2014 and 2019 for site 5 and 200 tons in 2019 at site 22 (fig. 27*A* and table 10). The smallest loads for total phosphorus at sites 5 and 22 were 1.4 and 1.9 tons in 2016, respectively (fig. 27*A* and table 10). Compared to the main-stem sites, total phosphorus loads were small in the lower basin tributaries, with loads ranging from 0.2 (2017) to 7.7 (2014 and 2019) tons in Antelope Creek (site 10), 1.2 (2016) to 13 (2014 and 2019) tons in Big Muddy Creek (site 18), and 1.2 (2016) to 8.4 (2014) tons Sweetbriar Creek (site 21; table 10).

Similar to the dissolved ions, most of the total phosphorus loads for main-stem sites 5 and 22 were transported in March, April, and June likely owing to snowmelt and early summer rains (fig. 27*B*). Monthly loads of total phosphorus ranged from nearly 0 ton in December to 13 tons in March at

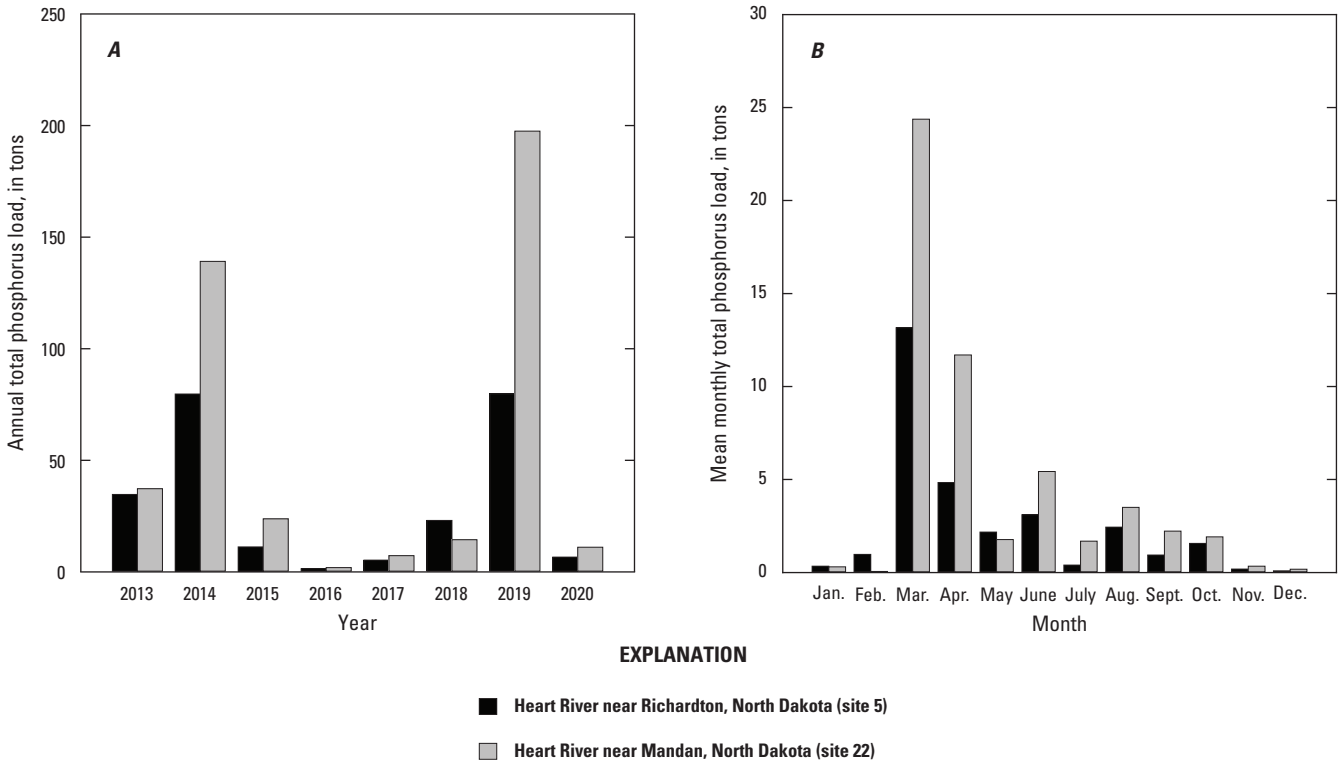

Figure 27. Estimated total phosphorus loads for Heart River near Richardton, North Dakota (site 5) and Heart River near Mandan, North Dakota (site 22), 2013–20. A, annual loads; and B, mean monthly loads.

site 5 (fig. 27*B*). At site 22, the monthly load of total phosphorus ranged from nearly 0 ton in February to 24 tons in March (fig. 27*B*).

The mean annual yields of total phosphorus for 2013–20 were largest on the main-stem site upstream from Lake Tschida (site 5) and Sweetbriar Creek (site 21), whereas the smallest yields were in the Big Muddy Creek (site 18; table 10, fig. 24*E*). The mean annual yield of total phosphorus for site 5 was 49 pounds per year per square mile (lbs/yr/mi^2), just slightly larger than site 21, which had a mean annual yield of 48 lbs/yr/mi^2 (fig. 24*E*, table 10). For site 18, the mean annual yield of total phosphorus was 22 lbs/yr/mi^2 (fig. 24*E*, table 10). Despite substantial contributions of phosphorus coming from the three major tributaries between sites 5 and 22, the most downstream Heart River site (site 22) had a mean annual yield of 33 lbs/yr/mi^2, which is just slightly larger than the yield for Antelope Creek (site 10) at 25 lbs/yr/mi^2 (fig. 24*E*, table 10). These differences are likely related to nutrient processes in Lake Tschida and in-stream processes are likely contributing to the smaller yield of total phosphorus at site 22.

The total phosphorus load was reduced by nearly 83 percent between the Heart River sites upstream (site 5) and downstream (site 7) of Lake Tschida (table 10), likely by processes in Lake Tschida such as algal uptake and sediment deposition. Of the total phosphorus load at site 22, 73 percent came from intervening sources and only 10 percent came from Lake Tschida at site 7. The three tributaries each contributed less than 7 percent of the total load. Different from the dissolved ions mass balance, 73 percent of total load at site 22 came from intervening flow, which is nearly twice the percentage of streamflow at site 22 owing to intervening flow (tables 10 and 11). Although a true mass balance is difficult to do for total phosphorus because it is not a conservative constituent, comparison among sites provides some indication of where the total phosphorus is being transported and transformed.

Much of the phosphorus that enters Lake Tschida from the upper basin does not get transported downstream to the lower basin, and much of the phosphorus in the lower basin was attributed to intervening flow. Most of the phosphorus is likely entering the Heart River through irrigation return flow and local runoff. The phosphorus is applied in fertilizers on the surface, and return flow from irrigation and local runoff and can transport some of the phosphorus to the Heart River. Phosphorus can also be transported by local runoff from livestock grazing areas and feedlots, which can affect the total phosphorus loads.

Implications

Salinity and nutrient conditions in the Heart River Basin were evaluated to determine how water quality varied spatially in the basin, how water quality changed temporally in the basin, and what factors were affecting the water-quality changes in the basin. The combination of analyses presented in this report address these questions for the Heart River Basin.

Spatial patterns emerged from the load and trend analysis that showed different areas of interest for salinity and nutrients in the basin. From the mass balance of TDS, sulfate, sodium, and chloride in the lower Heart River Basin, most of the loads at the farthest downstream main-stem site (site 22) were from intervening flows. Additionally, among the tributaries, Big Muddy Creek and Sweetbriar Creek were the two largest contributors to TDS, sulfate, sodium, and chloride loads at site 22. From the trend analysis of TDS, dissolved ions, and SAR, although consistent basinwide increases were evident, spatial patterns emerged among the tributaries and main-stem sites. The largest concentration increases were detected at the main-stem sites (sites 5 and 22), which indicates that tributaries are likely contributing to increasing concentrations in the Heart River. Antelope Creek (site 10) generally had the smallest increases in dissolved ion concentrations of the four sites analyzed for trends. The mass balance for total phosphorus is complicated by the nonconservative nature of nutrients, but the total phosphorus load was reduced by 83 percent between sites upstream (site 5) and downstream (site 7) from Lake Tschida. Most of the total phosphorus loads in the lower basin were transported through intervening flow, likely owing to groundwater inflow, irrigation return flow, and inputs from unmeasured tributaries. Trend results of nutrients for the upper basin site (site 5) and the lower basin site (site 22) indicated that concentrations were generally unchanging over time, except nitrate plus nitrite concentrations were likely decreasing in the upper basin.

In the mid-1970s, concentrations of TDS, most dissolved ions, and SAR began increasing with larger increases during the recent trend period (1999–2019), whereas total phosphorus and nitrate plus nitrite concentrations were generally unchanged during the recent trend period. Increases in TDS, sulfate, sodium, and SAR, usually used to evaluate salinity of irrigation water, ranged from 19 and 46 percent, overall, from 1974 to 2019, and the largest increases occurred from 1999 to 2019. SAR can be used to evaluate the salinity hazard of irrigation water, and the trends in the basin show the SAR values approaching 6, which is the highest SAR value recommended for continuous irrigation in North Dakota (Scherer and others, 2017). Nutrient concentrations generally were unchanging, except at site 5 where nitrate plus nitrite concentrations were likely decreasing. Because the nutrient data did not fully meet the data requirements for trend analysis, the trends related to nutrients should be used with caution. Continued data collection efforts in the basin, especially for nutrients, would produce a more robust dataset and better trend results in the future. Most of the nutrient conservation practices have been implemented in the upper basin, which is where the nitrate plus nitrite concentrations were likely decreasing, indicating that the conservation practices may be effectively reducing nitrate plus nitrite concentrations (Rita Sveen, NRCS, written commun., 2021).

Lake processes, geology, natural soil characteristics, hydroclimate, and irrigation practices contribute to water-quality changes spatially and temporally in the basin, and other than lake processes, these factors work together for a cumulative effect of causing increased salinity. Processes in Lake Tschida, such as sediment settling and adsorption, likely reduced dissolved ion concentrations, and algal uptake combined with sediment settling likely reduced nutrient concentrations. Another contributor to the differences in concentrations between the upper and lower basin, particularly for dissolved ions, could be the local geology. The upper basin drains large areas of the Sentinel Butte Formation, whereas the lower basin drains the Bullion Creek and Ludlow and Cannonball Formations. Differences in the water quality of the groundwater in these formations could affect the spatial and temporal water-quality changes in the basin. Of the basin soils, 71 percent are hydrologic group C and D, which are poorly drained soils (Soil Survey Staff, 2020), and irrigation on these soil types can produce evaporite deposits at or near the field surface (Al-Ghobari, 2011; Shahid, 2013). From the geochemical modeling, sulfate evaporites were determined to be the major geochemical control on the water-quality changes in the basin. The wet climatic period that began in the 1990s has increased base flow in the basin and in turn likely raised the groundwater table. The rise in groundwater dissolves minerals in the formerly unsaturated zone, increasing the salinity of groundwater discharge into the basin. Transition from flood to pivot irrigation has been occurring in the basin since the late 1990s (Chad Skretteberg, Western Heart River Irrigation District, written commun., 2021; James Weigel, Bureau of Reclamation, written commun., 2021) and can cause the accumulation of salts at or near the surface on poorly drained soils (Al-Ghobari, 2011; Shahid, 2013). Other than lake processes, the factors described above create a cumulative effect that is enhanced by producers using increasingly saline water from the Heart River and its tributaries to irrigate crops. The changing irrigation techniques and increasingly poorer water quality can cause evaporites to form at or near the soil surface, and thus in a wetter climate runoff increases the concentrations in the Heart River Basin by dissolving these evaporites. The increasing base-flow contributions observed from the wetter climate indicated a rise in the groundwater tables that began to dissolve minerals in the unsaturated zone (fig. 21).

Summary

The Heart River Basin is predominantly an agricultural basin in western North Dakota and is approximately 3,350 square miles. The U.S. Geological Survey, in cooperation with the U.S. Department of Agriculture Natural Resources Conservation Service and the Grant County Soil Conservation District, completed a study to assess spatial and temporal patterns of water quality in the Heart River Basin. The purpose of this report is to describe the methods and results of a study to evaluate salinity and nutrients in the Heart River Basin in western North Dakota. Water-quality and streamflow data used in the study were compiled from 1970 to 2020 using the National Water Quality Monitoring Council Water Quality Portal and National Water Information System database.

Changes in streamflow characteristics were investigated at three sites (Green River near New Hradec, North Dakota [site 1]; Heart River near Richardton, N. Dak. [site 5]; and Heart River near Mandan, N. Dak. [site 22]) from 1970 to 2020. No formal significance value was calculated for these trends, so interpretations should be made with caution. Visual observation of streamflow trends at sites 1, 5, and 22 indicated decreasing streamflow for maximum daily, mean daily, and 7-day minimum flows from 1970 until the late 1990s followed by increasing flow through 2020.

The spatial patterns of median concentrations in the basin tended to be similar among total dissolved solids (TDS), sulfate, sodium, chloride, and bicarbonate with the lowest median concentrations in the South Branch Heart River near South Heart, N. Dak. (site 4) and the highest median concentrations at one of three sites: Heart River near South Heart, N. Dak. (site 2); Hailstone Creek (site 17); or Big Muddy Creek near Almont, N. Dak. (site 18). For one-third of the selected sites in the Heart River Basin with sodium adsorption ratio (SAR) data, median values were greater 6, which is the maximum value recommended in North Dakota for continuously irrigated water.

Spatial patterns for median concentrations of nitrate plus nitrite differed from the other nutrient constituents. The lowest median nitrate plus nitrite concentrations were below the recensored reporting level of 0.03 milligram per liter (mg/L) at multiple sites and the highest median concentration was 0.8 mg/L at Antelope Creek (site 8). Median concentrations of total ammonia, dissolved phosphorus, and total phosphorus were similar, with the lowest median concentrations at the Heart River near Carson, N. Dak. (site 11) and the highest median concentrations at site 4 and Big Muddy Creek (site 15).

For the historical trend period (1974–2019), TDS concentrations have increased since the mid-1970s through 2019. During the recent trend period (1999–2019), increasing concentrations in TDS were observed across the Heart River Basin, and the magnitude of the increases was smaller at tributary sites compared to main-stem sites. During the historical trend period, sulfate and sodium concentrations have increased since the mid-1970s at all sites, but the increase was greater on main-stem sites during 1999–2019 than 1974–99. During the recent trend period, increases in sulfate and sodium concentrations were detected basinwide, and sulfate trends had larger increases in concentration compared to sodium. Chloride concentrations showed large, consistent, and significant increases starting in the mid-1970s through 2019, whereas potassium concentrations remained mostly constant with some small fluctuations during the same period. During the recent period, large increases (greater than 40 percent) in chloride

concentrations were detected, and potassium was mostly constant, although small (0.9 mg/L or less) decreases on tributaries and small (1.3 mg/L) increases on the main-stem sites were detected. Calcium and magnesium concentrations increased since the mid-1970s at all sites, except for a decrease at site 5 between 1974 and 1999. During the recent period, calcium and magnesium concentrations increased basinwide with percentage increases smaller for calcium than magnesium. Results of the historical trend analysis of SAR values indicated significant increases basinwide since the mid-1970s. Increasing values of SAR were observed basinwide, with lower SAR values at the end of the trend period on the tributaries than the main-stem sites.

Land use, agricultural practices, and hydroclimatic changes in the Heart River Basin, combined with naturally occurring and readily available sulfate and sodium in geologic formations, soils, and aquifers, likely contributed to the moderate to large sulfate and sodium concentrations increases. Chloride concentrations had larger increases from 1999 to 2019 compared to from 1974 to 1999, which were likely a result of a combination of sources such as deicing and dust-control chemicals, agricultural management and practices, and energy production. Potassium concentrations did not follow the trends observed with other constituents and remained constant with small fluctuations in concentration from 1974 to 2019. Overall, increasing concentrations of both calcium and magnesium were consistent basinwide and were likely related to anthropogenic effects and naturally occurring geologic effects. Because SAR is computed as the ratio of sodium to calcium and magnesium in the soil water, increasing concentrations in these constituents resulted in increasing SAR values. Trend results did not indicate increasing concentrations of nitrate plus nitrite and total phosphorus concentrations, but anthropogenic changes, conservation practices, and land use can affect nutrients in the basin.

Increasing trends in concentrations during the last several decades for all dissolved ions except potassium were detected in the Heart River Basin. Possible geochemical controls on these water-quality trends could be from minerals found in soils, bedrock geology, or agricultural products. From PHREEQC inverse modeling for period 1 (1974–99) in model zone 1 (Heart River reach from site 5 to site 6), eight reasonable models indicated that the clay mineral-water interactions and dissolution of evaporites control the geochemistry. Results of the inverse modeling for period 2 (1999–2019) in model zone 1 had eight reasonable models that indicated that the dissolution of evaporites was the major geochemical control. Three major differences were observed in period 2 compared to period 1: (1) gypsum was dissolving in five models, (2) dissolution of sylvite was the dominant source of potassium over hydrolysis of potassium feldspar, and (3) evaporite dissolution was 50 percent greater compared to period 1.

Results of the geochemical modeling for period 1 in model zone 2 (Heart River and Sweetbriar Creek reach from Heart River at Stark Bridge near Judson, N. Dak. [site 20] and Sweetbriar Creek near Judson, N. Dak. [site 21] to site 22), produced seven reasonable models, and the geochemical control of the system was the dissolution of the sulfate evaporite minerals of mirabilite, thenardite, konyaite, and gypsum. Geochemical modeling results for period 2 in model zone 2 produced 11 reasonable models and was also controlled by the dissolution of sulfate evaporite minerals. Mole transfers increased between period 1 and period 2 for the sulfate evaporites of mirabilite, thenardite, and konyaite.

Differences between models in the upper and lower basin indicated that geology controls some of the water-quality changes in the Heart River Basin. Carbonate dissolution was occurring in the upper basin, whereas these minerals generally precipitated out in the lower basin. The varying composition of sandstones produced different chemical reactions between zones in the basin. Groundwater was not considered because of too few data; therefore, geochemical evolution through the aquifers was not modeled. Sulfate evaporite minerals in soils in the Heart River Basin had the most geochemical control over the system.

Loads and yields were estimated for selected sites in the Heart River Basin from 2013 to 2020. Total, annual, and monthly loads were estimated for total dissolved solids, sulfate, sodium, chloride, and total phosphorus. Total loads were used to compute a simplified mass balance in the lower Heart River Basin. Annual loads estimated for the Heart River during 2013–20 at sites 5 and 22 were generally greatest in 2014 and the smallest in 2016 for TDS, sulfate, sodium, and chloride. Most of the annual loads of TDS, sulfate, sodium, and chloride are delivered in March through June in the Heart River at sites 5 and 22, likely owing to snowmelt and runoff from rainfall events. The mean annual yields of TDS and sodium from 2013 through 2020 generally were largest in Big Muddy Creek (site 18), whereas yields of sulfate and chloride were largest at Sweetbriar Creek (site 21) compared to the other selected sites in the Heart River Basin. Larger yields of TDS, sulfate, sodium, and chloride in sites located on Big Muddy Creek and Sweet Briar Creek in the lower Heart River Basin were likely a result of differences in geology and soils upstream from the selected sites.

A mass balance was estimated for TDS, sulfate, sodium, and chloride in the lower basin, specifically the reach on the Heart River from site 7 to site 22, using the total loads computed for 2013–20. Intervening flow is a large contributor to dissolved ion loads in the lower Heart River Basin and is an important part of understanding the transport of dissolved ions in the basin. The intervening flow can include groundwater discharge, irrigation return flow, local runoff, and input from smaller ephemeral tributaries. Tributaries in the lower Heart River Basin contributed portions of the TDS, sulfate, sodium, and chloride loads at the Heart River near Mandan (site 22) that generally were proportional to the streamflow contributions.

Annual loads for total phosphorus from 2013 to 2020 at sites 5 and 22 generally were largest in 2019 and smallest in 2016. Similar to the dissolved ions, most of the total phosphorus loads for main-stem sites 5 and 22 were transported in

March, April, and June, likely owing to snowmelt and early summer rains. The mean annual yields of total phosphorus for 2013–20 were largest on the main-stem site upstream from Lake Tschida (site 5) and the Sweetbriar Creek tributary (site 21), whereas the smallest yields were in the Big Muddy Creek tributary (site 18). Much of the phosphorus that enters Lake Tschida from the upper basin does not get transported downstream to the lower basin, and much of the phosphorus in the lower basin was attributed to intervening flow.

References Cited

Ackerman, D.J., 1980, Ground-water resources of Morton County, North Dakota: North Dakota State Water Commission County Ground-Water Studies 27, part III, 51 p. [Also available at http://www.swc.state.nd.us/info_edu/reports_and_publications/county_groundwater_studies/pdfs/Morton_Part_III.pdf.]

Al-Ghobari, H.M., 2011, Effect of irrigation water quality on soil salinity and application uniformity under center pivot systems in arid regions: Australian Journal of Basic and Applied Sciences, v. 5, no. 7, p. 72–80.

Brekke, D.W., 1979, Mineralogy and chemistry of clay-rich sediments in the contact zone of the Bullion Creek and Sentinel Butte Formations (Paleocene), Billings County, North Dakota: University of North Dakota, Master's thesis, 107 p. [Also available at https://commons.und.edu/theses/36.]

Brutsaert, W., 2008, Long-term groundwater storage trends estimated from streamflow records: Climatic perspective: Water Resources Research, v. 44, no. 2, 7 p. [Also available at https://doi.org/10.1029/2007WR006518.]

Bureau of Reclamation, 2020, HYDROMET data system: U.S. Bureau of Reclamation Missouri Basin Region, accessed February 2021 at https://www.usbr.gov/gp/hydromet/.

Bureau of Reclamation, 2021, Heart Butte unit history: U.S. Bureau of Reclamation, Heart Butte Unit, accessed May 2021 at https://www.usbr.gov/projects/index.php?id=465.

Carlson, C.G., 1982, Geology of Grant and Sioux Counties, North Dakota: North Dakota Geological Survey Bulletin 67—part 1, 37 p., 1 sheet, accessed August 2020 at https://www.swc.nd.gov/info_edu/reports_and_publications/county_groundwater_studies/.

Carlson, C.G., 1983, Geology of Morton County, North Dakota: North Dakota Geological Survey Bulletin 72—part 1, 42 p., 1 sheet, accessed August 2020 at https://www.swc.nd.gov/info_edu/reports_and_publications/county_groundwater_studies/.

Clayton, L., Carlson, C.G., Moore, W.L., Groenewold, G., Holland, F.D., Jr., and Moran, S.R., 1977, The Slope (Paleocene) and Bullion Creek (Paleocene) Formations of North Dakota: North Dakota Geological Survey Report of Investigation No. 59, 18 p., accessed August 2020 at https://www.dmr.nd.gov/ndgs/documents/Publication_List/pdf/RISeries/RI-59.pdf.

Cohn, T.A., 1995, Recent advances in statistical methods for the estimation of sediment and nutrient transport in rivers: Reviews of Geophysics, v. 33, no. S2, p. 1117–1123. [Also available at https://doi.org/10.1029/95RG00292.]

Cohn, T.A., Caulder, D.L., Gilroy, E.J., Zynjuk, L.D., and Summers, R.M., 1992, The validity of a simple statistical model for estimating fluvial constituent loads—An Empirical study involving nutrient loads entering Chesapeake Bay: Water Resources Research, v. 28, no. 9, p. 2353–2363. [Also available at https://doi.org/10.1029/92WR01008.]

Cohn, T.A., DeLong, L.L., Gilroy, E.J., Hirsch, R.M., and Wells, D.K., 1989, Estimating constituent loads: Water Resources Research, v. 25, no. 5, p. 937–942. [Also available at https://doi.org/10.1029/WR025i005p00937.]

Diaz, D.R., and Presley, D., 2017, Management of saline and sodic soils: Manhattan, Kans., Kansas State University, 4 p., accessed August 2021 at https://bookstore.ksre.ksu.edu/pubs/MF1022.pdf.

Dubrovsky, N.M., Burow, K.R., Clark, G.M., Gronberg, J.M., Hamilton, P.A., Hitt, K.J., Mueller, D.K., Munn, M.D., Nolan, B.T., Puckett, L.J., Rupert, M.G., Short, T.M., Spahr, N.E., Sprague, L.A., and Wilber, W.G., 2010, The quality of our Nation's waters—Nutrients in the Nation's streams and groundwater, 1992–2004: U.S. Geological Survey Circular 1350, 174 p. [Also available at https://water.usgs.gov/nawqa/nutrients/pubs/circ1350.]

Fenner, W.E., 1974, The foraminiferids of the Cannonball Formation (Paleocene, Danian) and their paleoenvironmental significance—Grant, Morton and Oliver counties, North Dakota: Grand Forks, N. Dak., University of North Dakota, Master's thesis, 146 p. [Also available at https://commons.und.edu/theses/92/.]

Franzen, D.W., and Bu, H., 2018, North Dakota clay mineralogy impacts crop potassium nutrition and tillage systems: Fargo, N. Dak., North Dakota State University, 12 p., accessed August 2021 at https://www.ndsu.edu/fileadmin/soils.del/pdfs/Clay_Mineralogy_2018.pdf.

Franzen, D., Wick, A., Augustin, C., and Kalwar, N., 2014, Saline and sodic soils: Fargo, N. Dak., North Dakota State University, 8 p., accessed August 2021 at https://www.ndsu.edu/soilhealth/wp-content/uploads/2014/07/Saline-and-Sodic-Soils-2-2.pdf.

Galloway, J.M., Vecchia, A.V., Vining, K.C., Densmore, B.K., and Lundgren, R.F., 2012, Evaluation of water-quality characteristics and sampling design for streams in North Dakota, 1970–2008: U.S. Geological Survey Scientific Investigations Report 2012–5216, 304 p. [Also available at https://doi.org/10.3133/sir20125216.]

Granato, G.E., DeSimone, L.A., Barbaro, J.R., and Jeznach, L.C., 2015, Methods for evaluating potential sources of chloride in surface waters and groundwaters of the conterminous United States: U.S. Geological Survey Open-File Report 2015–1080, 89 p. [Also available at https://doi.org/10.3133/ofr20151080.]

Helsel, D.R., Hirsch, R.M., Ryberg, K.R., Archfield, S.A., and Gilroy, E.J., 2020, Statistical methods in water resources: U.S. Geological Survey Techniques and Methods, book 4, chap. A3, 458 p. [Also available at https://doi.org/10.3133/tm4A3.] [Supersedes U.S. Geological Survey Techniques of Water-Resources Investigations, book 4, chap. A3, version 1.1.]

Hem, J.D., 1985, Study and interpretation of the chemical characteristics of natural water (3d ed.): U.S. Geological Survey Water-Supply Paper 2254, 263 p. [Also available at https://doi.org/10.3133/wsp2254.]

Hirsch, R.M., and De Cicco, L.A., 2015, User guide to Exploration and Graphics for RivEr Trends (EGRET) and dataRetrieval—R packages for hydrologic data (version 2.0, February 2015): U.S. Geological Survey Techniques and Methods book 4, chap. A10, 93 p. [Also available at https://doi.org/10.3133/tm4A10.]

Homer, C.G., Dewitz, J.A., Yang, L., Jin, S., Danielson, P., Xian, G., Coulston, J., Herold, N.D., Wickham, J.D., and Megown, K., 2015, Completion of the 2011 National Land Cover Database for the conterminous United States—Representing a decade of land cover change information: Photogrammetric Engineering and Remote Sensing, v. 81, no. 5, p. 345–354, accessed August 2021 at https://www.ingentaconnect.com/content/asprs/pers/2015/00000081/00000005/art00002.

Jacob, A.F., 1975, Criteria for differentiating the Tongue River and Sentinel Butte Formations (Paleocene), North Dakota: North Dakota Geological Survey, Report of Investigation 53, 60 p.

Keller, L.P., McCarthy, G.J., and Richardson, J.L., 1986a, Mineralogy and stability of soil evaporites in North Dakota: Soil Science Society of America Journal, v. 50, no. 4, p. 1069–1071, accessed August 2021 at https://doi.org/10.2136/sssaj1986.03615995005000040047x.

Keller, L.P., McCarthy, G.J., and Richardson, J.L., 1986b, Laboratory modeling of Northern Great Plains salt efflorescence mineralogy: Soil Science Society American Journal, 5 p., accessed August 2021 at https://doi.org/10.2136/sssaj1986.03615995005000050056x.

Kolars, K.A., Vecchia, A.V., and Ryberg, K.R., 2015, Stochastic model for simulating Souris River precipitation, evapotranspiration, and natural streamflow: U.S. Geological Survey Scientific Investigations Report 2015–5185, 55 p. [Also available at https://doi.org/10.3133/sir20155185.]

Langmuir, D., 1997, Aqueous environmental geochemistry: Upper Saddle River, N.J., Prentice-Hall, Inc., 599 p.

Linenberger, T.R., 1996, The Dickinson Unit, Heart Division, Pick-Sloan Missouri Basin Program: U.S. Bureau of Reclamation, 15 p., accessed August 2021 at https://www.usbr.gov/projects/pdf.php?id=158.

Lumley, T., 2020, Leaps—Regression subset selection: R package version 3.1, accessed https://cran.r-project.org/web/packages/leaps/index.html.

Maderak, M.L., 1966, Sedimentation and chemical quality of surface water in the Heart River drainage basin, North Dakota: U.S. Geological Survey Water Supply Paper 1823, 42 p. [Also available at https://doi.org/10.3133/wsp1823.]

Murphy, E.C., Nordeng, S.H., Juenker, B.J., and Hoganson, J.W., 2009, North Dakota stratigraphic column: North Dakota Geological Survey Miscellaneous Series 91, accessed August 2020 at https://www.dmr.nd.gov/ndgs/documents/Publication_List/pdf/Strat-column-NDGS-(2009).pdf.

Naplin, C.E., and Shaver, R.B., 1978, Ground-water resources of the New Salem area Morton County, North Dakota: North Dakota State Water Commission, North Dakota Ground-Water Studies No. 84, 72 p., accessed August 2021 at https://www.swc.nd.gov/info_edu/reports_and_publications/pdfs/gw_studies/gws_84_report.pdf.

National Water Quality Monitoring Council, 2020, Water Quality Portal: National Water Quality Monitoring Council web page, accessed December 1, 2020, at https://www.waterqualitydata.us.

Neter, J., Kutner, M.H., Nachtsheim, C.J., and Wasserman, W., 1996, Applied linear statistical models (4th ed.): New York, WCB McGraw-Hill, 1415 p.

North Dakota Administrative Code, 2020, Underground injection control: North Dakota State Legislature, Title 43, Article 2, Chapter 5, accessed August 2021 at https://www.legis.nd.gov/information/acdata/pdf/43-02-05.pdf.

North Dakota Department of Environmental Quality, 2021a, Watershed boundary data: North Dakota Department of Environmental Quality, accessed March 2021 at https://gishubdata-ndgov.hub.arcgis.com/.

North Dakota Department of Environmental Quality, 2021b, Harmful algal blooms: North Dakota Department of Environmental Quality, accessed March 2020 at https://deq.nd.gov/WQ/3_Watershed_Mgmt/8_HABS/Habs.aspx.

Nustad, R.A., and Vecchia, A.V., 2020, Water-quality trends for selected sites and constituents in the international Red River of the North Basin, Minnesota and North Dakota, United States, and Manitoba, Canada, 1970–2017: U.S. Geological Survey Scientific Investigations Report 2020–5079, 75 p. [Also available at https://doi.org/10.3133/sir20205079.]

Oblinger Childress, C.J., Foreman, W.T., Connor, B.F., and Maloney, T.J., 1999, New reporting procedures based on long-term method detection levels and some considerations for interpretations of water-quality data provided by the U.S. Geological Survey National Water Quality Laboratory: U.S. Geological Survey Open-File Report 99–193, 19 p. [Also available at https://doi.org/10.3133/ofr99193.]

Paerl, H.W., Fulton, R.S., Moisander, P.H., and Dyble, J., 2001, Harmful freshwater algal blooms, with an emphasis on cyanobacteria: The Scientific World, v. 1, p. 76–113, accessed August 2021 at https://doi.org/10.1100/tsw.2001.16.

Parkhurst, D.L., 1995, User's guide to PHREEQC—A computer program for speciation, reaction-path, advective-transport, and inverse geochemical calculations: U.S. Geological Survey Water-Resources Investigations Report 95–4227, 143 p. [Also available at https://pubs.usgs.gov/wri/1995/4227/report.pdf.]

Parkhurst, D.L., and Appelo, C.A.J., 1999, User's guide to PHREEQC (Version 2)—A computer program for speciation, batch-reaction, one-dimensional transport, and inverse geochemical calculations: U.S. Geological Survey Water-Resources Investigations Report 99–4259, 327 p. [Also available at https://doi.org/10.3133/wri994259.]

Parkhurst, D.L., and Appelo, C.A.J., 2013, Description of input and examples for PHREEQC version 3—A computer program for speciation, batch-reaction, one-dimensional transport, and inverse geochemical calculations: U.S. Geological Survey Techniques and Methods, book 6, chap. A43, 497 p. [Also available at https://doi.org/10.3133/tm6A43.]

Randich, P.G., 1979, Ground-water resources of Grant and Sioux Counties North Dakota: North Dakota State Water Commission County Ground-Water Studies 24, part III, 49 p., accessed August 2021 at http://www.swc.state.nd.us/info_edu/reports_and_publications/county_groundwater_studies/pdfs/Grant_Sioux_Part_III.pdf.

Ritter, D.F., Kochel, R.C., and Jerry, R.M., 2011, Process geomorphology: Long Grove, Ill., Waveland Press Inc., 152 p.

Richards, L.A., 1954, Diagnosis and improvement of saline and alkali soils: U.S. Department of Agriculture Handbook no. 60, 166 p., accessed August 2021 at https://www.ars.usda.gov/ARSUserFiles/20360500/hb60_pdf/hb60complete.pdf.

Runkel, R.L., Crawford, C.G., and Cohn, T.A., 2004, Load Estimator (LOADEST)—A FORTRAN program for estimating constituent loads in streams and rivers: U.S. Geological Survey Techniques and Methods, book 4, chap. A5, 69 p. [Also available at https://pubs.usgs.gov/tm/2005/tm4A5/pdf/508final.pdf.]

Runkel, R.L., 2013, Revisions to LOADEST, April 2013: U.S. Geological Survey, 6 p., accessed August 2021 at https://water.usgs.gov/software/loadest/doc/loadest_update.pdf.

Ryberg, K.R., Vecchia, A.V., Akyüz, F.A., and Lin, W., 2016, Tree-ring-based estimates of long-term seasonal precipitation in the Souris River region of Saskatchewan, North Dakota and Manitoba: Canadian Water Resources Journal, v. 41, no. 3, p. 412–428. [Also available at https://doi.org/10.1080/07011784.2016.1164627.]

Scherer, T.F., Franzen, D., and Cihacek, L., 2017, Soil, water and plant characteristic important to irrigation: Fargo, N. Dak., North Dakota State University Extension Service, accessed May 2021 at https://www.ag.ndsu.edu/publications/crops/soil-water-and-plant-characteristics-important-to-irrigation#section-9.

Shahid, S.A., 2013, Irrigation-induced soil salinity under different irrigation systems—Assessment and management—Short technical note: Climate Change Outlook and Adaptation, v. 1, no. 1, p. 19–24, accessed January 2021 at https://www.researchgate.net/publication/263773729_Irrigation-Induced_Soil_Salinity_Under_Different_Irrigation_Systems_-_Assessment_and_Management_Short_Technical_Note.

Simonds, W.J., 1996, The Heart Butte Unit, Heart Division, Pick-Sloan Missouri Basin Program: U.S. Bureau of Reclamation, 13 p., accessed August 2021 at https://www.usbr.gov/projects/pdf.php?id=163.

Smakhtin, V.U., 2001, Low flow hydrology—A review: Journal of Hydrology (Amsterdam), v. 240, no. 3–4, p. 147–186. [Also available at https://doi.org/10.1016/S0022-1694(00)00340-1.]

Soil Survey Staff, 2020, Gridded Soil Survey Geographic (gSSURGO) database for North Dakota: U.S. Department of Agriculture, Natural Resources Conservation Service, accessed August 2021 at https://gdg.sc.egov.usda.gov/.

Tatge, W.S., Nustad, R.A., and Galloway, J.M., 2022, Data and scripts used in water-quality trend and load analysis in the Heart River Basin, North Dakota, 1970–2020: U.S. Geological Survey data release, access February 2022 at https://doi.org/10.5066/P987APZ8.

Tornes, L.H., and Brigham, M.E., 1993, Nutrients, suspended sediment, and pesticides in waters of the Red River of the North Basin, Minnesota, North Dakota, and South Dakota, 1970–90: U.S. Geological Survey Water Resources Investigations Report 93–4231, 62 p. [Also available at https://doi.org/10.3133/wri934231.]

Trapp, H., Jr., and Croft, M.G., 1975, Geology and groundwater resources of Hettinger and Stark Counties, North Dakota: North Dakota State Water Commission County Ground-Water Studies 16, part I, 51 p., accessed August 2021 at http://www.swc.state.nd.us/info_edu/reports_and_publications/county_groundwater_studies/pdfs/Hettinger_Stark_Part_I.pdf.

Turnbull, B.W., and Weiss, L.A., 1978, A likelihood ratio statistic for testing goodness of fit with randomly censored data: Biometrics, v. 34, no. 3, p. 367–375. [Also available at https://doi.org/10.2307/2530599.]

U.S. Census Bureau, 2010, Quickfacts Dickinson city, North Dakota and Mandan city, North Dakota: accessed August 2020, at https://www.census.gov/quickfacts/fact/table/dickinsoncitynorthdakota,ND/PST045219.

U.S. Department of Agriculture, 1972, Hydrologic soil groups, chap. 7 *of* U.S. Department of Agriculture, Hydrology National Engineering Handbook, Part 630: U.S. Department of Agriculture, 5 p., accessed August 2021 at https://directives.sc.egov.usda.gov/OpenNonWebContent.aspx?content=22526.wba.

U.S. Department of Agriculture, 2019, Fertilizer use and price: U.S. Department of Agriculture Economic Research Service, accessed February 2021 at https://www.ers.usda.gov/data-products/fertilizer-use-and-price.aspx.

U.S. Energy Information Administration, 2013, North Dakota oil production reaches new high in 2012, transported by trucks and railroads: U.S. Energy Information Administration, accessed February 24, 2017, at https://www.eia.gov/todayinenergy/detail.php?id=10411.

U.S. Geological Survey, variously dated, National field manual for the collection of water-quality data: U.S. Geological Survey Techniques of Water-Resources Investigations, book 9, chaps. A1–A9 [variously paged], accessed March 18, 2015, at https://pubs.water.usgs.gov/twri9A.

U.S. Geological Survey, 2020, USGS water data for the Nation: U.S. Geological Survey National Water Information System database, accessed July 31, 2020, at https://doi.org/10.5066/F7P55KJN.

Vecchia, A.V., 2003, Water-quality trend analysis and sampling design for streams in North Dakota 1971–2000: U.S. Geological Survey Water-Resources Investigations Report 2003–4094, 73 p. [Also available at https://doi.org/10.3133/wri034094.]

Vecchia, A.V., 2005, Water-quality trend analysis and sampling design for streams in the Red River of the North Basin, Minnesota, North Dakota, and South Dakota, 1970–2001: U.S. Geological Survey Scientific Investigations Report 2005–5224, 54 p. [Also available at https://doi.org/10.3133/sir20055224.]

Vecchia, A.V., 2008, Climate simulation and flood risk analysis for 2008–40 for Devils Lake, North Dakota: U.S. Geological Survey Scientific Investigations Report 2008–5011, 28 p. [Also available at https://doi.org/10.3133/sir20085011.]

Vecchia, A.V., and Nustad, R.A., 2020, Time-series model, statistical methods, and software documentation for R–QWTREND—An R package for analyzing trends in streamwater quality: U.S. Geological Survey Open-File Report 2020–1014, 51 p. [Also available at https://doi.org/10.3133/ofr20201014.]

Wilcox, L.V., 1955, Classification and use of irrigation waters: U.S. Department of Agriculture Circular No. 969, 19 p., accessed August 2021 at https://www.ars.usda.gov/arsuserfiles/20360500/pdf_pubs/P0192.pdf.

Williams-Sether, T., 1999, From dry to wet, 1988–97, North Dakota: U.S. Geological Survey Fact Sheet 075–99, 4 p. [Also available at https://doi.org/10.3133/fs07599.]

Appendix 1. Statistical Summary Tables

Table 1.1. Summary statistics of selected major ion constituents for sites in the Heart River Basin, 1970–2020.

[<, less than; --, no data]

Site number (fig. 1)	Number of observations	Number of censored values	Percent of data that is censored	Beginning sample year	Ending sample year	Number of years of sample record	Concentration						
							Minimum	Maximum	10th percentile	25th percentile	Median	75th percentile	90th percentile
Total dissolved solids, in milligrams per liter													
1	274	7	3	1972	2020	48	92.0	3,110.0	234	458	685	803	985
2	179	7	4	1975	2020	45	203	3,680.0	588	1,020	1,700	2,300	2,780
3	32	0	0	1978	1981	3	209	3,460.0	324	720	1,150	2,270	2,980
4	36	0	0	1979	1983	4	220	1,720.0	299	355	510	935	1,400
5	359	0	0	1972	2020	48	242	2,880.0	590	854	1,180	1,400	1,600
6	77	0	0	1989	2012	23	250	1,850.0	405	639	960	1,270	1,406
7	15	0	0	1972	2019	47	434	1,320.0	499	629	769	986	1,040
10	163	8	5	1972	2020	48	279	2,130.0	494	664	885	1,090	1,480
11	16	0	0	2008	2019	11	577	1,140.0	605	696	936	993	1,090
17	29	0	0	2011	2012	1	925	3,200.0	1,250	1,680	2,150	2,420	2,600
18	104	10	10	1991	2020	29	274	3,270.0	475	941	1,460	1,700	2,180
19	117	0	0	1971	1995	24	193	1,090.0	357	623	759	897	1,000
20	93	2	2	1988	2019	31	162	1,540.0	535	754	889	1,050	1,210
21	110	8	7	1972	2020	48	88.0	2,500.0	337	675	1,020	1,410	1,740
22	488	1	0	1971	2020	49	156	2,240.0	568	825	1,000	1,200	1,380
Sulfate, in milligrams per liter													
1	167	0	0	1972	2020	48	8	2,050	84	190	250	318	425
2	111	0	0	1975	2020	45	59	2,130	280	495	810	1,130	1,610
3	24	0	0	1978	1996	18	57	1,700	96	243	484	990	1,400
4	31	0	0	1979	1996	17	8	910	39	82	170	315	518
5	276	0	0	1972	2020	48	105	1,430	295	420	609	772	916
6	48	0	0	1989	2012	23	98	1,100	200	288	425	563	744
7	14	0	0	1972	2019	47	210	724	285	320	381	514	543
10	147	0	0	1972	2020	48	90	1,270	187	294	404	573	785
11	16	0	0	2008	2019	11	252	606	276	324	455	515	542
17	29	0	0	2011	2012	1	512	1,870	612	895	1,160	1,370	1,490
18	83	0	0	1991	2020	29	114	1,960	252	455	619	917	1,270
19	59	0	0	1971	1995	24	75	530	148	250	340	400	454

Table 1.1. Summary statistics of selected major ion constituents for sites in the Heart River Basin, 1970–2020.—Continued

[<, less than; --, no data]

Site number (fig. 1)	Number of observations	Number of censored values	Percent of data that is censored	Beginning sample year	Ending sample year	Number of years of sample record	Concentration						
							Minimum	Maximum	10th percentile	25th percentile	Median	75th percentile	90th percentile
Sulfate, in milligrams per liter—Continued													
20	64	0	0	1988	2019	31	41	831	239	340	415	520	604
21	85	0	0	1972	2020	48	22	1,500	139	270	491	851	1,040
22	351	0	0	1971	2020	49	55	1,220	260	380	462	572	733
Sodium, in milligrams per liter													
1	166	0	0	1972	2020	48	15	690	42	103	160	190	240
2	110	0	0	1975	2020	45	32	971	149	262	485	680	814
3	24	0	0	1978	1996	18	22	1,100	38	113	277	508	868
4	30	0	0	1979	1996	17	21	380	36	59	120	190	311
5	276	0	0	1972	2020	48	39	690	110	172	241	306	341
6	48	0	0	1989	2012	23	40	405	61	120	199	280	320
7	14	0	0	1972	2019	47	75	265	97	114	149	198	211
10	146	0	0	1972	2020	48	32	331	66	98	124	152	212
11	16	0	0	2008	2019	11	101	258	112	120	174	195	225
17	29	0	0	2011	2012	1	149	632	239	340	411	489	525
18	82	0	0	1991	2020	29	49	695	141	282	413	470	549
19	59	0	0	1971	1995	24	30	230	58	110	150	190	200
20	64	0	0	1988	2019	31	22	315	102	158	190	230	260
21	84	0	0	1972	2020	48	13	457	86	169	259	321	385
22	351	0	0	1971	2020	49	19	576	118	170	218	270	323
Chloride, in milligrams per liters													
1	166	8	4.8	1972	2020	48	<0.1	30.0	2.9	4.5	6.2	10.0	14.7
2	111	7	6.3	1975	2020	45	3.3	100.0	5.9	11.4	19.0	29.1	35.0
3	24	0	0.0	1978	1996	18	1.8	15.2	3.3	4.0	5.2	7.0	9.6
4	31	0	0.0	1979	1996	17	1.6	47.0	3.0	3.8	4.8	9.1	15.0
5	276	3	1.1	1972	2020	48	<0.1	127.0	7.7	12.0	19.0	27.4	35.8
6	48	0	0.0	1989	2012	23	3.1	48.0	4.3	9.6	13.0	17.7	25.9
7	14	0	0.0	1972	2019	47	2.8	21.1	11.4	14.5	15.9	16.8	17.4
10	146	68	46.6	1972	2020	48	<0.1	31.4	5.8	8.9	15.0	15.0	15.5

Table 1.1. Summary statistics of selected major ion constituents for sites in the Heart River Basin, 1970–2020.—Continued

[<, less than; --, no data]

Site number (fig. 1)	Number of observations	Number of censored values	Percent of data that is censored	Beginning sample year	Ending sample year	Number of years of sample record	Concentration						
							Minimum	Maximum	10th percentile	25th percentile	Median	75th percentile	90th percentile
Chloride, in milligrams per liters—Continued													
11	16	0	0.0	2008	2019	11	7.3	18.7	8.6	10.9	15.0	16.6	17.3
17	29	25	86.2	2011	2012	1	<3.0	30.0	15.0	15.0	30.0	30.0	30.0
18	79	11	13.9	1991	2020	29	<0.1	34.6	5.1	6.6	8.3	12.0	15.2
19	59	0	0.0	1971	1995	24	1.7	21.0	3.3	4.7	6.5	8.9	12.0
20	63	2	3.2	1988	2019	31	1.1	21.2	6.7	8.4	11.2	14.0	16.5
21	82	8	9.8	1972	2020	48	<0.3	22.1	3.5	5.0	9.6	15.7	18.6
22	349	14	4.0	1971	2020	49	<0.1	303.0	6.7	9.6	14.0	17.5	21.8
Potassium, in milligrams per liter													
1	165	0	0	1972	2020	48	3.7	16.0	4.5	5.3	6.3	8.1	9.3
2	110	0	0	1975	2020	45	3.7	24.0	6.1	7.2	8.3	9.8	11.6
3	24	0	0	1978	1996	18	4.9	20.2	5.7	8.3	9.7	11.3	14.7
4	31	0	0	1979	1996	17	2.2	48.4	3.3	5.3	7.8	10.0	13.7
5	276	0	0	1972	2020	48	4.3	19.6	8.0	8.9	10.1	11.4	13.0
6	48	0	0	1989	2012	23	4.6	16.0	7.7	9.0	11.0	12.0	13.9
7	14	0	0	1972	2019	47	6.2	13.1	7.9	11.3	11.5	11.9	13.1
10	146	0	0	1972	2020	48	4.5	19.7	7.1	8.8	10.7	12.4	14.6
11	16	0	0	2008	2019	11	8.2	13.6	10.0	10.6	11.7	12.3	13.0
17	29	0	0	2011	2012	1	6.2	17.2	9.5	10.4	11.1	12.7	13.7
18	82	0	0	1991	2020	29	3.9	15.5	7.4	8.7	10.0	12.0	14.0
19	59	0	0	1971	1995	24	4.1	14.0	6.3	7.0	8.0	10.0	12.0
20	64	0	0	1988	2019	31	4.1	14.0	7.1	9.4	10.9	11.9	12.9
21	84	0	0	1972	2020	48	2.7	14.3	5.1	7.1	10.4	12.1	13.1
22	351	0	0	1971	2020	49	2.5	26.2	7.5	8.5	9.8	11.0	12.1
Calcium, in milligrams per liter													
1	166	0	0	1972	2020	48	7	108	16	26	40	49	58
2	110	0	0	1975	2020	45	9	154	22	32	52	70	93
3	24	0	0	1978	1996	18	12	120	16	22	30	50	68
4	29	0	0	1979	1996	17	2	94	7	13	21	44	63

Table 1.1. Summary statistics of selected major ion constituents for sites in the Heart River Basin, 1970–2020.—Continued

[<, less than; --, no data]

Site number (fig. 1)	Number of observations	Number of censored values	Percent of data that is censored	Beginning sample year	Ending sample year	Number of years of sample record	Concentration						
							Minimum	Maximum	10th percentile	25th percentile	Median	75th percentile	90th percentile
Calcium, in milligrams per liter—Continued													
5	276	0	0	1972	2020	48	20	203	41	57	74	92	120
6	48	0	0	1989	2012	23	21	120	29	39	50	64	90
7	14	0	0	1972	2019	47	34	77	40	46	49	57	65
10	146	0	0	1972	2020	48	23	147	45	57	79	93	120
11	16	0	0	2008	2019	11	44	65	47	49	52	59	62
17	29	0	0	2011	2012	1	55	184	78	120	134	146	149
18	82	0	0	1991	2020	29	17	129	24	36	58	76	113
19	58	0	0	1971	1995	24	18	90	35	44	56	63	69
20	64	0	0	1988	2019	31	15	91	39	48	54	63	71
21	84	0	0	1972	2020	48	10	147	23	31	54	84	112
22	351	0	0	1971	2020	49	18	158	41	50	61	77	93
Magnesium, dissolved, in milligrams per liter													
4	30	0	0	1979	1996	17	0.3	69.2	1.5	5.6	9.7	24.3	46.1
3	24	0	0	1978	1996	18	8.6	100.0	9.5	15.0	23.7	43.8	54.2
1	166	0	0	1972	2020	48	3.5	118.0	7.9	16.0	28.0	34.3	39.8
19	59	0	0	1971	1995	24	9.5	56.0	16.6	28.0	36.0	42.5	47.4
6	48	0	0	1989	2012	23	11.0	100.0	17.8	25.8	36.5	47.6	70.2
2	110	0	0	1975	2020	45	3.3	140.0	12.9	19.0	37.7	53.0	77.4
7	14	0	0	1972	2019	47	23.0	67.4	26.8	31.9	38.4	47.7	51.5
20	64	0	0	1988	2019	31	6.5	81.3	25.2	33.0	39.0	47.1	60.0
18	82	0	0	1991	2020	29	8.5	141.0	17.2	31.4	45.3	65.5	99.7
22	351	0	0	1971	2020	49	0.6	124.0	26.3	37.0	45.5	58.2	74.7
21	84	0	0	1972	2020	48	3.2	134.0	16.0	27.0	46.0	73.7	90.4
11	16	0	0	2008	2019	11	27.9	61.7	30.2	36.3	48.7	51.3	55.5
5	276	0	0	1972	2020	48	11.0	143.0	28.7	36.9	53.4	69.3	85.9
10	146	0	0	1972	2020	48	18.0	155.0	40.2	55.2	68.8	88.9	115.5
17	29	0	0	2011	2012	1	44.3	188.0	60.0	89.5	112.0	124.0	142.8

Table 1.1. Summary statistics of selected major ion constituents for sites in the Heart River Basin, 1970–2020.—Continued

[<, less than; --, no data]

Site number (fig. 1)	Number of observations	Number of censored values	Percent of data that is censored	Beginning sample year	Ending sample year	Number of years of sample record	Concentration						
							Minimum	Maximum	10th percentile	25th percentile	Median	75th percentile	90th percentile
Bicarbonate, in milligrams per liter													
1	134	0	0	1972	2020	48	59	563	122	231	370	420	453
2	87	0	0	1975	2020	45	75	1,160	181	344	523	748	867
3	12	0	0	1978	1981	3	66	1,240	237	266	379	589	920
4	11	0	0	1979	1981	2	84	422	90	150	199	280	372
5	258	0	0	1972	2020	48	102	1,030	212	290	353	404	448
6	27	0	0	1989	2012	23	113	717	188	250	325	409	507
7	14	0	0	1972	2019	47	175	352	196	235	248	269	302
10	138	0	0	1972	2020	48	122	561	253	317	383	412	450
11	16	0	0	2008	2019	11	216	395	234	251	282	320	329
17	29	0	0	2011	2012	1	212	687	331	419	523	592	617
18	62	0	0	1991	2020	29	124	918	283	489	606	723	842
19	54	0	0	1971	1992	21	116	535	162	238	307	383	436
20	43	0	0	1988	2019	31	106	514	216	315	348	405	427
21	82	0	0	1972	2020	48	56	721	178	340	410	468	563
22	289	0	0	1971	2020	49	38	1,030	247	320	380	452	556
Sodium absorption ratio, unitless													
1	166	0	0	1972	2020	48	1.2	12.0	2.1	3.7	4.5	5.3	6.5
2	110	0	0	1975	2020	45	2.0	26.0	5.2	7.6	12.2	16.0	19.0
3	16	0	0	1978	1981	3	2.2	27.0	4.0	5.3	8.5	17.0	20.5
4	19	0	0	1979	1983	4	2.2	17.0	3.1	4.5	7.7	12.0	16.2
5	276	0	0	1972	2020	48	1.6	10.4	3.1	4.1	5.1	5.9	6.9
6	48	0	0	1989	2012	23	1.8	12.4	2.0	3.7	4.9	5.9	7.8
7	14	0	0	1972	2019	47	2.3	5.4	3.0	3.2	3.9	4.6	4.8
10	146	0	0	1972	2020	48	1.1	4.6	1.8	2.2	2.5	2.8	3.3
11	16	0	0	2008	2019	11	2.8	6.4	3.0	3.2	4.0	4.6	4.9
17	29	0	0	2011	2012	1	3.2	9.8	4.7	5.6	6.2	7.4	8.1
18	82	0	0	1991	2020	29	2.2	18.0	4.5	7.0	8.8	10.3	11.9
19	58	0	0	1971	1995	24	1.4	5.7	2.1	2.9	3.7	4.3	4.9

Table 1.1. Summary statistics of selected major ion constituents for sites in the Heart River Basin, 1970–2020.—Continued

[<, less than; --, no data]

Site number (fig. 1)	Number of observations	Number of censored values	Percent of data that is censored	Beginning sample year	Ending sample year	Number of years of sample record	Concentration						
							Minimum	Maximum	10th percentile	25th percentile	Median	75th percentile	90th percentile
Sodium absorption ratio, unitless—Continued													
20	64	0	0	1988	2019	31	1.2	6.8	3.1	4.0	4.6	5.3	6.0
21	84	0	0	1972	2020	48	0.9	11.1	3.2	4.8	5.9	6.9	7.7
22	351	0	0	1971	2020	49	1.0	9.0	3.3	4.2	5.1	6.0	6.7
Silica, in milligrams per liter													
1	146	14	10	1972	2020	48	1.6	16.7	2.0	3.6	5.6	8.2	11.0
2	103	1	1	1975	2020	45	1.5	49.8	4.6	6.3	8.7	11.6	14.0
3	16	0	0	1978	1981	3	0.4	12.0	0.7	3.1	5.0	7.7	9.3
4	19	0	0	1979	1983	4	1.6	130.0	5.5	6.7	9.1	13.0	23.8
5	144	23	16	1972	2020	48	1.3	14.7	2.0	2.8	5.0	7.5	9.9
6	27	2	7	1989	2012	23	2.0	11.0	2.6	4.4	5.9	7.3	8.6
7	14	0	0	1972	2019	47	2.1	9.4	3.9	4.3	5.1	6.1	8.5
10	59	10	17	1972	2020	48	2.0	17.4	2.0	2.6	4.2	8.0	10.3
11	13	4	31	2018	2019	1	2.0	12.6	2.0	2.0	3.2	6.1	10.2
17	0	--	--	--	--	--	--	--	--	--	--	--	--
18	61	2	3	1991	2020	29	2.0	14.5	4.2	5.4	7.6	9.8	12.7
19	57	0	0	1971	1994	23	0.4	25.0	2.7	3.4	4.8	5.9	7.8
20	41	0	0	1988	2019	31	2.0	23.0	3.4	4.4	5.2	6.8	9.1
21	78	6	8	1972	2020	48	0.7	15.4	2.0	3.5	5.4	7.3	9.2
22	215	3	1	1971	2020	49	1.0	15.0	3.1	4.5	5.9	7.3	9.6

Table 1.2. Summary statistics of selected nutrient constituents for sites in the Heart River Basin, 1970–2020.

[<, less than; --, no data]

Site number (fig. 1)	Number of observations	Number of censored values	Percent of data that is censored	Beginning sample year	Ending sample year	Number of years of sample record	Concentration						
							Minimum	Maximum	10th percentile	25th percentile	Median	75th percentile	90th percentile
Nitrate plus nitrite, milligrams per liter as nitrogen													
1	52	34	65	1979	2020	41	<0.03	2.96	<0.03	<0.03	<0.03	0.11	0.30
2	56	39	70	1979	2020	41	<0.03	1.5	<0.03	<0.03	<0.03	0.16	0.41
3	8	5	63	1979	1981	2	<0.03	0.69	<0.03	<0.03	0.10	0.20	0.43
4	11	6	55	1980	1983	3	<0.03	1.5	<0.03	0.10	0.10	0.62	0.88
5	257	141	55	1981	2020	39	<0.03	2.23	<0.03	<0.03	<0.03	0.27	0.84
8	75	12	16	2013	2014	1	<0.03	10	<0.03	0.13	0.80	1.96	2.95
9	75	45	60	2013	2014	1	<0.03	5.08	<0.03	<0.03	<0.03	0.61	1.31
10	107	48	45	2012	2020	8	<0.03	5.52	<0.03	<0.03	0.05	0.41	1.15
11	3	1	33	2008	2009	1	<0.03	0.46	0.1	0.205	0.38	0.42	0.44
12	37	23	62	2011	2012	1	<0.03	1.19	<0.03	<0.03	<0.03	0.1	0.63
13	32	18	56	2011	2012	1	<0.03	1.96	<0.03	<0.03	<0.03	0.06	0.57
14	37	12	32	2011	2012	1	<0.03	1.66	<0.03	<0.03	0.17	0.77	1.02
15	57	44	77	2015	2016	1	<0.03	2.00	<0.03	<0.03	<0.03	<0.03	0.13
16	61	36	59	2015	2016	1	<0.03	1.94	<0.03	<0.03	<0.03	0.1	0.34
17	106	73	69	2011	2016	5	<0.03	1.97	<0.03	<0.03	<0.03	0.05	0.39
18	102	80	78	2012	2020	8	<0.03	1.11	<0.03	<0.03	<0.03	<0.03	0.32
20	0	--	--	--	--	--	--	--	--	--	--	--	--
21	32	15	47	2012	2020	8	<0.03	0.78	<0.03	<0.03	0.04	0.31	0.48
22	349	142	41	1979	2020	41	<0.03	1.43	<0.03	<0.03	0.09	0.20	0.50
Ammonia, total, in milligrams per liter as nitrogen													
1	77	36	47	1977	2020	43	<0.03	0.59	<0.03	<0.03	0.04	0.09	0.15
2	81	37	46	1975	2020	45	<0.03	2.10	<0.03	<0.03	0.05	0.13	0.33
3	21	4	19	1978	1996	18	<0.03	0.51	<0.03	0.04	0.07	0.12	0.22
4	27	3	11	1979	1996	17	<0.03	0.45	0.042	0.054	0.09	0.14	0.38
5	173	116	67	1994	2020	26	<0.03	4.37	<0.03	<0.03	<0.03	0.06	0.22
8	195	98	50	2013	2020	7	<0.03	0.98	<0.03	<0.03	<0.03	0.08	0.21
9	201	157	78	2013	2020	7	<0.03	0.70	<0.03	<0.03	<0.03	<0.03	0.10
10	233	184	79	2012	2020	8	<0.03	0.82	<0.03	<0.03	<0.03	<0.03	0.08

Table 1.2. Summary statistics of selected nutrient constituents for sites in the Heart River Basin, 1970–2020.—Continued

[<, less than; --, no data]

Site number (fig. 1)	Number of observations	Number of censored values	Percent of data that is censored	Beginning sample year	Ending sample year	Number of years of sample record	Concentration						
							Minimum	Maximum	10th percentile	25th percentile	Median	75th percentile	90th percentile
Ammonia, total, in milligrams per liter as nitrogen—Continued													
11	3	3	100	2008	2009	1	<0.03	0.03	<0.03	<0.03	<0.03	<0.03	0.03
12	67	54	81	2011	2020	9	<0.03	0.15	<0.03	<0.03	<0.03	<0.03	0.04
13	61	32	52	2011	2020	9	<0.03	0.46	<0.03	<0.03	<0.03	0.07	0.15
14	68	43	63	2011	2020	9	<0.03	2.03	<0.03	<0.03	<0.03	0.05	0.11
15	97	30	31	2015	2018	3	<0.03	0.40	<0.03	<0.03	0.06	0.09	0.14
16	91	32	35	2015	2018	3	<0.03	0.30	<0.03	<0.03	0.04	0.07	0.13
17	196	115	59	2011	2020	9	<0.03	0.37	<0.03	<0.03	<0.03	0.04	0.08
18	152	100	66	2012	2020	8	<0.03	0.61	<0.03	<0.03	<0.03	0.04	0.08
19	2	1	50	2017	2017	<1	<0.03	0.04	0.03	0.03	0.04	0.04	0.04
21	32	17	53	2012	2020	8	<0.03	0.41	<0.03	<0.03	<0.03	0.10	0.22
22	258	159	62	1978	2020	42	<0.03	0.76	<0.03	<0.03	<0.03	0.06	0.17
Phosphorus, dissolved, in milligrams per liter as phosphorus													
1	77	38	49	1977	2020	43	<0.02	0.39	<0.02	<0.02	0.023	0.06	0.11
2	80	13	16	1977	2020	43	<0.02	0.35	<0.02	0.04	0.08	0.13	0.20
3	14	3	21	1978	1981	3	<0.02	0.34	<0.02	0.03	0.055	0.09	0.25
4	17	3	18	1979	1983	4	<0.02	0.52	<0.02	0.04	0.1	0.18	0.25
5	114	74	65	2005	2020	15	<0.02	0.41	<0.02	<0.02	<0.02	0.03	0.06
8	0	--	--	--	--	--	--	--	--	--	--	--	--
9	0	--	--	--	--	--	--	--	--	--	--	--	--
10	32	23	72	2012	2020	8	<0.02	0.08	<0.02	<0.02	<0.02	<0.02	0.02
11	1	1	100	2008	2008	<1	<0.02	<0.02	<0.02	<0.02	<0.02	<0.02	<0.02
12	0	--	--	--	--	--	--	--	--	--	--	--	--
13	0	--	--	--	--	--	--	--	--	--	--	--	--
14	0	--	--	--	--	--	--	--	--	--	--	--	--
15	0	--	--	--	--	--	--	--	--	--	--	--	--
16	0	--	--	--	--	--	--	--	--	--	--	--	--
17	0	--	--	--	--	--	--	--	--	--	--	--	--
18	33	16	48	2012	2020	8	<0.02	0.19	<0.02	<0.02	0.023	0.051	0.08

Table 1.2. Summary statistics of selected nutrient constituents for sites in the Heart River Basin, 1970–2020.—Continued

[<, less than; --, no data]

Site number (fig. 1)	Number of observations	Number of censored values	Percent of data that is censored	Beginning sample year	Ending sample year	Number of years of sample record	Concentration						
							Minimum	Maximum	10th percentile	25th percentile	Median	75th percentile	90th percentile
Phosphorus, dissolved, in milligrams per liter as phosphorus—Continued													
20	0	--	--	--	--	--	--	--	--	--	--	--	--
21	32	8	25	2012	2020	8	<0.02	0.27	<0.02	0.03	0.06	0.09	0.18
22	223	185	83	1978	2020	42	<0.02	0.11	<0.02	<0.02	<0.02	<0.02	0.04
Phosphorus, total, in milligrams per liter as phosphorus													
1	81	3	4	1977	2020	43	<0.02	0.42	0.03	0.04	0.07	0.12	0.17
2	85	0	0	1975	2020	45	0.04	1.90	0.06	0.09	0.14	0.23	0.32
3	25	0	0	1978	1996	18	0.05	0.91	0.07	0.13	0.21	0.38	0.49
4	31	0	0	1979	1996	17	0.06	7.40	0.07	0.19	0.28	0.64	1.57
5	174	19	11	1994	2020	26	<0.02	1.05	<0.02	0.03	0.05	0.08	0.14
8	195	2	1	2013	2020	7	<0.02	0.42	0.06	0.08	0.09	0.13	0.18
9	201	38	19	2013	2020	7	<0.02	0.26	<0.02	0.02	0.04	0.07	0.12
10	233	85	36	2012	2020	8	<0.02	0.37	<0.02	<0.02	0.03	0.05	0.10
11	3	2	67	2008	2009	1	<0.02	0.04	<0.02	<0.02	<0.02	0.03	0.03
12	67	0	0	2011	2020	9	0.026	0.19	0.04	0.06	0.08	0.10	0.13
13	61	0	0	2011	2020	9	0.034	0.33	0.07	0.11	0.14	0.20	0.28
14	68	5	7	2011	2020	9	<0.02	0.86	0.02	0.04	0.06	0.09	0.16
15	97	0	0	2015	2018	3	0.09	1.13	0.17	0.25	0.51	0.70	0.88
16	91	0	0	2015	2018	3	0.03	0.66	0.04	0.05	0.08	0.12	0.17
17	196	10	5	2011	2020	9	<0.02	0.92	0.03	0.03	0.05	0.07	0.10
18	152	0	0	2012	2020	8	0.03	0.68	0.04	0.04	0.06	0.10	0.18
20	2	2	100	2017	2017	<1	<0.02	<0.02	<0.02	<0.02	<0.02	<0.02	<0.03
21	32	1	3	2012	2020	8	<0.02	0.31	0.04	0.07	0.10	0.14	0.22
22	300	131	44	1978	2020	42	<0.02	1.60	<0.02	<0.02	0.03	0.05	0.13

Table 1.3. Summary statistics of selected field measurements and physical properties for sites in the Heart River Basin, 1970–2019.

[--, no data]

Site number (fig. 1)	Number of observations	Number of censored values	Percent of data that is censored	Beginning sample year	Ending sample year	Number of years of sample record	Concentration						
							Minimum	Maximum	10th percentile	25th percentile	Median	75th percentile	90th percentile
Specific conductance, in microsiemens per centimeter at 25 degrees Celsius													
1	561	0	0	1971	2020	49	150	6,930	425	770	1,070	1,280	1,520
2	216	0	0	1975	2020	45	226	4,850	775	1,570	2,320	3,320	4,190
3	40	0	0	1978	1996	18	243	4,740	336	485	1,390	2,680	4,060
4	61	0	0	1979	1996	17	222	2,500	291	338	641	937	1,610
5	566	0	0	1971	2020	49	220	4,800	853	1,220	1,680	2,030	2,380
6	215	0	0	1988	2012	24	398	3,500	870	1,180	1,630	2,000	2,370
7	38	0	0	1971	2019	48	510	1,880	849	923	1,080	1,460	1,520
10	214	0	0	1971	2020	49	357	2,790	677	850	1,070	1,320	1,560
11	27	0	0	2008	2019	11	964	1,660	1,030	1,130	1,390	1,480	1,630
17	0	--	--	--	--	--	--	--	--	--	--	--	--
18	240	0	0	1991	2020	29	161	4,260	704	1,380	2,120	2,440	2,900
19	269	0	0	1971	1995	24	118	2,900	560	870	1,150	1,370	1,520
20	234	0	0	1988	2019	31	260	2,660	839	1,180	1,370	1,570	1,760
21	238	0	0	1971	2020	49	145	3,280	470	903	1,460	2,000	2,480
22	732	0	0	1971	2020	49	240	3,500	825	1,140	1,420	1,650	2,000
pH, in standard units													
1	254	0	0	1972	2020	48	6.5	8.9	7.5	7.8	8.2	8.4	8.6
2	185	0	0	1975	2020	45	6.8	8.8	7.7	8.0	8.3	8.4	8.5
3	40	0	0	1978	1996	18	6.9	9.1	7.3	7.6	8.2	8.5	8.6
4	56	0	0	1979	1996	17	6.9	9.1	7.2	7.6	8.1	8.3	8.5
5	491	0	0	1972	2020	48	4.7	10.1	7.8	8.0	8.3	8.5	8.6
6	82	0	0	1989	2012	23	7.0	9.1	7.7	8.0	8.2	8.4	8.6
7	26	0	0	1972	2019	47	7.4	8.8	7.9	8.0	8.2	8.3	8.6
10	204	0	0	1972	2020	48	7.0	9.1	8.1	8.2	8.3	8.4	8.5
11	29	0	0	2008	2019	11	7.9	8.6	8.1	8.2	8.4	8.4	8.5
17	29	0	0	2011	2012	1	7.9	8.5	8.1	8.2	8.3	8.3	8.4
18	155	0	0	1991	2020	29	7.1	9.3	7.9	8.2	8.4	8.5	8.6
19	81	0	0	1971	1995	24	6.6	8.7	7.7	8.0	8.2	8.3	8.5

Table 1.3. Summary statistics of selected field measurements and physical properties for sites in the Heart River Basin, 1970–2019.—Continued

[--, no data]

Site number (fig. 1)	Number of observations	Number of censored values	Percent of data that is censored	Beginning sample year	Ending sample year	Number of years of sample record	Concentration						
							Minimum	Maximum	10th percentile	25th percentile	Median	75th percentile	90th percentile
pH, in standard units—Continued													
20	115	0	0	1988	2019	31	6.9	8.8	7.8	8.2	8.4	8.4	8.5
21	139	0	0	1972	2020	48	6.8	9.0	8.0	8.1	8.3	8.5	8.6
22	745	0	0	1971	2020	49	6.9	9.1	7.8	8.1	8.3	8.5	8.5

For more information about this publication, contact:

Director, USGS Dakota Water Science Center
821 East Interstate Avenue, Bismarck, ND 58503
1608 Mountain View Road, Rapid City, SD 57702
605–394–3200

For additional information, visit: https://www.usgs.gov/centers/dakota-water

Publishing support provided by the
Rolla Publishing Service Center

ISSN 2328-0328 (online)
https://doi.org/10.3133/sir20225013